Coordination Polymers

Functional Porous Coordination Polymers

Susumu Kitagawa, Ryo Kitaura, and Shin-ichiro Noro*

Keywords:
coordination polymers · dynamic properties · inclusion compounds · metal–organic frameworks · microporous materials

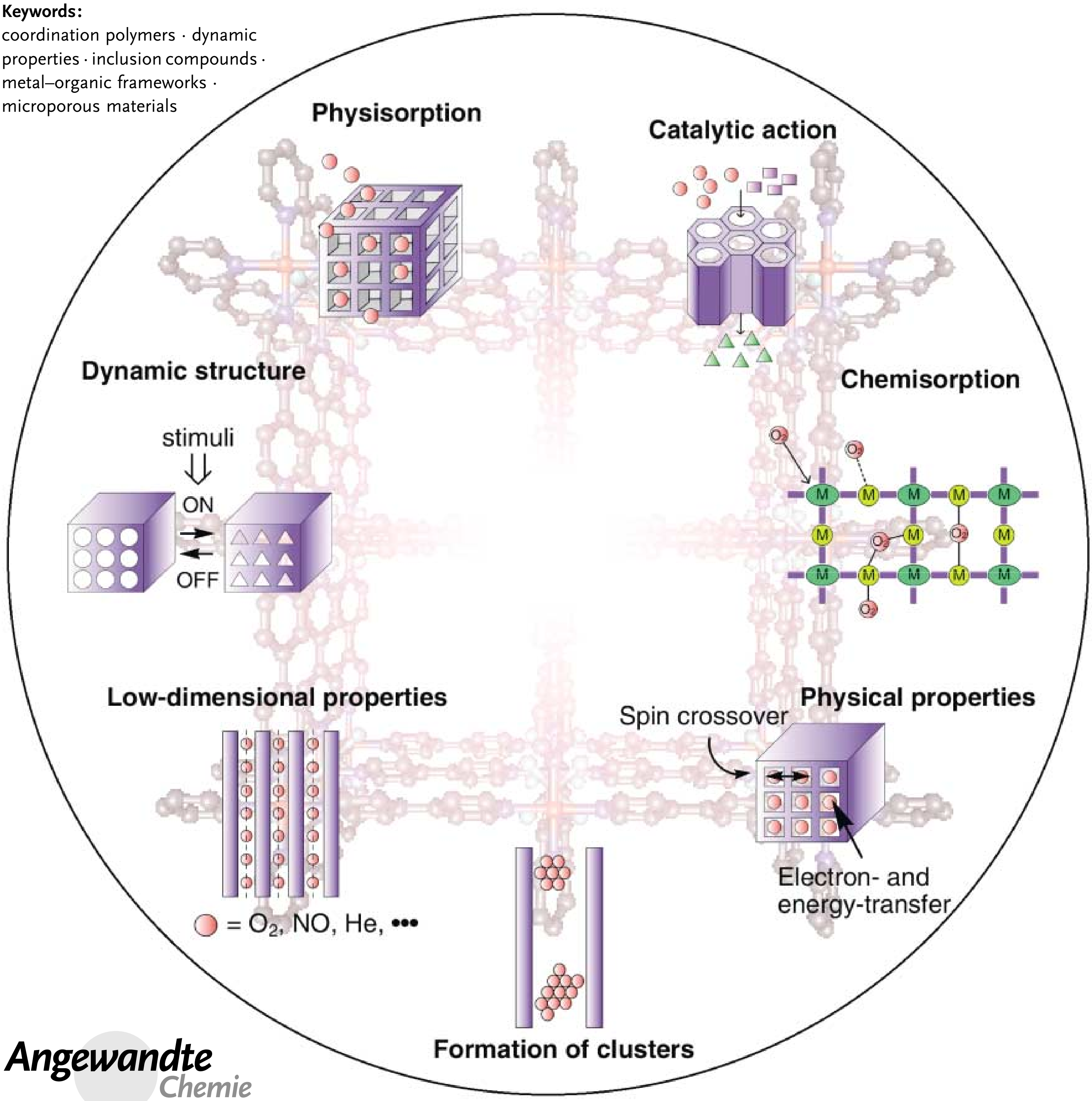

Angewandte Chemie

DOI: 10.1002/anie.200300610

The chemistry of the coordination polymers has in recent years advanced extensively, affording various architectures, which are constructed from a variety of molecular building blocks with different interactions between them. The next challenge is the chemical and physical functionalization of these architectures, through the porous properties of the frameworks. This review concentrates on three aspects of coordination polymers: 1) the use of crystal engineering to construct porous frameworks from connectors and linkers ("nanospace engineering"), 2) characterizing and cataloging the porous properties by functions for storage, exchange, separation, etc., and 3) the next generation of porous functions based on dynamic crystal transformations caused by guest molecules or physical stimuli. Our aim is to present the state of the art chemistry and physics of and in the micropores of porous coordination polymers.

From the Contents

1. Introduction

Recently, remarkable progress has been made in the area of molecular inorganic–organic hybrid compounds. The synthesis and characterization of infinite one-, two-, and three-dimensional (1D, 2D, and 3D) networks has been an area of rapid growth. Coordination compounds with infinite structures have been intensively studied, in particular, compounds with backbones constructed from metal ions as connectors and ligands as linkers, the so-called coordination polymers.[1–22] The phrase, "coordination polymers" appeared in the early 1960s, and the area was first reviewed in 1964.[23] Versatile synthetic approaches for the assembly of target structures from molecular building blocks have been developed. The key to success is the design of the molecular building blocks which direct the formation of the desired architectural, chemical, and physical properties of the resulting solid-state materials. In a surprisingly short time, the structural chemistry has attained a very mature level. Figure 1 shows the extraordinary increase in the number of articles published in this area. Coordination polymers have now taken an important position in the porous-materials area and added a new category to the conventional classification (Figure 2).

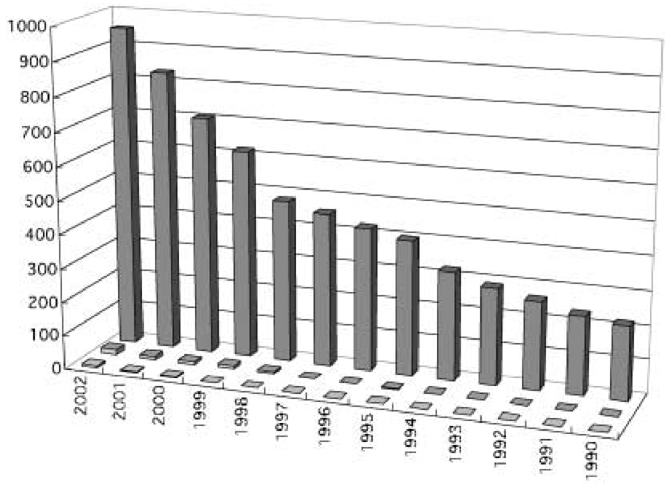

Figure 1. The number of published articles containing the keywords "coordination polymers" (back), "porous coordination polymers" (middle), and "adsorption of porous coordination polymers" (front), survey by SciFinder.

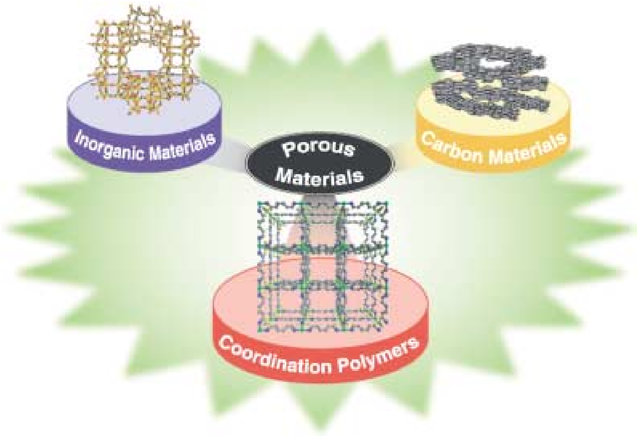

Figure 2. Classes of porous materials.

---

[*] Prof. Dr. S. Kitagawa, Dr. R. Kitaura,[+] Dr. S.-i. Noro[++]
Department of Synthetic Chemistry and
Biological Chemistry, Graduate School of Engineering
Kyoto University, Katsura
Nisikyo-ku, Kyoto 615-8510 (Japan)
Fax: (+81) 75-383-2732
E-mail: kitagawa@sbchem.kyoto-u.ac.jp

[+] Current Address:
Toyota Central R&D Laboratories, Inc.
Nagakute, Aichi, 480–1192 (Japan)

[++] Current Address:
Supramolecular Science Laboratory
RIKEN (The Institute of Physical and Chemical Research)
2-1 Hirosawa, Wako-shi, Saitama, 351-0198 (Japan)

DOI: 10.1002/anie.200300610

Porous compounds have attracted the attention of chemists, physicists, and materials scientists because of interest in the creation of nanometer-sized spaces and the novel phenomena in them. There is also commercial interest in their application in separation, storage, and heterogeneous catalysis. Until mid 1990s, there were basically two types of porous materials, namely, inorganic and carbon-based materials. In the case of microporous inorganic solids, the largest two subclasses are the aluminosilicates and aluminophosphates. Zeolites are 3D crystalline, hydrated alkaline or alkaline-earth aluminosilicates with the general formula $M^{n+}_{x/n}[(AlO_2)_x(SiO_2)_y]^{x-}\cdot w\,H_2O$[24–26] (M = metal). Their framework, built from corner-sharing TO_4 tetrahedra (T = Al, Si), defines interconnected tunnels or cages in which water molecules and M ions are inserted. The porosity is then provided through the elimination of the water molecules, the framework usually remains unaffected by this. The cavities, whose structure is usually determined by the number of polyhedra surrounding the pore, were initially exploited for molecular-sieve requirements in gas separation and catalytic processes. Synthetic zeolites were first observed in 1862.[27] Aluminophosphates ($AlPO_4$s) consist of tetrahedra of Al^{3+} and P^{5+} ions linked by corner-sharing oxygen atoms, and which build up a 3D neutral framework with channels and/or pores of molecular dimensions.[28] Many aluminophosphates have crystal structures, which are not observed in zeolites. The first publication on microporous crystalline aluminophosphates appeared in 1982.[29] Since then, not only several related crystalline oxides, such as silicoaluminophosphates, metallosilicates, metalloaluminophosphate, and metallophosphates, but also porous chalcogenides, halides, and nitrides, have been discovered.[30,31] Mesoporous materials have also been extensively studied; they afford intriguing and useful porous properties, characteristic of meso-sized structures.[32–35]

The activated carbons have a high open porosity and a high specific surface area, but have a disordered structure. The essential structural feature is a twisted network of defective hexagonal carbon layers, cross-linked by aliphatic bridging groups. The width of the layers varies, but typically is about 5 nm. Simple functional groups and heteroelements are incorporated into the network and are bound to the periphery of the carbon layers. Herein, we focus on the regular microporous structures; therefore, we will not consider the activated carbons further.

Recently, porous coordination polymers have been developed, which are beyond the scope of the former two classes of porous materials. They are completely regular, have high porosity, and highly designable frameworks. Their syntheses occur under mild conditions and the choice of a certain combination of discrete molecular units leads to the desired extended network, this is the so-called bottom-up method. The structural integrity of the building units is maintained throughout the reactions which allows their use as modules in the assembly of extended structures. Werner complexes, [β-M(4-methylpyridyl)$_4$(NCS)$_2$] (M = Ni^{II} or Co^{II}),[36] Prussian blue compounds,[37–39] and Hofmann clathrates and their derivatives have frameworks that are built of CN linkages between square-planar or tetrahedral tetracyanometallate(II) units and octahedral metal(II) units coordinated by complementary ligands,[39–41] which are known to be materials that can reversibly absorb small molecules. There is an early report on use of organic bridging ligands to form the porous coordination polymer $[Cu(NO_3)(\text{adiponitrile})_2]_n$ with a diamond net, however, the adsorption behavior was not reported.[42] Since the early 1990s, research on the structures of porous coordination polymers has increased greatly, and examples with functional micropores soon started to appear. In 1990, Robson et al. reported a porous coordination polymer capable of an anion exchange.[43] The catalytic properties of the 2D [Cd^{II}(4,4′-bpy)$_2$] (bpy = bipyridine)[*] coordination polymer were studied by Fujita et al. in 1994.[44] In 1995, the adsorption of guest molecules was studied by the groups of Yaghi[45] and Moore[46], and in 1997 we reported gas adsorption at ambient temperature.[47]

2. Principles in Synthesis

2.1. Connectors and Linkers

Coordination polymers contain two central components, connectors and linkers. These are defined as starting reagents with which the principal framework of the coordination polymer is constructed. In addition, there are other auxiliary components, such as blocking ligands, counteranions, and nonbonding guests or template molecules (Figure 3). The important characteristics of connectors and linkers are the

---

[*] A list of abbreviations is given in the Appendix on p. 2368 and 2369.

Susumu Kitagawa obtained his PhD from Kyoto University in 1979 and then joined the Department of Chemistry of Kinki University as an assistant professor. He was promoted to associate professor in 1988 and then moved to Tokyo Metropolitan University as a professor in 1992, and since 1998 he has been a professor in Department of Synthetic Chemistry and Biological Chemistry, Kyoto University. His research interests are centered on the chemistry of organic–inorganic hybrid compounds, particularly the chemical and/or physical properties of porous coordination polymers.

Ryo Kitaura was born in 1974. He studied Chemistry and Physical Chemistry, and received his doctoral degree with Professor S. Kitagawa in 2003 from the Kyoto University. Since 2003 he has worked at Toyota central R&D laboratories. His current research interests focus on chemistry and physics in nanospace of microporous coordination polymers.

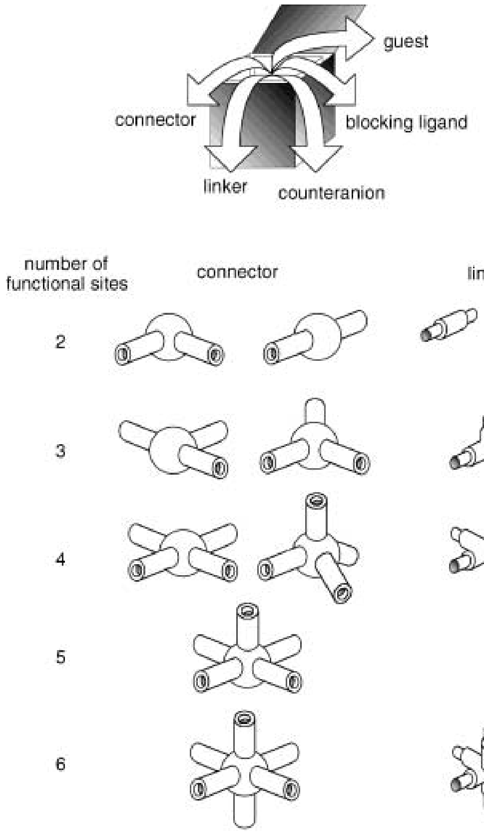

Figure 3. Components of coordination polymers.

number and orientation of their binding sites (coordination numbers and coordination geometries).

Transition-metal ions are often utilized as versatile connectors in the construction of coordination polymers. Depending on the metal and its oxidation state, coordination numbers can range from 2 to 7, giving rise to various geometries, which can be linear, T- or Y-shaped, tetrahedral, square-planar, square-pyramidal, trigonal-bipyramidal, octahedral, trigonal-prismatic, pentagonal-bipyramidal, and the corresponding distorted forms (Figure 3). For instance, Ag^{I}[8,15] and Cu^{I}[10] ions with d^{10} configuration have various coordination numbers and geometries which can be realized by changing reaction conditions, such as solvents, counteranions, and ligands. The large coordination numbers from 7 to 10 and the polyhedral coordination geometry of the lanthanide ions are useful for the generation of new and unusual network topologies. In addition, coordinatively unsaturated lanthanide ion centers can be generated by the removal of coordinated solvent molecules. The vacant sites could be utilized in chemical adsorption, heterogeneous catalysis, and sensors.[48,49] Instead of a naked metal ion, the metal-complex connectors have the advantage of offering control of the bond angles and restricting the number of coordination sites; sites that are not required can be blocked by chelating or macrocyclic ligands that are directly bound to a metal connector, and thus leave specific sites free for linkers. This "ligand-regulation" of a connector is very useful. The polymer $\{[Ni(C_{12}H_{30}N_6O_2)(1,4\text{-bdc})]\cdot 4H_2O\}_n$ ($C_{12}H_{30}N_6O_2$ = macrocyclic ligand; bdc = benzenedicarboxylate) forms 1D chains, in which each axial site of the nickel–macrocyclic unit is occupied by bridging 1,4-bdc ligands, and the chains are linked together by the hydrogen-bonding interactions to give rise to a 3D network.[50]

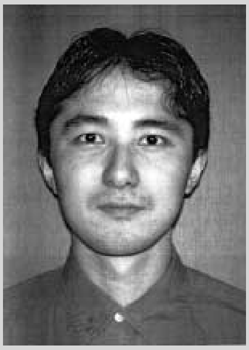

Shin-ichiro Noro, born in Kanagawa in 1975, received his PhD from Kyoto University in 2003 under the supervision of Professor S. Kitagawa with research on crystal engineering of functional coordination polymers. He is currently a special postdoctoral researcher at the RIKEN (The Institute of Physical and Chemical Research), working in the research group of Dr. T. Wada (Supramolecular Science Laboratory).

Linkers afford a wide variety of linking sites with tuned binding strength and directionality (Figure 4). Halides (F, Cl, Br, and I) are the smallest and simplest of all linkers. Quasi-

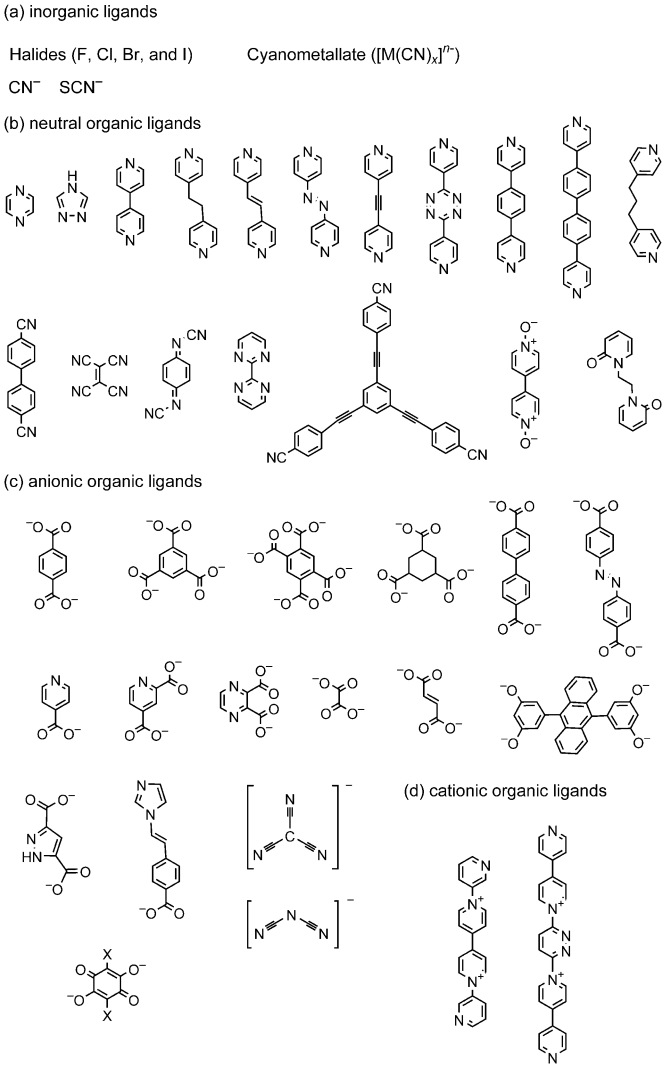

Figure 4. Examples of linkers used in coordination polymers.

1D halogen-bridged mixed-valence compounds (MX chains) formulated as $\{[M^{II}(AA)_2][M^{IV}(AA)_2X_2]\cdot 4Y\}_n$ (M^{II}–M^{IV} = Pt^{II}–Pt^{IV}, Pd^{II}–Pd^{IV}, Ni^{II}–Pt^{IV}, Pd^{II}–Pt^{IV}, Cu^{II}–Pt^{IV}; X = Cl, Br, I, and mixed halides; AA = ethylenediamine, 1,2-diaminocyclohexane, etc.; Y = ClO_4, BF_4, halides, etc.) have been extensively investigated because of their physical properties.[51,52] A series of mixed-valence Cu^I/Cu^{II}-X (X = Cl, Br) chain compounds has pinned charge-density waves.[53] Halides can also coexist in the coordination frameworks with neutral organic ligands.[54–57] The CN^- and SCN^- ions have a similar bridging ability to halides.[58–61] Cyanometallate anions have various geometries, for example, linear, as in $[M(CN)_2]^-$ (M = Au[62,63] and Ag[64–66]), trigonal, as in $[Cu(CN)_3]^{2-}$,[67] tetrahedral, as in $[Cd(CN)_4]^{2-}$,[68–71] square planar, as in $[M(CN)_4]^{2-}$ (M = Ni,[41] Pd,[72–74] and Pt[72,75]), octahedral, as in $[M(CN)_6]^{3-}$ (M = Fe,[76–80] Co,[76,81,82] Cr,[83–85] and Mn[86,87]), and pentagonal bipyramidal, as in $[Mo(CN)_7]^{4-}$.[88–91] The octacyanometallates, $[M(CN)_8]^{n-}$ (M = Mo and W), in particular have various coordination geometries, for example, square-antiprism, dodecahedron, or bicapped trigonal-prism.[91–93] This structural diversity makes the cyanometallates useful and practical connectors modules.

The most frequently used neutral organic ligands are pyrazine (pyz) and 4,4′-bpy.[7,11,14,19] An example of a coordination polymer with the 4,4′-bpy ligand is illustrated in Figure 5.[94] Recent efforts have been devoted to utilization of long bridging ligands with appropriate spacers.[95–100] For example, treatment of a longer ligand, L = 9,9-diethyl-2,7-bis(4-pyridylethynyl)fluorene, with copper nitrate in ethanol leads to the exceptionally large, noninterpenetrating, square-grid polymer $\{[Cu(L)_2(NO_3)_2]\cdot x(\text{solvent})\}_n$ with grid dimensions of 25 × 25 Å^2.[100]

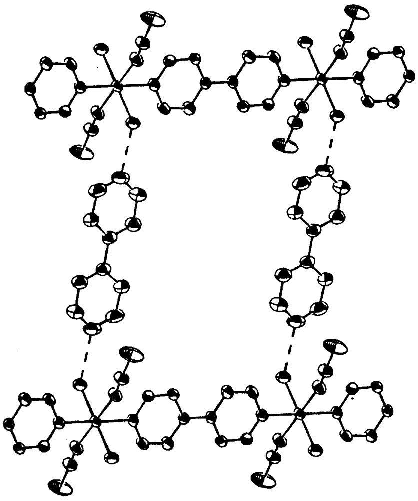
Figure 5. Section of the structure of $\{[Co(NCS)_2(4,4'\text{-bpy})(H_2O)_2]\cdot 4,4'\text{-bpy}\}_n$. Dotted lines indicate hydrogen bonds.[94]

Di-,[4,101,102] tri-,[4,103–106] tetra-,[107,108] and hexacarboxylate[109,110] molecules are typical anionic linkers. Coordination polymers having nonsymmetric anionic ligands (generally described as pyridine-X-COO^- (X = spacer)) have been extensively studied.[5] 1,4-Dihydroxy-2,5-benzoquinone and its derivatives are also often used and give rise a variety of frameworks, in which they act as linear linkers.[13] The crystal structure of $[Cu(ca)(pyz)]_n$ (H_2ca = chloranilic acid) is made up of parallel sheets, which consist of square arrays formed by Cu^{II} ions and ca^{2-} and pyz linkers.[111]

There are few examples of coordination polymers with cationic organic ligands, which is naturally a result of their very low affinity for cationic metal ions.[112–116] Novel cationic ligands based on *N*-aryl pyridinium and viologen derivatives were developed and successfully employed.[112–114]

2.2. Design of Motifs

Excellent reviews about the structural topologies of the frameworks of coordination polymers and/or inorganic materials have been published,[2,3,7,8,14,19,31,117–123] and, therefore, topological features are only described briefly herein.

Various combinations of the connector(s) and linker(s) mentioned in the previous section affords various specific structural motifs. Figure 6 shows representative motifs of frameworks constructed from various types of connectors and a linear linker. A linear chain is a simple 1D motif. The Ag^I ion tends to form a linear chain with several linear linkers as a result of its preference for a coordination number of two.[8]

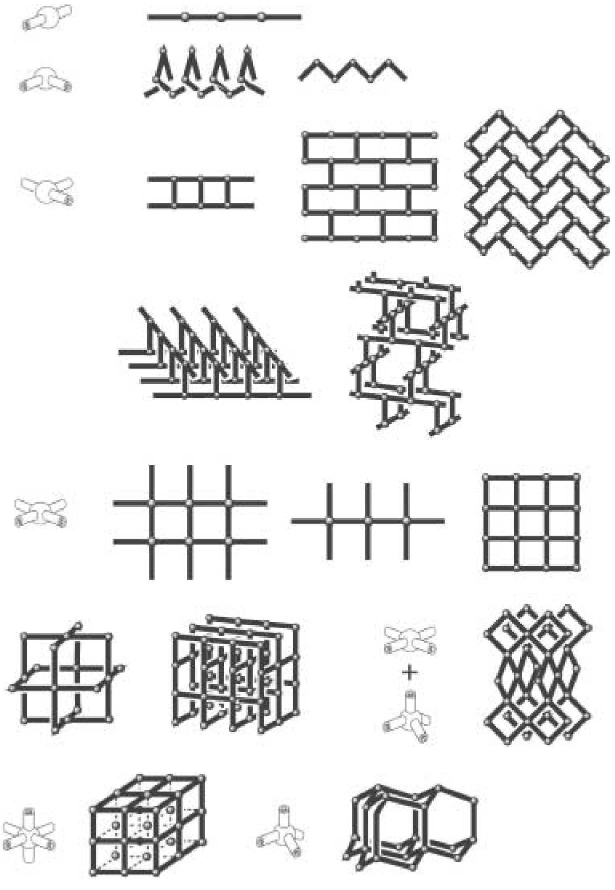

Figure 6. The structural frameworks that can be constructed by using different connectors and linear linkers.

Square-grid networks exemplify a particularly simple and commonly reported example of predictable 2D metal–organic networks. Square-grid coordination polymers are based upon 1:2 metal:ligand complexes with linear bifunctional linkers. A ligand L and $Ni(NO_3)_2$ form a mutually interpenetrated 2D grid structure $\{[Ni(L)_2(H_2O)_2]\cdot 2NO_3\}_n$ (L = 9,10-bis(4-pyridyl)anthracene) in the presence of benzene (Figure 7).[124] A T-shaped metal connector generates unique structural motifs, such as the brick wall,[99] herringbone,[125] and bilayer[47,126] (see Figure 6). To create such a T-shaped module, the NO_3^- ion is often utilized, which through chelation blocks four coordination sites of heptacoordinate metal ions, such as Cd^{II} and Co^{II}. The remaining three coordination sites are bridged by bifunctional ligands, creating the T-shaped module with metal:ligand ratio of 1:1.5. The Cu^{II} center of $\{[Cu_2(4,4'\text{-bpy})_5(H_2O)_4]\cdot x(\text{anion})\cdot 2H_2O\cdot 4EtOH\}_n$ (x(anions) = $4PF_6^-$ and $2PF_6^-$ and $2ClO_4^-$) has an octahedral coordination environment with four nitrogen atoms of 4,4′-bpy ligands in the equatorial plane and two oxygen atoms of H_2O molecules at the axial sites.[126] They, however, represent the bilayer motif with the T-shape module because one of the four 4,4′-bpy ligands coordinated to the Cu^{II} ions occurs as a terminal mode. Diamond nets, which containtetrahedral nodes[5,43,127] and the B net in CaB_6,[128–131] which contains octahedral nodes, are classical examples of the 3D motif. Other new 3D networks have been described in recent years.[132–138] $\{[Zn(\text{nicotinate})_2]\cdot MeOH\cdot 2H_2O\}_n$ is the first example of a 3D coordination polymer that possesses a $4^2\cdot 8^4$ topology[139] based solely upon square-planar nodes.[135]

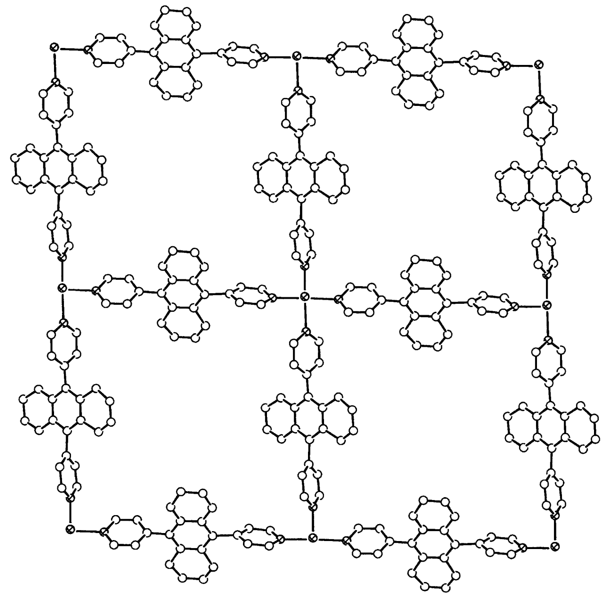

Figure 7. The 2D square grid network of $\{[Ni\{9,10\text{-bis}(4\text{-pyridyl})\text{anthracene}\}_2(H_2O)_2]\cdot 2NO_3\}_n$.[124]

The synthesis of homochiral, porous materials is a particularly interesting objective, because such chiral porous coordination polymers could be of use for applications in heterogeneous asymmetric catalysis and enantioselective separations.[100,140–143] Strategies for forming homochiral frameworks exploit enantiopure organic ligands,[100,140–142] or the use of helical chains or helical frameworks.[143] The inherent chirality of this architecture comes from spatial disposition rather than the presence of chiral centers. $[Ni(4,4'\text{-bpy})(bz)_2(MeOH)_2]_n$ self-assembles as a helical architecture based on octahedral metal connectors with linear spacer ligands (Figure 8).[143] The helical chains pack in a staggered fashion but align in a parallel fashion. Therefore, the bulk crystal is chiral as every helix in an individual crystal is of the same handedness.

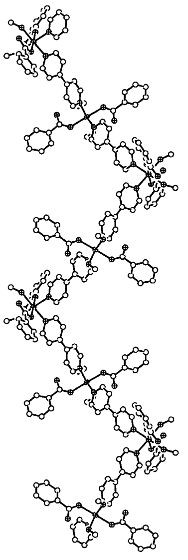

Figure 8. The 1D helical structure of $\{[Ni(bz)_2(4,4'\text{-bpy})(MeOH)_2]\cdot\text{guest}\}_n$ (guest = nitrobenzene, benzene, veratrole, phenol, chloroform, and dioxane).[143]

Polynuclear clusters constructed from two or more metal ions and multidentate carboxylate linkers, such as 1,4-bdc and 1,3,5-btc, (so-called "secondary building units" (SBUs)), can have special coordination numbers and geometries. When such polytopic units are copolymerized with metal ions, it is common to find linked cluster entities in the assembled solid. Each cluster is considered to be an SBU, in that it is a conceptual unit which was not employed in the synthesis as a distinct molecular building block. However, specific SBUs can be generated in situ under the correct chemical conditions.[21] Because the metal ions are locked into their positions by the carboxylate groups, the SBUs are sufficiently rigid to produce extended frameworks of high structural stability. Such frameworks are also neutral, obviating the need for counterions in their cavities. In clusters with terminal ligands, the reactivity of the metal site can be studied through the removal of these ligands, which frees a coordination site.

Anionic molybdenum oxides, which are prepared in situ by hydrothermal reactions, are useful building blocks for the construction of novel frameworks. A large number of organodiamine–molybdenum oxide composite materials have been thoroughly investigated (Figure 9).[7,144]

Charge is an important factor in the rational construction of functional coordination polymers. Since most of transition-metal connectors are cationic, an anionic source must be included to neutralize the overall charge. Frequently used anionic sources are inorganic anions, such as ClO_4^-, BF_4^-, NO_3^-, NCS^-, PF_6^-, NO_2^-, SiF_6^{2-}, CN^-, $CF_3SO_3^-$, SO_4^{2-}, N_3^-, and halide, which are introduced together with metal ions from the corresponding metal, sodium, and potassium salts. These anions exist as free guests, counterions, or linkers in the coordination polymers. An important characteristic of inorganic anions is their ability to act as hydrogen-bond-acceptor sites through their O and F atoms. $\{[Mn(NO_3)_2(azpy)(H_2O)_2]\cdot 2EtOH\}_n$ (azpy = 4,4′-azopyridine) is composed of 1D linear chains, each of which is bridged by hydrogen bonds between coordinated H_2O donor groups and NO_3^- acceptor

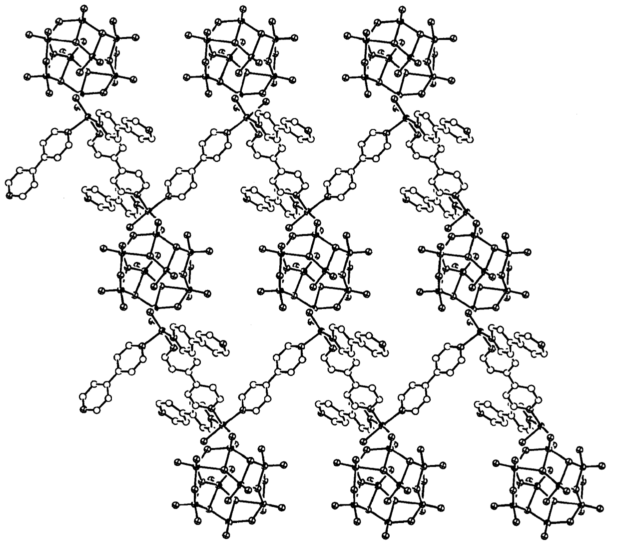

Figure 9. Crystal structure of $[\{Ni(4,4'\text{-}bpy)_2(H_2O)_2\}_2Mo_8O_{26}]_n$. The connection of the cluster SBUs to the polymeric cationic chains results in a 2D framework.[144]

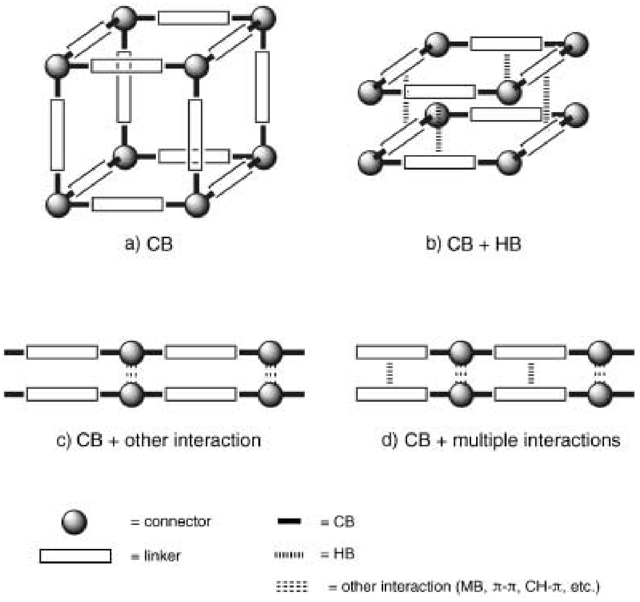

Figure 10. Combinations of interactions participating in the construction of a coordination polymer.

groups to form a unique 3D "log cabin" network.[145] Inorganic anions are also used as spacers between magnetic chains and layers.[16]However, the disadvantage of inorganic anions is that when using them it is difficult to create a highly porous neutral framework. To make neutral coordination frameworks anionic organic ligands are used, such as polycarboxylates (e.g. oxalate and benzenetricarboxylate), and 1,4-dihydroxybenzoquinone, pyridinecarboxylate, and their derivatives.[4,5,13] These organic anions can coexist with neutral organic ligands, such as bipyridine derivatives, and are therefore good candidates for the construction of high-dimensional frameworks.

The bonding interactions of coordination polymers are classified into four types as shown in Figure 10: a) coordination bond (CB) only, b) coordination bond and hydrogen bond (CB + HB), c) coordination bond + other interaction, such as metal–metal bond (MB), π–π (PP), CH–π (HP) interactions, and d) coordination bond + mixture of interactions (for instance, HB + PP, HB + MB, or MB + PP). The stability of 3D motifs increases with increasing coordination bond contribution. 1D and 2D motifs often aggregate through additional weak bonds (HB, PP, HP) to give 3D frameworks. In some cases, 1D and 2D motifs are linked by guest molecules through weak interactions. Of course, even 3D motifs interact with each other by such weak interactions (for example, when interpenetration occurs). Figure 11 shows examples of coordination polymers classified on the basis of the types of bond combinations. Many 1D linear M–L (L = bipyridine ligands) coordination polymers are linked by hydrogen bonds between free ligands and coordinated H_2O or alcohol molecules to form 2D rectangular grids, each of which in turn is linked by π–π interactions between the pyridine rings of the ligands (type d: CB + HB + PP).[94,146–150] In $\{[Ag(2,4'\text{-}bpy)]\cdot ClO_4\}_n$, adjacent helical chains are linked by weak ligand-unsupported metal–metal interactions ($Ag\cdots Ag = 3.1526(6)$ Å), which results in an open 2D network with compressed hexagons as building units (Figure 11 c; type c: CB + MB).[151] The Cu^{II} ions of $\{[Cu(dhbc)_2(4,4'\text{-}bpy)]\cdot H_2O\}_n$ (Hdhbc = 2,5-dihydroxybenzoic acid) are connected by 4,4'-bpy ligands to produce straight chains, which are linked by dhbc units to give a 2D sheet motif.[152] The

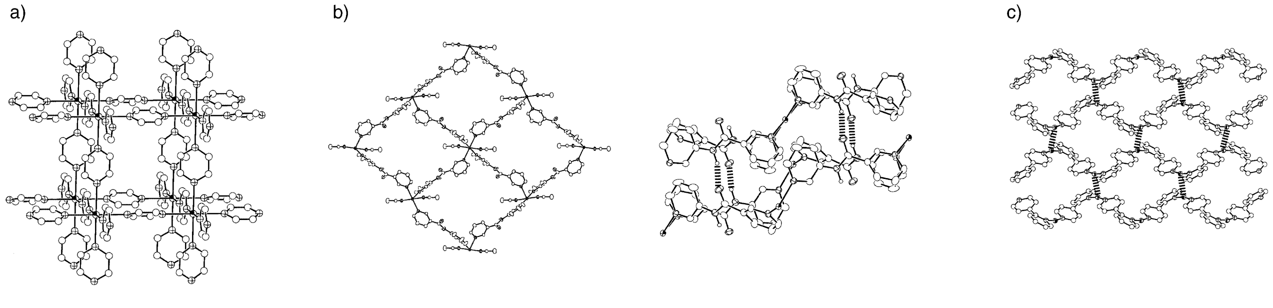

Figure 11. Examples of coordination polymers with various bond combinations. a) 3D framework (the B net in CaB_6) of $\{[Ag(pyz)_3]\cdot SbF_6\}_n$ (type a).[128] b) 2D sheet structure (left) and the stacking of two sheets linked by amide hydrogen bonds (right) in $[Co(NCS)_2(3\text{-}pna)_2]_n$ (type b: CB + HB).[153] c) 2D network consisting of helical chains linked by Ag–Ag bonds (dashed lines) in $\{[Ag(2,4'\text{-}bpy)]\cdot ClO_4\}_n$ (type c: CB + MB).[151]

distance of 3.44 Å between the planes of the nearest-neighbor dhbc ligands indicates the presence of π–π stacking interactions (type c: CB + PP). Amide-containing ligands are useful for the stabilization of coordination frameworks because they have both hydrogen-bond donor (NH) and hydrogen-bond acceptor (CO) sites.[153,154] The crystal structure of $[Co(NCS)_2(3\text{-pna})_2]_n$ (pna = *N*-pyridylnicotinamide) has a 2D sheet composed of a nearly square grid with the dimensions 7.3 × 12.9 Å^2.[153] The adjacent sheets stack along the *c* axis, and are offset by 0.5(*a* + *b*) along the *ab* plane so that the NCS group protrudes through the midpoint of the cavity of the adjacent sheet. The interlayer separation is about 3 Å. A hydrogen-bonding link of the NH···O=C (N···O = 2.874(4) Å) type between the adjacent sheets affords a 3D network (Figure 11 b, type b: CB + HB).

Interpenetration frequently occurs in the coordination polymers with a large grid. In some cases the coordination frameworks generate open voids, cavities, and channels, which can make up more than half the volume of the crystal. These large spaces are usually occupied by solvent molecules or counteranions. In other cases remarkable interpenetrating structures form, in which the voids constructed by one framework are occupied by one or more independent frameworks. Such entangled structures can only be disentangled by destroying internal bonds. Until recently examples of such structures were rare, but they are now being reported with ever increasing frequency, as a result of the developments in the chemistry of microporous coordination polymers. A detailed review on interpenetration has been published.[2] It is noteworthy that one of the first examples of coordination networks, reported many years ago, is a sixfold interpenetrated diamondoid net based on Cu^I ions and the flexible bidentate ligand adiponitrile.[42] The highest interpenetration (tenfold) ever found within diamond nets with exclusively coordinative bonds was recently reported for $\{[Ag(ddn)_2]\cdot NO_3\}_n$.[155]

For creating highly porous coordination polymers, it is naturally very important to avoid interpenetration. $\{[Zn_3(OH)_2(bpdc)_2]\cdot 4\,def\cdot 2\,H_2O\}_n$ (bpdc = 4,4′-biphenyldicarboxylate, def = *N*,*N*′-diethylformamide) has a 3D structure constructed from infinite Zn-O-C SBUs and long bpdc linkers, the Zn-O links (within the SBUs) and the Ph–Ph links (between the SBUs) provide a noninterpenetrated framework that is an amplification of the Al net in $SrAl_2$ (Figure 12).[156] The two following distances are important in this case for the formation of a noninterpenetrated net: a short distance between the carboxylate linkers along the [001] direction, and a longer distance between the SBUs in the [110] direction. The small separation allows the long linkers to come together such that the phenyl rings of each bpdc linker form CH···π interactions (3.73 Å) to adjacent linkers resulting in an impassable wall of bpdc units. For the construction of an interpenetrated structure in this coordination polymer, an additional bpdc unit would have to fit between adjacent linkers, which is impossible. Other structural types, such as the B net in CaB_6, can be amenable to the same strategy, for example, in the structure of $[M(AF_6)(4,4'\text{-bpy})_2]_n$ (M = Zn^{II}, A = Si;[129] M = Cu^{II}, A = Si;[130] M = Cu^{II}, A = Ge[126]). Cd^{II} coordination polymers with fluorinated ligands are not apt to be interpenetrated, owing to weak intermolecular forces among fluorinated compounds. These compounds tend instead to interact with guest molecules to form clathrate compounds.[157] From thick 2D layers of $[Cu(pzdc)]_n$ (pzdc = pyrazine-2,3-dicarboxylate) and pillar ligands L the 3D pillared-layer coordination polymers $[Cu_2(pzdc)_2(L)]_n$ (L = pyz, 4,4′-bpy, and its derivatives) are constructed.[158,159] Because of the absence of effective windows in the layers, it is impossible for interpenetration to occur in the 3D networks.

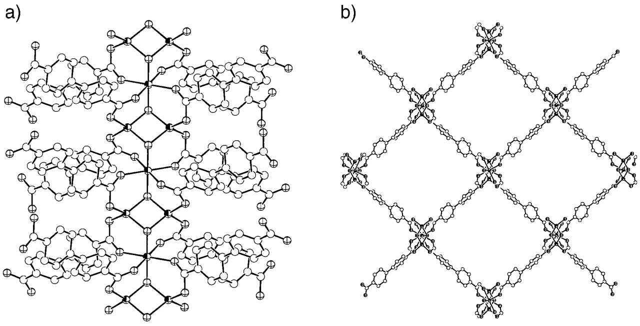

Figure 12. a) The crystal structure of $\{[Zn_3(OH)_2(bpdc)_2]\cdot 4\,def\cdot 2\,H_2O\}_n$ which contains infinite Zn-O-C SBUs that are linked together by bpdc links. b) View of 1D channels running along the *c* axis.[156]

On the other hand, interpenetration affords very stable structures.[145,152,160–163] Thus, we have synthesized several interpenetrated coordination polymers with the azpy ligand which is longer than 4,4′-bpy. The resulting robust interpenetrated frameworks showed gas-adsorption properties.[145] A 3D doubly interpenetrated coordination polymer of $[Cu(1,4\text{-bdc})(4,4'\text{-bpy})_{0.5}]_n$ (the B net of CaB_6) has stable and dynamic channels, which give hysteretic adsorption isotherms.[152,161] Moreover, a considerably longer ligand could give highly porous interpenetrated coordination polymers. $\{[Tb_2(adb)_3]\cdot 20\,dmso\}_n$ (adb = 4,4′-azodibenzoate) with a long dicarboxylate linker has a doubly interpenetrating structure with each framework having an idealized simple cubic 6-connected net (the B net of CaB_6). Despite the presence of doubly interpenetrating networks, at least 20 dmso guest molecules per SBU occupy the pores, or a volume representing 71 % of the crystal volume, the greatest value observed for interpenetrating structures.[164]

The synthesis of coordination polymers with different linkers (at least two kinds) has been attempted not only to generate diverse structures but also to give multifunctional frameworks. There are two kinds of linker combination known to date; neutral–neutral and neutral–anionic. $\{[Cu(4,4'\text{-bpy})(pyz)(H_2O)_2]\cdot 2\,PF_6\}_n$ is the first example of a coordination polymer containing two different types of neutral ligands.[165] This coordination polymer comprises 2D rectangular grids, which superimpose in an off-set fashion to give smaller rectangular channels. The combination of linear bipyridine ligands (4,4′-bpy, 1,4-bis(4-pyridyl)benzene, 9,10-bis(4-pyridyl)anthracene, and 4,4′-bis(4-pyridyl)biphenyl), selectively affords polymers of the form $\{[Ni(NO_3)_2(L1)(L2)]\cdot guest\}_n$ which have rectangular grids of various dimensions.[96] Coordination polymers with both anionic and neutral organic linkers are far more common because of the ease of charge compensation.[111,158,159,166–181] $[Cu_2(bpm)(ox)Cl_2]_n$ (bpm = 2,2′-bipyrimidine, ox = oxalate) consists of alternate μ-bpm and μ-ox bridged Cu^{II} chains which are further connected through inorganic chloride linkers, thus forming a corrugated 2D framework.[176] The crystal structure of $[Cu_2(bpm)(suc)_{0.5}(ClO_4)_2(OH)(H_2O)_2]_n$ (suc = succinate) consists of a chain of bpm-bridged dinuclear Cu^{II} units linked by a carboxylate group from the succinate anion and a hydroxy group.[166] Coordinated ClO_4^- ions also bridge the adjacent chains. This polymer possesses four different linkers including two inorganic linkers (OH and ClO_4^-).

Coordination polymers with two kinds of connectors (heterometallic polymers) are of great interest owing to their possible applications for the functionalization of micropores and/or microchannels and the construction of molecular-based magnets. Therefore, a new type of donor building block has been developed, which is a hybrid inorganic–organic bridging ligand, the so-called metalloligand.[6,182–201] A metalloligand has several advantages: 1) simple to prepare multifunctional ligands. Multifunctional organic bridging ligands require many intricate synthetic steps while multifunctional metalloligands can be obtained from combination of simple connectors and linkers, 2) modification of coordination ability is possible. Owing to the Lewis acidity and electrostatic effect of metal ions, the coordination properties of the functional groups in the metalloligand can be modified, 3) amphoteric properties. In addition to Lewis basic coordination sites, metalloligands also provide a Lewis acidic site at the metal ion, 4) two functions for the metal ions. Two roles of metal ions can be utilized, one is to link connectors to afford the backbone of a framework. The other is to make a branch in the backbone. This advantage also contributes to the chemical or physical properties of the coordination polymer. Homometallic coordination polymers and also heterometallic ones can be systematically synthesized.

Early reports on metalloligands are of Cu^{II} complexes with oxamate, oxamide, benzoate, and propionate (Figure 13).[182–184,202] $[RuCl_2(pyz)_4]$ has four equatorial pyrazine molecules, the free *exo*-oriented N-donor atoms of which are in square-planar orientation. The complex reacts with Ag^I salts to form 2D and 3D bimetallic networks.[191] Metalloporphyrins are one of the most widely used metalloligands,[6,192,194,203] which can have peripheral substituents capable of metal-binding, such as pyridine,[192] carboxylate,[194] and cyanide.[192] The structural analysis of $\{Cu[Cu(tpyp)]\}_n$ (H_2tpyp = 5,10,15,20-tetra(4-pyridyl)-21*H*,23*H*-prophyrin) shows a PtS-related framework.[192] This framework occupies less than half the volume of the crystal, the remaining space is occupied by highly disordered solvent molecules and anions.

The oxalate-bridged polymeric compounds of general formula, $\{cat[M^{1,II}M^{2,III}(ox)_3]\}_n$ (cat^+ = monovalent cation; $M^{1,II}$: divalent metal ion), are constructed from metalloligands $[M^{2,III}(ox)_3]^{3-}$ (M^2 = Cr,[196] Fe,[198] and Ru[199]). A similar metalloligand $[Cr(dto)_3]^{3-}$ is used to create bimetallic assemblies of $\{NPr_4[MCr(dto)_3]\}_n$ (M = Fe, Co, Ni, Zn).[200]

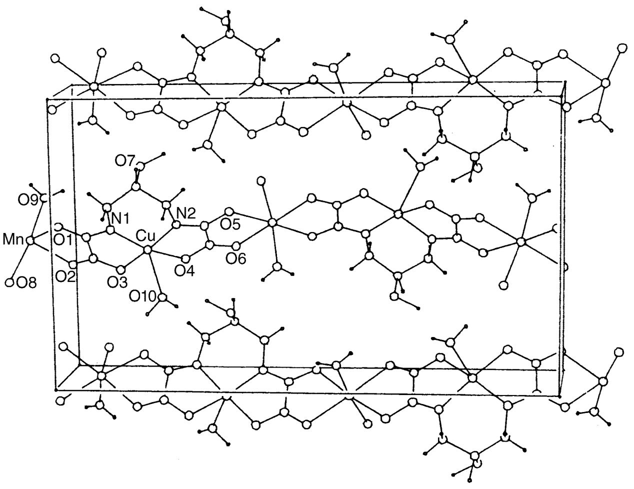

Figure 13. Perspective view of three neighboring chains in $[MnCu(pbaOH)(H_2O)_3]_n$.[202]

The immobilization of coordinatively unsaturated metal centers (UMCs) into porous frameworks is a very attractive idea because a regular arrangement of metal centers in a certain space induces regioselectivity or shape- or size-selectivity towards guest molecules. Moreover, the combination of a catalytic center with porous properties and effective isolation from species toxic to the catalyst leads to efficient tailor-made reaction systems, which approach the peptide architecture of enzymes in biological systems.[204] The immobilization of UMCs in porous hosts has been tried by using zeolites, polymeric matrices, and clays by means of ion-exchange or impregnation. However, by these methods it was not possible to generate sufficiently isolated and uniformly distributed UMCs and the environment around the UMC is not clearly defined. If the UMC can be directly incorporated into the channel walls of microporous coordination polymers, completely isolated and uniformly distributed catalytic centers would be realized. For this purpose, a new synthetic scenario has been developed, that is, "two-step self-assembly". First, a metalloligand is synthesized, which acts not only as a framework linker but also as a UMC (M^1). Second, the metalloligand is added to another metal ion (M^2), which acts as a node in the framework. Consequently, two kinds of metal centers coexist in a framework (Figure 14), and the metal ion in the channel wall presents a large surface to guest molecules. Utilization of the metalloligand, $\{[Cu(2,4\text{-}pydca)_2(H_2O)]\cdot 2Et_3NH\}$ (pydca = 2,4-pyridine dicarboxylate) as a linker provides the porous coordination polymer,

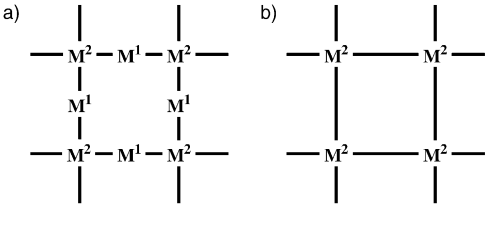

Figure 14. Metal frameworks with a) two kinds of metal units (coordinatively saturated M^2 and unsaturated M^1), and b) coordinatively saturated M^2.

$\{[ZnCu(2,4\text{-}pydca)_2(H_2O)_3(dmf)]\cdot dmf\}_n$, where the Zn^{II} ion at the node of the network acts as a connector and the Cu^{II} ion in the channel wall is available for guest coordination.[189] Other metalloligands, $[M(H_2salphdc)]$ ($M = Co^{II}$ and Cu^{II}), with the Schiff base ligand, $H_4salphdc$, were recently synthesized.[201] Single crystals of $\{[Zn_3Cu_2(OH)_2(salphdc)_2]\cdot 2\,dmf\}_n$, whose topology is identical to that of the Al net in $SrAl_2$, contain large 1D channels approximately 14 × 14 Å^2 (Figure 15). Interestingly, coordinatively unsaturated Cu^{II} ions line up along the *c* axis every 6.1 Å. This kind of framework have been expected but not realized.[407] To our knowledge, this is the first example in which metallo-Schiff base moieties are embedded in the pore wall of 3D porous framework. The X-ray powder diffraction (XRPD) pattern of as-prepared $\{[Zn_3Cu_2(OH)_2(salphdc)_2]\cdot 2\,dmf\}_n$ measured at 298 K is in good agreement with that of the simulated pattern obtained from single-crystal diffraction. The pattern indicates that the porous structure is maintained until 573 K. Instead of the Cu^{II} ion, the Co^{II} ion can be introduced as a UMC. $[Zn_3Co_2(OH)_2(salphdc)_2]$ was synthesized by a similar procedure to $\{[Zn_3Cu_2(OH)_2(salphdc)_2]\cdot 2\,dmf\}_n$. The X-ray diffraction pattern is in good agreement with that of $\{[Zn_3Cu_2(OH)_2(salphdc)_2]\cdot 2\,dmf\}_n$, which indicates that the same 3D framework with coordinatively unsaturated Co^{II} ions was formed. Various metal complexes with Schiff base ligands show unique catalytic activities,[205–207] suggesting an interesting possibility for design of pore walls for catalytic porous compounds.

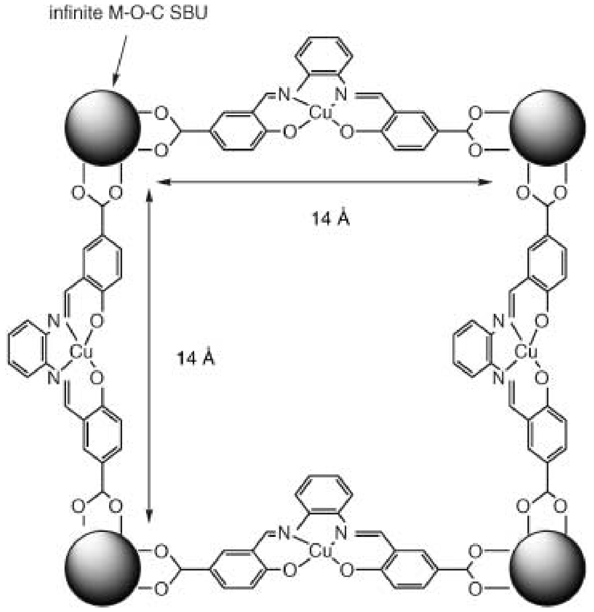

Figure 15. Structure of $\{[Zn_3Cu_2(OH)_2(salphdc)_2]\cdot 2\,dmf\}_n$; view along the *c* axis.

2.3. Nanospace Engineering

Inorganic porous compounds, such as zeolites or activated carbons with high stability of their frameworks are widely used, for example, in separation, catalysis, exchange, nonlinear optics, electro devices, ship in bottle synthesis. Zeolites have high crystallinity with regular channels or cavities but a low porosity (and in some cases high surface areas).[208–214] On the other hand, activated carbons have high porosity with a broad pore size distribution, so that many of the channels or cavities are often superfluous and unnecessary for the required porous functions, which leads to poor storage/separation capacity for a specific guest. In addition, the control and fine-tuning of the frameworks for both classes of porous compounds are not easy by current synthetic methods. Recently, organic porous compounds linked by hydrogen bonds have been reported.[215–221] Many of them show unique catalytic properties, but their frameworks are liable to collapse or deform after removal of guest molecules from the micropores. Coordination polymers are mainly constructed from coordination bonds with the aid of other interactions, such as hydrogen and metal–metal bonds, π–π, CH–π, electrostatic, and van der Waals interactions, and, therefore, networks that are both robust and flexible can be made. The bridging organic ligands used as building blocks can be modified easily enabling the preparation of tailored structures. The transition-metal ions required for catalytic sites can be readily introduced into the pore walls.[30,31,222–225] Moreover, the pore walls are principally constructed from organic molecules, producing a “light material”. Thus, the field of porous coordination polymer chemistry has shown quite spectacular advances in the last decade.

The following points should be taken into consideration when creating porous coordination polymers: 1) it is impossible to synthesize compounds containing vacant space because nature dislikes vacuums. In other words the pores will always be filled with some sort of guest or template molecules. Therefore, it is very important to select appropriate, size-fitting guest molecules, which are volatile or exchangeable, 2) large linkers, which extend the distance between nodes (connectors) of a framework, are often used for the preparation of large micropores, however, with such linkers interpenetration frequently occurs. Regulation of interpenetration (Section 2.2.) is an important challenge in crystal engineering, 3) an alternative strategy is to design a framework, in which the spaces occur topologically. For example, the diamond net and the B net in CaB_6 are frequently used in the construction of highly porous coordination polymers.

Based on spatial dimensions there are four types of porous structures, as illustrated in Figure 16. 0D cavities (dots) are completely surrounded by wall molecules. In these cavities, a certain guest can be isolated or dispersed in the solid. Channels (1D), layers (2D), and intersecting channels (3D), are frequently utilized to accommodate or exchange guests.

Following a suggestion in 1998, porous coordination compounds were classified in the three categories, 1st, 2nd, and 3rd generation (Figure 17).[11] The 1st generation compounds have microporous frameworks, which are sustained only with guest molecules and show irreversible framework collapse on removal of guest molecules. The 2nd generation compounds have stable and robust porous frameworks, which show permanent porosity without any guest molecules in the

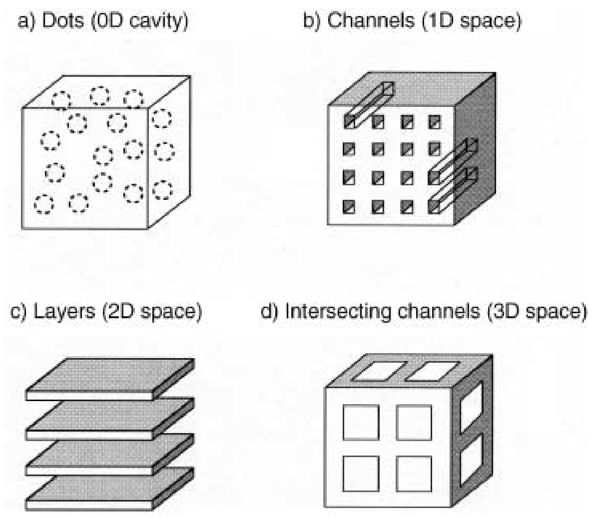

Figure 16. Classes of porous structures based on spatial dimensions.

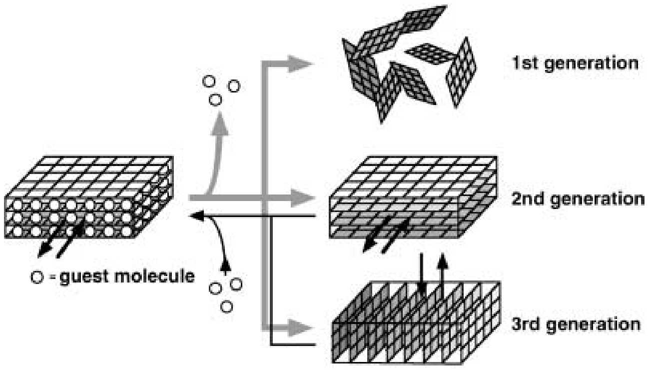

Figure 17. Classification of porous compounds as 1st, 2nd, and 3rd generation.

pores. The 3rd generation compounds have flexible and dynamic frameworks, which respond to external stimuli, such as light, electric field, guest molecules, and change their channels or pores reversibly. Many inorganic porous materials constructed by covalent bonds are classified as the 2nd generation compounds. On the other hand, porous coordination polymers could afford not only robust "2nd generation compounds" but also flexible and dynamic "3rd generation ones".

3. Porous Structures

3.1. Dots (0D Cavities)

Nanosized pores, which are isolated from the others and scattered in the solid, occur in several coordination-polymer solids and are divided into two categories: solid without windows and solids with windows but these windows are very small compared to the guest molecules. In any case, guest molecules are unable to pass out of these cavities. An interpenetrated 3D network of $\{[Zn(CN)(NO_3)(tpt)_{2/3}]\cdot 3/4\,C_2H_2Cl_4\cdot 3/4\,CH_3OH\}_n$ provides a barrier impenetrable to even the smallest molecules (with the possible exception of H_2), effectively isolating each cavity from its neighbors and from the outside world (Figure 18).[226] The cavities, sealed-off in this manner, are exceptionally spacious, the distance across the inner shell from one Zn_4 square to the opposite and parallel Zn_4 square is the unit cell length, 23.448(4) Å. The cavity is large enough to accommodate approximately nine 1,1,2,2-tetrachloroethane molecules, together with nine molecules of methanol, all of which are highly disordered and essentially a liquid. In the 3D oxalate network structures $\{[M^{II}(2,2'\text{-bpy})_3][M^{I}M^{III}(ox)_3]\}_n$ the negatively charged oxalate backbone provides perfect cavities for tris(bipyridyl) complex cations. The size of the cavity can be adjusted by variation of the metal ions of the oxalate backbone.[227,228]

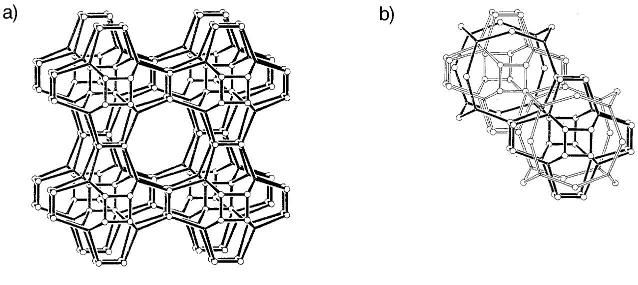

Figure 18. a) Part of one individual infinite 3D network and b) two independent, equivalent, and interpenetrating frameworks (distinguished by "full" and "open" lines) of $\{[Zn(CN)(NO_3)(tpt)_{2/3}]\cdot 3/4\,C_2H_2Cl_4\cdot 3/4\,CH_3OH\}_n$. Tpt units are represented by three spokes radiating from a point at the center of the triazine ligands. ZnCNZn units are represented by direct Zn–Zn links.[226]

3.2. Channels (1D Space)

A large number of coordination polymers with regular 1D channels have been synthesized and crystallographically characterized. There are several sizes and shapes of 1D channel. For example, $\{[Ni(NO_3)_2(4,4'\text{-bis(4-pyridyl)biphenyl})_2]\cdot 4(o\text{-xylene})\}_n$ has big 2D square-grid networks (19.9 × 20 Å^2), each of which stacks to create large rectangular channels (ca. 10 × 20 Å^2).[229] $\{[Zn(in)_2]\cdot 2H_2O\}_n$ (in = isonicotinate) has a 3D, twofold interpenetrated network characteristic of a 6^48^2-b net, similar to that of α-quartz, and forms pseudohexagonal channels with diameters of about 8.6 Å.[230] $\{[Ni(acac)_2(L)]\cdot 3\,MeCN\cdot 6\,H_2O\}_n$ (L = 2,2′-diethoxy-1,1′-binaphthalene-6,6′-bis(4-vinylpyridine); acac = acetylacetonate) has two sizes of chiral 1D channels, 17 × 17 Å^2 and 7 × 11 Å^2.[231]

On the macroscopic scale, pillared layer structures are frequently been found in ancient buildings, such as the Parthenon in Athens. Even on the microscopic scale, the pillared layer motif is very useful for the construction of various porous frameworks because simple modification of a pillar module can control the porous structures and properties.[12] The Cu^{II} coordination polymer, $[Cu_2(pzdc)_2(pyz)]_n$ (CPL-1; coordination polymer 1 with pillared layer structure), has a pillared layer structure, and is a suitable system for the design of porous structures and properties.[158]

The Cu^{II} center in CPL-1 has a distorted square-pyramidal coordination environment formed by three carboxylate oxygen atoms, one nitrogen atom of pzdc, and one nitrogen atom of pyz (Figure 19a). 2D sheets constructed from Cu^{II} and pzdc units, which have no voids large enough for molecules to pass through, are linked by pyz ligands affording a 3D porous pillared layer structure (Figure 19b). There are 1D channels with dimensions of approximately 4×6 Å^2 which run along the a axis between the 2D sheets, and in which one water molecule is included per Cu^{II} ion.

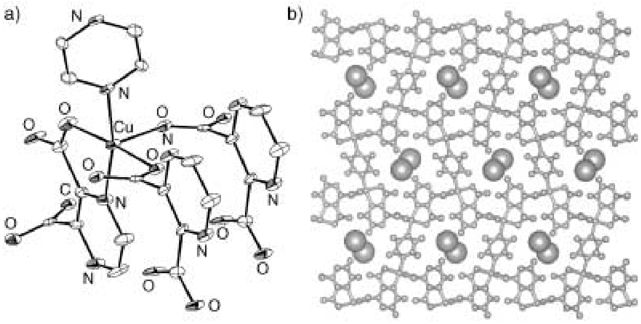

Figure 19. a) Coordination environment of the Cu^{II} ion and b) 3D structure along the a axis of CPL-1. Guest H_2O molecules, which are represented by space filling model, are accommodated in each channel.[158]

The channel dimensions and surface properties of this pillared layer coordination network can be controlled by modification of the pillar ligands. For this purpose, various pillar ligands, which have a variety of lengths and functionalities (Figure 20), were employed to give a series of compounds, $\{[Cu_2(pzdc)_2L]\cdot n\,H_2O\}_n$ (L = pyz (CPL-1, $n=1$),[158] bpy (CPL-2, $n=4$),[158] pyre (CPL-3, $n=4$),[159] azpy (CPL-4, $n=5$),[159] dpe (CPL-5, $n=4$),[159] and pia (CPL-6, $n=5$)[158]). For such a series of complexes which have a similar basic framework, Rietveld analyses of the X-ray powder diffraction patterns are useful for structure determination. Modification of the pillar ligands enables us to realize systematic control not only of the pore size (approximately 8×6, 8×3, 10×6, and 10×6 Å^2 for CPL-2, 3, 4 and 5, respectively) but also of the surface functionality.

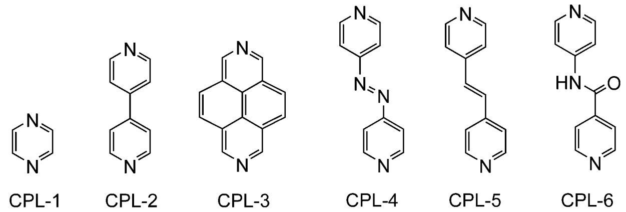

Figure 20. Linker ligands used as pillars in $\{[Cu_2(pzdc)_2L]\cdot n\,H_2O\}_n$.

3.3. Layers (2D Space)

While there are dozens of 2D coordination polymers, few have been reported in which several guests can be incorporated between the layers. The 1D motif of $\{Cu(ca)(ROH)_2\}$ contains hydrogen-bonding sites, ca-O (hydrogen-bond acceptor) and ROH (hydrogen-bond donor).[111] $[Cu(ca)(H_2O)_2]$ has a layer structure and the distance between the copper atoms in the different sheets is 8.45 Å. In fact, the compound obtained, $[Cu(ca)(H_2O)_2]$, is thermodynamically unstable without intercalated molecules, which tightly link the layers[232] through hydrogen-bonding interactions (Figure 21). In $\{[Cu(ca)(H_2O)_2]\cdot phz\}_n$ (phz = phenazine) the phz molecules intercalate and stack in columns that are separated by 3.18 Å (nearest neighbor C···C distance).[232] The interlayer distance (nearest neighbor Cu···Cu distance) is 9.25 Å. Molecules of 2,5-dimethylpyrazine (dmpyz) also form columnar stacks between the sheets. Interestingly, there are two types of phases (α and β) in the compound, $\{[Cu(ca)(H_2O)_2]\cdot dmpyz\}_n$. In the α- and β-phases, the stacking mode of dmpyz is similar, whereas the coordination mode of dmpyz is different and the two phases have different colors. This result also indicates that the layer spacing is flexible, a characteristic of coordination polymer frameworks. The spacing between the layers in $\{[Cu(ca)(H_2O)_2]_n\}_m$, ranges from 8.45 to 11.0 Å. The intercalation is governed by several factors: The inter-

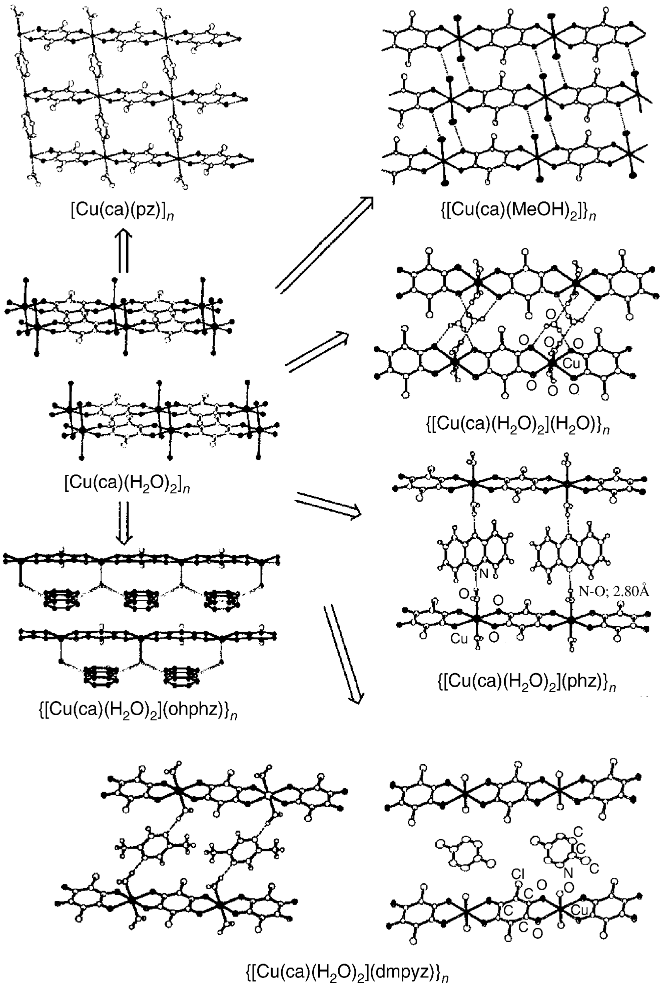

Figure 21. Intercalation of various guests between the layers in the coordination polymer $[Cu(ca)(H_2O)_2]_n$.[232]

calated molecules has 1) a π-electron structure with which to form a stacked column, and 2) hydrogen-bonding sites in opposing directions for linking the layers. When condition (1) is not fulfilled, for example, with 1,2,3,4,6,7,8,9-octahydrophenazine (ohphz), which has a nonplanar structure, no intercalated stacked ohphz columns are formed. The ohphz still has hydrogen-bonding capability and can bind to the water molecules in the same chain (Figure 21).

The intercalation compounds $\{[M(ca)(H_2O)_2]\cdot L\}_n$ (M = Fe^{II}, Co^{II}, and Mn^{II}, L = H_2O and phz) have also been synthesized and characterized.[233,234] For $\{[M(ca)(H_2O)_2]\cdot H_2O\}_n$, the crystal structures consists of uncoordinated guest water molecules and 1D zigzag $[M(ca)(H_2O)_2]_n$ chains. The adjacent chains are interlinked by hydrogen bonds, thus forming layers. The water molecules are intercalated between the $\{[M(ca)(H_2O)_2]_n\}_m$ layers. The intercalation mode of the water molecules is different from that in the compounds $\{[M(ca)(H_2O)_2]\cdot phz\}_n$ (M = Fe^{II}, Co^{II}, and Mn^{II}), which are isomorphous to $\{[Cu(ca)(H_2O)_2]\cdot phz\}_n$.

The molecular assemblies obtained here reveal three key factors that control the crystal structures: 1) hydrogen bonds support a 2D sheet, $\{[M(ca)(H_2O)_2]_n\}_m$, which is flexible and amenable to intercalation of various kinds of molecules, 2) the intercalated guest molecules affect the sheet structure and dynamics of $\{[M(ca)(H_2O)_2]_n\}_m$, and 3) the choice of a metal ion mediates the fine-tuning of the sheet structures and the orientation of the guest molecules.

Another instructive example of this class of materials is the 2D bimetallic phases $\{(\text{cation})[M^{II}M^{III}(ox)_3]\}_n$ (M^{II} = Mn, Fe, Co, Cu, Zn; M^{III} = Cr, Fe) first reported by Okawa et al.,[195,235] which behave as ferro-,[196] ferri-,[199,236,237] or canted antiferromagnets[238,239] with critical temperatures ranging from 5 to 44 K. Their structures[197,240] consist of an extended anionic network formed by oxalate-bridged hexagonal layers of the two metal atoms. These layers are separated by an organic counterion of the type $[XR_4]^+$ (X = N, P; R = Ph, *n*Pr, *n*Bu), which may act as a template controlling the formation of the net structure and thus determining the interlayer separation, as well as its packing.[197] It is possible to replace this electronically "innocent" cation by an electroactive one, to confer new properties, such as electrical conductivity, thermal spin transition, and nonlinear optical activity, on the magnetic material. The first successful attempt to combine an organic donor with a polymeric bimetallic oxalato complex afforded the semiconducting hybrid salt $[\text{bedt-ttf}]_2[CuCr(ox)_3]$ (bedt-ttf = bis(ethylenedithio)tetrathiafulvalene).[241] The hybrid was obtained by electrocrystallization as a microcrystalline powder. It is worth noting that not only the electrical properties of the bimetallic magnetic units but also the nonlinear optical properties of the organic dyes in between the layers can be realized.[242,243] Pure, magnetic multilayered materials with organometallic decamethylmetallocenium cations as counterions $[Z^{III}(Cp^*)_2]$ (Z^{III} = Fe, Co; Cp* = C_5Me_5) show spontaneous magnetization below T_c (Figure 22).[244,245] Crystalline $[\text{bedt-ttf}]_3[MnCr(ox)_3]$ displays ferromagnetism and metallic conductivity.[246]

$[Cd(1,5\text{-nds})(H_2O)_2]_n$ is a layered metal sulfonate coordination polymer.[247] It can selectively and reversibly intercalate ammonia and amines quantitatively without dehydration and form stable adducts, by a solid–vapor reaction at room temperature. Amines are intercalated with the aid of different interactions. Two equivalents of amine molecules are intercalated with the formation of coordination bonds by replacing the coordinated H_2O molecules, while a further equivalent of amine is anchored by weak intermolecular interactions. Guest-driven solid-to-solid phase transformations are also observed.

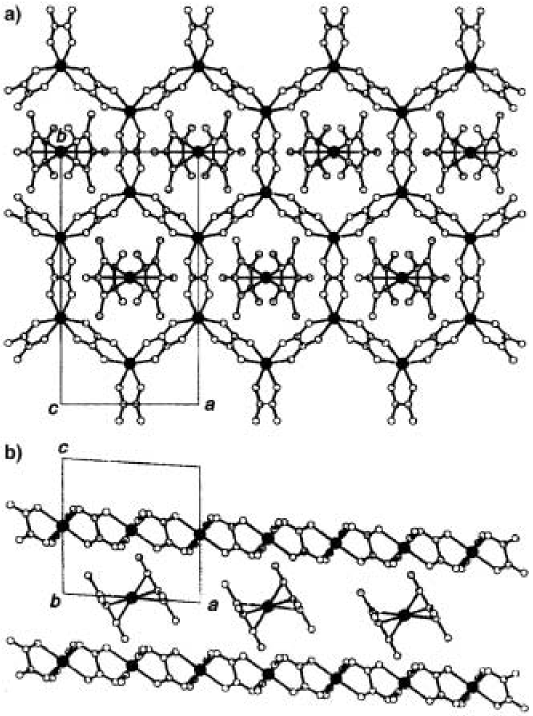

Figure 22. View of the structure of $\{[FeCp^*_2][MnFe(ox)_3]\}_n$ a) in the *ab* plane showing the honeycomb magnetic layers, b) in the *ac* plane.[244,245]

$[Ag(CF_3SO_3)]_n$ forms a layer host structure, in which alcohol guests are intercalated with the aid of coordination bonds between Ag^I and the alcohol to give $[Ag(CF_3SO_3)(L)_{0.5}]_n$ (L = alcohols). Interestingly, a wide range of guests can be exchanged, that is, straight primary alcohols containing an even number of carbon atoms ranging from ethanol (C_2H_5OH) to eicosanol ($C_{20}H_{41}OH$).[248]

3.4. Intersecting Channels (3D Space)

3D intersecting channels, which frequently occur in zeolites, are constructed by the interconnection of 1D channels from various directions. Coordination polymers with such 3D channels are rare owing to the framework instability associated with high porosity. $\{[Ni_6(1,3,5\text{-btc})_4(4,4'\text{-bpy})_6(MeOH)_3(H_2O)_9]\cdot\text{guest}\}_n$ has a 3D porous framework constructed from 2D $Ni_3(1,3,5\text{-btc})_2$ layers and pillared by 4,4'-bpy ligands, which gives hexagonal-shaped channels (12.3 and 11.0 Å in diameter) running parallel to the stacking direction.[249] In addition, there are three 1D channels (8 × 4.4 Å^2) between the layers, forming and overall 3D framework of intersecting channels. In $\{[Zn_4O(1,4\text{-}bdc)_3]\cdot 8\,dmf\cdot C_6H_5Cl\}_n$) (IRMOF-1; IRMOF = isoreticular metal–organic framework), octahedral Zn-O-C clusters are linked by benzene supports to afford a primitive cubic structure (the B net in CaB_6) and an exceptionally rigid and highly porous structure with 3D intersecting channels. The simple and facile synthetic method indicates that the use of other dicarboxylate linkers under similar conditions would yield the same type of frameworks with diverse pore sizes and functionalities. Indeed, using linkers other than 1,4-bdc yielded IRMOF-2 through to IRMOF-16 (Figure 23). In IRMOF-2 through IRMOF-7, 1,4-bdc linkers with bromo, amino, *n*-propoxy, *n*-pentoxy, cyclobutyl, and fused benzene functional groups were introduced into the desired structure in which their substituent groups point into the voids. Some of the IRMOFs have mesopores (> 20 Å) as well as the lowest crystal density of any material reported to date.

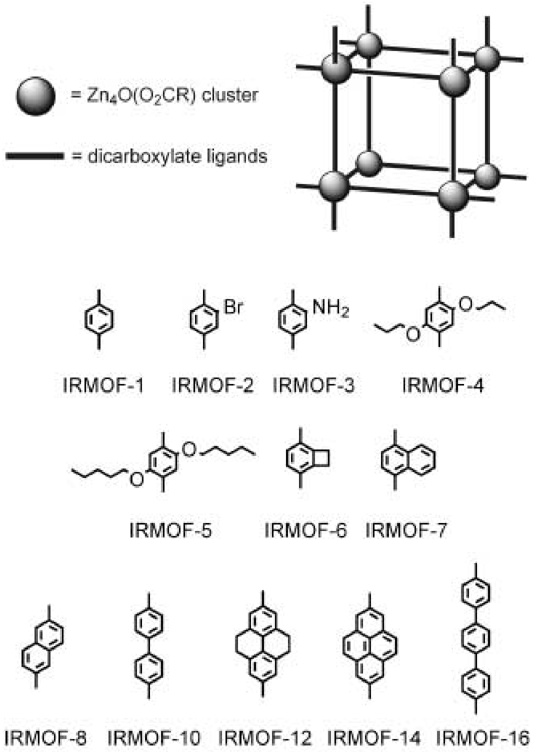

Figure 23. Dicarboxylate linkers used in the preparation of IRMOF materials.

4. Functions of Coordination Polymers

4.1. Overview of Microporous Properties

Porous properties have attracted the attention of chemists, physicists, and material scientists because of not only industrial applications, such as separation, heterogeneous catalysis, and gas storage but also because of scientific interest in the formation of molecular assemblies, such as clusters and 1D arrays, and in the anomalous physical properties of confined molecules can be studied. The adsorption of guest molecules onto the solid surface plays an essential role in determining the properties of porous compounds. This adsorption is governed not only by the interaction between guest molecules and the surfaces but also by the pore size and shape. Pores are classified according to their size as shown in Table 1.[250] There is no essential difference between adsorption by a macropore and adsorption onto a single surface, and both are explained well by the Brunauer–Emmett–Teller (BET) equation.[251] The adsorption by a mesopore is dominated by capillary condensation, which is responsible for a sharp adsorption rise around the mid relative-pressure region. This effect is not attributable to molecule–solid interactions but to a purely geometrical requirement, which is illustrated well by the Kelvin equation. The adsorption in the micropore should not be considered as that of molecules onto a solid surface but as the filling of molecules into a nanospace where a deep potential field is generated by the overlapping of all the wall potentials. In this case, the adsorption isotherm shows a steep rise at very low relative pressure and a plateau after saturation. There are six representative adsorption isotherms that reflect the relationship between porous structure and sorption type.[252,253] This IUPAC classification of adsorption isotherms is shown in Figure 24. These adsorption isotherms are characteristics of adsorbents that are microporous (type I), nonporous and macroporous (types II, III, and VI), and mesoporous (types IV and V). The differences between types II and III and between types IV and V arise from the relative strength of fluid–solid and fluid–fluid attractive interactions. When the fluid–solid attractive interaction is stronger than that of fluid–fluid, the adsorption isotherm should be of types II and IV,

Table 1: Classification of pores.

Pore type	Pore size [Å]
Ultramicropore	< 5
Micropore	5–20
Mesopore	20–500
Macropore	> 500

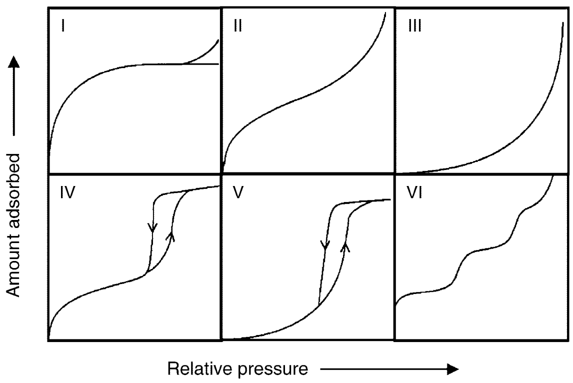

Figure 24. IUPAC classification of adsorption isotherms.

and opposite situation leads to types III and V. The type VI isotherm represents adsorption on nonporous or macroporous solid surfaces where stepwise multiplayer adsorption occurs. Many articles have been published on the adsorption processes in zeolites and activated carbons.[31,33,254–262]

Porous coordination polymers have a variety of coordination architectures with uniform and/or dynamic pore structures. In the conventional porous materials, such as activated carbons and inorganic zeolites, pore shapes are often slit-like or cylindrical, respectively. On the other hand, the pore shapes of coordination polymers are not necessarily modeled by slit-like and cylindrical pores because they have crystallographically well-defined shapes, such as squares, rectangles, and triangles. Unprecedented adsorption profiles have been found in porous coordination polymers, which are characteristic of the uniform microporous nature. For example, a square pore possesses four corner sites where a deeper attractive potential for guests is formed by the two pore walls than at the midpoint of the wall (Figure 25).[263] In this case, two-step adsorption is expected in the low relative-pressure region corresponding to the presence of the two different sites. $[Cu(bpdc)(dabco)_{0.5}]_n$ (dabco = 1,4-diazabicyclo[2.2.2]octane), with the B net of CaB_6, has a uniform square cross-sectional 1D channel with dimensions of 10.5×10.5 Å^2.[264–266] The Ar adsorption isotherm measured at 87.3 K shows two steps at relative pressure around 10^{-2} which correspond to pore sizes of about 9.5 and 12 Å, respectively (Figure 26).[267]

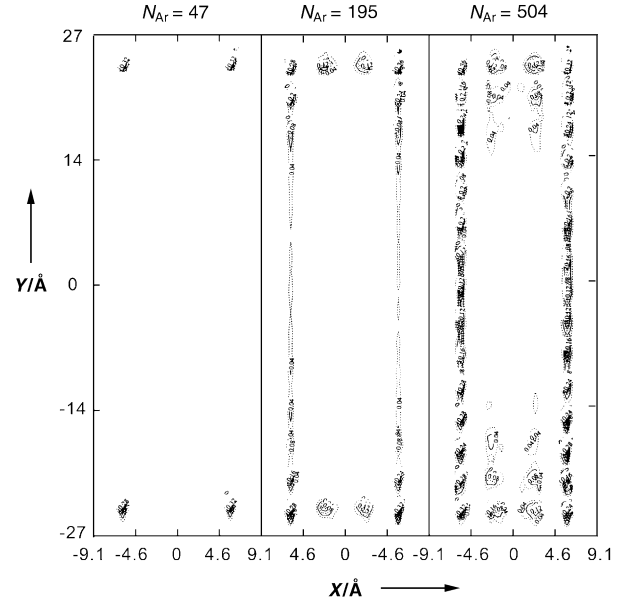

Figure 25. Contours of constant local density of adsorbed Ar molecules for several values of the pore loading (Monte Carlo computer simulations for the pore size $18.2 \times 54.6 \times$ Å^3). N_{Ar} is the number of argon molecules adsorbed. These local densities have been averaged along the direction of the pore axis and thus show where adsorption is occurring in a cross-sectional view down the pore axis.[263]

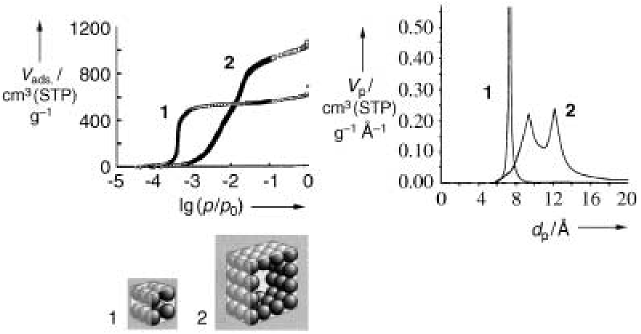

Figure 26. Ar adsorption isotherms at 87.3 K (left) and pore size distributions (right) for coordination polymers $[Cu(1,4\text{-}bdc)(dabco)_{0.5}]_n$ (**1**) and $[Cu(bpdc)(dabco)_{0.5}]_n$ (**2**). Schematic views show the Ar filling of the micropore.[264] $V_{ads.}$ = adsorbed volume, V_p = pore volume, D_p = pore diameter, STP = standard temperature and pressure.

The six types of adsorption isotherms assume that the porous host structures are not altered through the sorption process. If the porous hosts have a flexible and dynamic nature, for example, when a structure transformation from nonporous to microporous occurs during the adsorption, the adsorption isotherm has a novel profile, dissimilar to the conventional type (Figure 24). In this case, the adsorption isotherm could be a combination of types I and II or III. In Figure 27, the adsorption isotherm follows the type II isotherm at low concentration (pressure), that of a nonporous phase. After a certain point A, the isotherm begins to approach type I with a sudden rise. At point B the structural transformation from nonporous to porous is complete. If many structural transformations occur, a multistep adsorption profile would be observed. This phenomenon is one of the advantages of coordination polymers with flexible and dynamic frameworks based on weak interactions, such as coordination bonds, hydrogen bonds, π–π stacking interactions, and van der Waals forces. Structural flexibility accompanied with a certain structural transformation can even occur in inorganic porous materials. Several examples of flexible inorganic networks are known.[211,268–272] The structural change in inorganic networks, however, is not so drastic

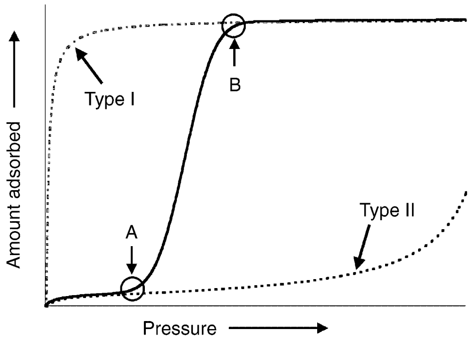

Figure 27. Adsorption isotherms observed when porous frameworks undergo a structure transformation from nonporous to porous. Dashed lines represent the Type I (micropore filling) and Type II (surface adsorption) isotherms. Points A and B indicate the gate-opening and gate-closing pressures which accompany the start and end of the structure transformation, respectively.

as that of coordination polymers because of their robust frameworks characteristic of strong bonds, such as Si/Al–O bonds. A framework in which the pore size could be changed by temperature was found in a zeolite containing octahedral and tetrahedral motifs.[273] However, on guest adsorption the framework is not flexible but robust.

The structural stability is an important factor in the study of the microporous functions of coordination polymers. There are two types of the stability: 1) whether or not a framework is maintained on the removal of the guest molecules from the pores, 2) thermal stability, a stable framework at high temperature tends to require strong bonding between building blocks but in certain cases the stability depends on the mode of framework. X-ray powder diffraction (XRPD) and thermogravimetric (TG) measurements are commonly used to investigate the structural stability. TG data provides information about the temperatures T_1 and T_2, at which guest removal and framework decomposition occur, respectively, but no information on framework stability. The XRPD pattern of a desolvated porous framework, which is obtained by heating above T_1 but below T_2, affords direct information of the framework stability: structural analysis indicates robustness/flexibility of a framework or preservation of the crystalline phase or formation of an amorphous one. Recently, direct detection of vacant channels by single-crystal X-ray diffraction after the removal of guest molecules was reported.[229,274] According to these analyses, porous coordination polymers are thermally less stable than inorganic materials owing to the presence of the weaker coordination bonds. Typical T_2 values for this kind of frameworks is below 473 K though some coordination polymers do have a high thermal stability where T_2 is above 573 K (for example, materials with strong M–O bonds).[131]

The specific surface area is one of the most important factors for evaluating the pore capacity, and is associated with the number of guest molecules accommodated by direct contact. Table 2 shows values of the surface area and pore volume of representative stable porous coordination polymers as determined by gas-adsorption studys.[47,130,158,265,275–278] Recently, the specific surface areas attainable with coordination polymers have increased from 500 m^2 g^{-1}, comparable to that of zeolites, to a very large value, 4500 m^2 g^{-1}. This value is much higher than the ideal value of carbon materials, 2630 m^2 g^{-1}, which is calculated as the sum of two surfaces of graphite planes. In practice, the thinner the walls of the pores are, the higher the specific surface area is. In the case of inorganic zeolites, the pore walls are constructed with a thickness of at least several Si, O, and Al atoms, whereas coordination polymers afford thin walls, for instance, only one carbon atom thick when the wall is of 4,4′-bpy, which shows that almost all the atoms constructing porous frameworks can be used as a surface. In addition to the high porosity, one of the most interesting porous properties is the regularity of the pore distribution in the solid. Regular pore distribution can be readily realized for coordination polymers as well as inorganic porous materials. Molecules confined in restricted space can show group properties and form molecular assemblies that are not realized in the bulk state. Utilization of this nanosized space found in precisely designed uniform pores has just begun (see Section 5).

Based on the accumulated crystallographic and adsorption data of porous coordination polymers, Monte Carlo (MC) simulations of small-molecule adsorption have been performed, an approach that is common in carbon and inorganic materials chemistry.[279–281] For the simulation, the porous coordination polymers have an advantage, their well-characterized regular structure precludes the need to make assumptions about the host structures. The MC simulations were carried out using formal HF-based and B3LYP-based charge densities for the frameworks $[Zn(1,4\text{-bdc})]_n$ and $[Cu_3(1,3,5\text{-btc})_2]_n$.[282] The isosteric heats of adsorption for N_2, Ar, and H_2, are small and lie in the range of values for physisorption (< 10 kcal mol^{-1}). In the case of the $[Cu_3(1,3,5\text{-btc})_2]_n$ framework, the adsorbed Ar tends to distribute in a four-leaf-clover-like shape. The effect of axially coordinated water molecules influences the adsorption; the amount of adsorbed Ar at low pressure in the presence of coordinated water is higher than that of water-free $[Cu_3(1,3,5\text{-btc})_2]_n$, while the value for water coordinated $[Cu_3(1,3,5\text{-btc})_2]_n$ is smaller than that for water-free $[Cu_3(1,3,5\text{-btc})_2]_n$ (Figure 28). The

Table 2: Values of the surface area (*a*) and pore size (d_p) and pore volume (*V*) of stable porous coordination polymers.

Formula	d_p [Å]	a [m^2 g^{-1}]	V (micropore) [mL g^{-1}]
$[Co_2(NO_3)_4(4,4'\text{-bpy})_3]_n$	3×6	–	0.15
$[Cu_2(pzdc)_2(4,4'\text{-bpy})]_n$	9×6	846	0.22
$[Cu_2(pzdc)_2(pia)]_n$	11×6	1013	0.27
$[Cu(SiF_6)(4,4'\text{-bpy})_2]_n$	8.0	1337	0.56
$[Cu_2(1,3,5\text{-btc})_3]_n$	9.0	692	0.33
$[Cu(1,4\text{-bdc})]_n$	6.0	545	0.22
$[Cu(1,4\text{-bdc})(dabco)_{1/2}]_n$	7.4	1947 (3894[a])	0.71
$[Cu(L1)(dabco)_{1/2}]_n$[b]	9.5	3013 (4520[a])	1.08
$[Cu(bpdc)(dabco)_{1/2}]_n$	10.8	3265	1.27
$[Zn_4O(1,4\text{-bdc})_3]_n$	11.2	2900[c]	1.04
$[Zn_4O(L2)_3]_n$[d]	9.3	2630[c]	0.60
$[Zn_4O(bpdc)_3]_n$	15.4	1936[c]	0.69

[a] The surface areas were determined by BET plots using 2 a_m at corner sites (a_m is the cross section of a probe molecule). [b] L1 = *trans*-$^-$OOC-Ph-CH=CH-COO$^-$. [c] The surface areas were determined by Langmuir plots. [d] L2 is shown in Figure 23 as the ligand of IRMOF-6.

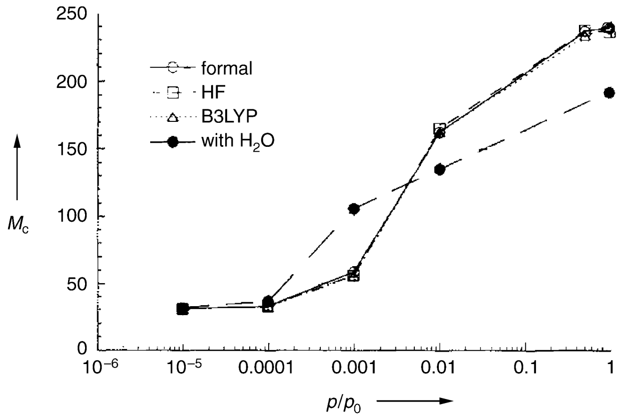

Figure 28. Calculated isotherms of adsorbed Ar in $[Cu_3(1,3,5\text{-btc})_2]$. Three models for the charge densities on each atom of the framework are used: formal charge, HF/4-31G, and B3LYP4-31G. M_c = molecules per cell.[282]

coordinating water enhances adsorption but also narrows the cavity available for Ar.

4.2. Robust Frameworks with Nanospace

4.2.1. Gas Storage

The ability to store a desired compound is a typical property of porous materials. Table 3 lists porous coordination polymers classified based on functions, properties as hosts for guests or reactants, and generation category according to the structural flexibility and stability (see Figure 17).

The adsorption of gases at ambient temperature is important for applications, such as storage and transport. A useful strategy for the creation of suitable adsorbents is to prepare stable frameworks without guest molecules (2nd generation compounds; Figure 17). The first report on the gas-adsorption properties of those compounds at ambient temperature appeared in 1997. The framework reported is best described as tongue-and-groove (bilayer) structure, $\{[M_2(4,4'\text{-bpy})_3(NO_3)_4]\cdot x\,H_2O\}_n$ (M = Co, $x = 4$; Ni, $x = 4$; Zn, $x = 2$), formed from $M(NO_3)_2$ and 4,4′-bpy units (Figure 29a).[47] The effective micropore cross section for the dried sample is about 3×6 Å^2 (based on van der Waals radii; Figure 29b). This host reversibly adsorbs CH_4, N_2, and O_2 in the pressure range of 0–36 atm without collapse of the crystal framework (Figure 29c). Similar coordination polymers capable of the gas adsorption have since been synthesized.[126,130,131,145,264–266,276–278,285,306,308,311,314,323,329] The adsorption of N_2 or Ar gas at low temperature is generally used for the evaluation of micropores. The N_2 adsorption isotherms measured at 77 K on CPL-1, CPL-2, and CPL-5 are given in Figure 30.[277] All CPL samples show typical isotherms of type I, which confirms the presence of micropores and the absence of mesopores. The almost vertical rise of the N_2 adsorption isotherms at low relative pressures indicates that the size of micropores is extremely uniform, characteristic of coordination polymers. From the α_s-analysis and the Dubinin–Radushkevich (DR) equation, several micropore parameters, such as micropore volume, surface area, and isosteric heat of adsorption are obtained. The pore size distribution of $[Cu(SiF_6)(4,4'\text{-bpy})_2]_n$, which has a 3D porous network constructed from 2D grid layers of $[Cu(4,4'\text{-bpy})_2]_n$ and columns of AF_6 anions (Figure 31a), were calculated from Ar adsorption at 87.3 K according to the Horvath–Kawazoe (HK) method.[126,130] The differential pore volume plot, shows a single sharp peak around 8 Å (Figure 31b). This compound has quite a uniform square pore (8×8 Å^2) as shown in Figure 31a. The result is in good agreement with the crystallographic structure.

Methane is the main component of natural gas, which is an important candidate for clean transportation fuels. The storage of methane by adsorbents has been pursued vigorously as an alternative to compressed gas storage at high pressure. However, none of the conventional adsorbents have afforded sufficient CH_4 storage to meet the conditions required for commercial viability. Even in activated carbons with large specific surface area and micropores, a high percentage of the mesopores and macropores are not effective for CH_4 adsorption because the single surface can not trap CH_4 molecules and therefore the large voids are useless. To achieve higher adsorption capacity, it is necessary to ensure that micropores with sizes well suited to methane molecules are densely and uniformly distributed in the solid. Porous coordination polymers are therefore good candidates as adsorbents for CH_4 storage.

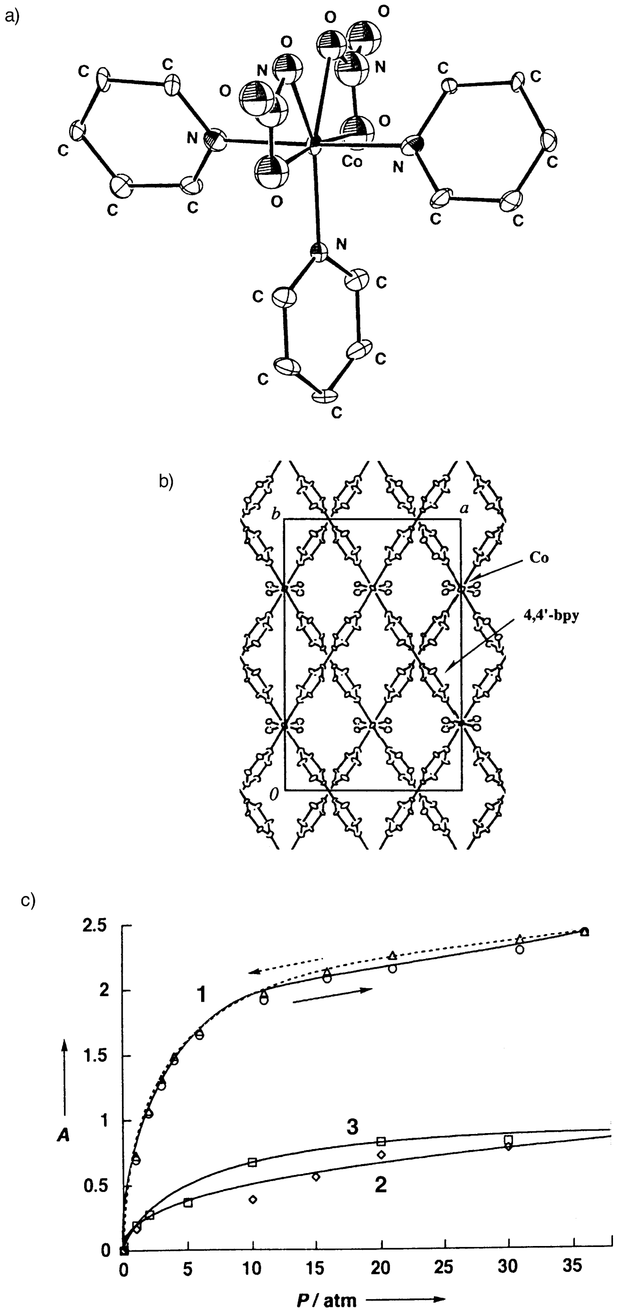

Figure 29. a) ORTEP drawing of the Co^{II} center in $\{[Co_2(4,4'\text{-bpy})_3(NO_3)_4]\cdot 4\,H_2O\}_n$, b) view of the infinite framework along the *c* axis, c) isotherms of the adsorption of CH_4 (open circle (adsorption); open triangle (desorption)), N_2 (open rhombus), and O_2 (open square) by $[Co_2(NO_3)_4(4,4'\text{-bpy})_3]_n$ at 298 K in the range 1–36 atm; A = absolute adsorption in mmol of adsorbed gas per gram of anhydrous sample.[47]

Table 3: Selected functional microporous coordination polymers.[a]

Compound	Function[b]	Guests or reactants	Generation type[c]	References
$[\mathrm{Ti_2Cl_2}(i\mathrm{PrO})_2\mathrm{L1}]_n$ and $[\mathrm{Zr_2}(t\mathrm{BuO})_4\mathrm{L1}]_n$				[283, 284]
	AD	N_2, hexane, benzene, ethyl acetate		
$\{[\mathrm{V(OH)(1,4\text{-}bdc)}]\cdot 0.75\,\mathrm{H_21,4\text{-}bdc}\}_n$			CCT	[285]
	AD	N_2, Et_2O		
	AD	trimethylbenzene, 2-methyl-1-propanol	CCT	
$\{[\mathrm{Cr(OH)(1,4\text{-}bdc)}]\cdot 0.75\,\mathrm{H_21,4\text{-}bdc}\}_n$			CCT	[286, 287]
	AD	N_2		
	AD	H_2O	3rd-II-1	
$\{[\mathrm{Cr(OH)(1,4\text{-}bdc)}]\cdot 0.75\,\mathrm{H_21,4\text{-}bdc}\}_n$ H_2O-containing host	GE	dmf	CCT	
$\{[\mathrm{Fe_2(NCS)_4(azpy)_4}]\cdot \mathrm{EtOH}\}_n$			3rd-II-1	[288]
	AD	EtOH, MeOH, 1-PrOH	3rd-II-1	
$\{[\mathrm{Fe[Ni(bpca)_2]_{1.5}}]\cdot 2\,\mathrm{ClO_4}\cdot 4.5\,\mathrm{CHCl_3}\cdot 3\,\mathrm{MeOH}\cdot 10\,\mathrm{H_2O}\}_n$			[d]	[289]
	AE	PF_6^-	[d]	
	GE	$CHBr_3$	[d]	
$\{[\mathrm{Co_{1.5}[Co(tcpp)](py)_3(H_2O)}]\cdot 11\,\mathrm{py}\}_n$			2nd	[203]
	AD	hydrophilic guests, N_2		
	selective AD	H_2O from benzene, toluene, thf solutions		
$\{[\mathrm{Co_2(4,4'\text{-}bpy)_3(NO_3)_4}]\cdot 4\,\mathrm{H_2O}\}_n$			2nd[e]	[47]
	AD	N_2, O_2, CH_4		
$\{[\mathrm{Co(NCS)_2(3\text{-}pia)_2}]\cdot 2\,\mathrm{EtOH}\cdot 11\,\mathrm{H_2O}\}_n$			CAT	[153]
	AD	thf, H_2O, Me_2CO	CAT	
$[\mathrm{Co(NCS)_2(3\text{-}pia)_2}]_n$	Selective AD	ring ethers, Me_2CO	3rd-II-1	[153]
$\{[\mathrm{Co_2(azpy)_3(NO_3)_4}]\cdot \mathrm{Me_2CO}\cdot 3\,\mathrm{H_2O}\}_n$			CAT	[145]
	AD	CH_4		
$\{[\mathrm{Co(NCS)_2(azpy)_2}]\cdot 0.5\,\mathrm{EtOH}\}_n$			2nd[e]	[145]
	AD	CH_4		
$\{[\mathrm{M_3(1,3,5\text{-}btc)_2(H_2O)_{12}}]_n$ (M = Co, Ni, Zn)			2nd (Zn) 3rd-I (Co, Ni)	[106]
	AD	NH_3	2nd (Zn) CAT (Co, Ni)	
$\{[\mathrm{Co(1,3,5\text{-}Hbtc)(py)_2}]\cdot 1.5\,\mathrm{py}\}_n$			2nd	[45]
	selective AD	aromatic guests		
$\{[\mathrm{Co_3(citrate)_2(4,4'\text{-}bpy)_4(H_2O)_2}]\cdot 4\,\mathrm{H_2O}\}_n$			3rd-II-1	[290]
	AD	MeOH, EtOH		
$\{[\mathrm{Co_2(H_2O)_4}][\mathrm{Re_6S_8(CN)_6}]\cdot 10\,\mathrm{H_2O}\}_n$			CCT or CAT	[291]
	GE	bulkier guests (alcohol, nitrile, ether, dmf, etc)	3rd-II-1	
$\{[\mathrm{Co(H_2O)_3}]_4[\mathrm{Co_2(H_2O)_4}]\ [\mathrm{Re_6Se_8(CN)_6}]\cdot 44\,\mathrm{H_2O}\}_n$			CCT or CAT	[291]
	GE	see above	3rd-II-1	
$\{[\mathrm{Co_3(bpdc)_3(4,4'\text{-}bpy)}]\cdot 4\,\mathrm{dmf}\cdot \mathrm{H_2O}\}_n$				[292]
	AD	hydrocarbons		
$\{[\mathrm{Co_5(im)_{10}}]\cdot 2\,(\text{3-methyl-1-butanol})\}_n$			2nd	[293]
	GE	EtOH, toluene, xylene	2nd	
$\{[\mathrm{Ni_2(4,4'\text{-}bpy)_3(NO_3)_4}]\cdot 2\,\mathrm{EtOH}\}_n$			2nd	[294, 295]
	AD	MeOH	CCT	[295, 296]
	AD	N_2, Ar, CO_2, N_2O	3rd[f]	[295, 296]
		toluene	2nd	[295]
$\{[\mathrm{Ni(L2)_2(NO_3)_2}]\cdot 4\,(o\text{-xylene})\}_n$			[d]	[297]
	GE	mesitylene, styrene, nitrobenzene, cyano benzene	CCT	
$\{[\mathrm{Ni(L2)_2(NO_3)_2}]\cdot 1.7\,(\text{mesitylene})\}_n$			2nd[e]	[297]
	GE	nitrobenzene, *o*-xylene	2nd[e]	
	AD	ben		
$\{[\mathrm{Ni_3(L3)_3(ctc)_2}]\cdot 16\,\mathrm{H_2O}\}_n$			3rd-II-1	[298]
	GE	$\{[\mathrm{Cu(NH_3)_4}]\cdot 2\mathrm{ClO_4}\}$	2nd[e]	
	AD	MeOH, EtOH, PhOH	3rd-II-1	
$\{[\mathrm{Ni_3(1,3,5\text{-}btc)_2(py)_6(eg)_6}]\cdot x(\mathrm{eg})\cdot y(\mathrm{H_2O})\}_n$			2nd[e]	[299]
	AD	MeOH, EtOH	CCT[g]	

Table 3: (Continued)

Compound	Function[b]	Guests or reactants	Generation type[c]	References
$\{[Ni_3(1,3,5\text{-btc})_2(py)_6(1,2\text{-pd})_3]\cdot 11\,(1,2\text{-pd})\cdot 8\,(H_2O)\}_n$			CAT	[299]
	AD	EtOH, 2-methyl-1-butanol	CAT	
$\{[Ni_3(L4)_3(1,3,5\text{-btc})_2]\cdot 18\,H_2O\}_n$			3rd-I	[103]
	AD	PhOH		
$\{[Ni_7(suc)_4(OH)_6(H_2O)_3]\cdot 7\,H_2O\}_n$			3rd-II-1	[300]
	AD	N_2		
$\{[Ni(4,4'\text{-bpy})_{2.5}(H_2O)_2]\cdot 2\,ClO_4\cdot 1.5\,(4,4'\text{-bpy})\cdot 2\,H_2O\}_n$	AE	PF_6^-	[d,e]	[301]
$\{[Cu_2(pzdc)_2(dpyg)]\cdot 8\,H_2O\}_n$			3rd-II-1	[167]
	AD	MeOH	3rd-II-1	
$\{[Cu(1,4\text{-bdc})(py)_2(H_2O)]\cdot py\cdot H_2O\}_n$			2nd[e]	[302]
	AD	N_2		
$[Cu(\text{dicarboxylate}(1))(dabco)_{0.5}]_n$			2nd[e]	[264–266]
	AD	Ar, CH_4		
$\{[Cu(AF_6)(4,4'\text{-bpy})_2]\cdot 8\,H_2O\}_n$			2nd[e]	[126,130]
(A = Si and Ge)	AD	CH_4, Ar		
	AD	H_2O	CCT	[126]
$\{[Cu_2(pzdc)_2(PL)]\cdot x\,(H_2O)\}_n$			2nd[e]	[158,159,277,303]
	AD	N_2, CO_2, Ar, CH_4		
	AD	O_2	2nd	[303]
$\{[Cu(dhbc)_2(4,4'\text{-bpy})]\cdot H_2O\}_n$			CCT	[152]
	AD	N_2, O_2, CO_2, CH_4, MeOH	3rd-II-1	
$[Cu(1,4\text{-bdc})(4,4'\text{-bpy})_{0.5}]_n$	AD	N_2, CH_4, MeOH	3rd-II-1	[161]
$\{[Cu_2(bz)_4(pyz)]\cdot 2\,MeCN\}_n$			[d]	[304]
	AD	N_2		
$[Cu(\text{dicarboxylate}(2))]_n$			[d]	[305,306]
	AD	N_2, Ar, O_2, Xe, CH_4		
$\{[Cu_2(o\text{-Br-}1,4\text{-bdc})_2(H_2O)_2]\cdot 8\,dmf\cdot 2\,H_2O\}_n$			1 st	[138]
	GE	$CHCl_3$, benzene, MeCN MeOH, EtOH, thf, dmso	2nd[e]	
$\{[Cu_3(btb)_2(H_2O)_3]\cdot 9\,dmf\cdot 2\,H_2O\}_n$			2nd[e]	[160]
	AD	N_2, Ar, CO, CH_4, CCl_4, CH_2Cl_2, benzene, C_6H_{12}, *m*-xylene		
	GE	organic solvents	2nd[e]	
$\{[Cu_{24}(1,3\text{-bdc})_{24}(dmf)_{14}(H_2O)_{10}]\cdot 50\,H_2O\cdot 6\,dmf\cdot 6\,EtOH\}_n$			[d]	[307]
	GE	H_2O	CCT	
$\{[Cu_2(atc)(H_2O)_2]\cdot 4\,H_2O\}_n$			3rd-II-1	[137]
	AD	N_2, Ar, CH_2Cl_2, benzene, CCl_4, C_6H_{12}		
$\{[Cu(pymo)_2]\cdot 2.25\,H_2O\}_n$			2nd	[308]
	AD	N_2		
	AD	$MClO_4$ (M = NH_4, Li, Na,K, Rb)	CCT	
$\{[Cu_3(L4)_3(1,3,5\text{-btc})_2]\cdot 18\,H_2O\}_n$			2nd	[309]
	GE	MeOH, EtOH		
	GE	PhOH	CCT	
$[Cu(L5)_2]_n$	AD	various guests	3rd-II-1 h]	[310–313]
	AD	coordinating solvents	3rd-II-1	
$\{[Cu(4,4'\text{-bpy})(BF_4)_2(H_2O)_2]\cdot 4,4'\text{-bpy}\}_n$	AD	N_2, Ar, CO_2	3rd[f]	[314]
$\{[Cu_5(bpp)_8(SO_4)_4(EtOH)(H_2O)_5]\cdot SO_4\cdot EtOH\cdot 25.5\,H_2O\}_n$			3rd-I	[315]
	AD	MeOH, MeCN	3rd-I	
$\{[Cu(CF_3SO_3)_2(4,4'\text{-bpy})_2]\cdot \text{solvent}\}_n$			2nd[e]	[134]
	AD	amyl acetate, $MeNO_2$, 4-methyl-2-pentanone, *n*-decane, tetrachloroethane	CCT	
$\{[Cu(tcnb)(thf)]\cdot PF_6\}_n$			3rd-II-1[i]	[316]
$\{[Cu_3(ptmtc)_2(py)_6]\cdot 2\,EtOH\cdot H_2O\}_n$			3rd-I	[317]
	AD	MeOH	3rd-I	
$\{[Cu(in)]\cdot 2\,H_2O\}_n$			2nd[e]	[318]
	Selective AD	MeOH, EtOH, 1-PrOH	CCT	
$\{[Cu(4,4'\text{-bpy})_{1.5}]\cdot NO_3\cdot 1.5\,H_2O\}_n$	AE	SO_4^{2-}, BF_4^-	[d,e]	[319]

Table 3: (Continued)

Compound	Function[b]	Guests or reactants	Generation type[c]	References
$\{[Cu(L6)(ox)_{0.5}(H_2O)_2]\cdot 3\,NO_3\cdot 20\,H_2O\}_n$			3rd-I	[116]
	AE	PF_6^-, p-$MePhSO_3^-$	CCT	
	GE	NH_3	2nd[e]	
$\{[Zn_3(OH)_2(bpdc)_2]\cdot 4\,def\cdot 2\,H_2O\}_n$			CAT[j]	[156]
	GE	benzene, $CHCl_3$, *i*PrOH, thf, toluene	2nd	
$\{[Zn_3(OH)_2(ndc)_2]\cdot 4\,def\cdot 2\,H_2O\}_n$			CAT[j]	[156]
	GE	benzene, chloroform, *i*PrOH, thf, toluene	2nd	
	AD	benzene		
$\{[Zn_4O(dicarboxylate)_3]\cdot x\,(def)\}_n$			2nd[e]	[131, 276]
(MOF-5 and IRMOF-1 ~16)	AD	Ar, N_2, C_6H_{12}, CCl_4, CH_2Cl_2, benzene, CH_4, $CHCl_3$		
(MOF-5, IRMOF-6 and-8)	AD	H_2		[320]
$\{[ZnO(tta)(dma)_2]\cdot 3\,dma\cdot 21\,H_2O\}_n$			[d]	[321]
	AD	N_2, Ar, CH_2Cl_2, CCl_4, benzene, C_6H_{12}		
$\{[Zn(1,4\text{-}bdc)]\cdot dmf\cdot H_2O\}_n$			[d]	[322, 323]
	AD	N_2, CO_2, CH_2Cl_2, $CHCl_3$, benzene, C_6H_{12}		
$\{[Zn_3(1,4\text{-}bdc)_3]\cdot 6\,MeOH\}_n$			3rd-II-1	[323, 324]
	AD	N_2, Ar, CO_2, CH_2Cl_2, benzene, CCl_4, C_6H_{12}, MeOH		
$\{[Zn_2(1,3,5\text{-}btc)(NO_3)]\cdot 5\,EtOH\cdot H_2O\}_n$			2nd	[323, 325]
	AD	EtOH		
	selective GE	dmf, alcohols		
$\{[Zn_3I_6(tpt)_2]\cdot 6(solvent)\}_n$			CCT	[162]
(solvent = $PhNO_2$ and PhCN)	GE	benzene, mesitylene, *cis*-stilbene, $CHCl_3$	2nd[e]	
$\{[Zn(1,4\text{-}bdc)(H_2O)]\cdot dmf\}_n$			3rd-I	[326]
	AD	MeOH	CAT	
$\{[Zn(in)]\cdot 2\,H_2O\}_n$			2nd[e]	[230]
	AD	N_2		
$\{[Zn_3O(L7)_6]\cdot 2\,H_3O\cdot 12\,H_2\}_n$			3rd-I	[141]
	AE	I_3^-, PF_6^-, p-$CH_3C_6H_4SO_3^-$	[e]	
	CE	alkali-metal ions	2nd[e]	
	Enantioselective CE	$[Ru(2,2'\text{-}bpy)_3]^{2+}$	[e]	
$\{[Zn(dimto)_2]\cdot x\,(dmf)\}_n$				[327]
	GE	MeCN	[e]	
MeCN-exchanged material			2nd[e]	
$[Mo(dicarboxylate(3))]_n$	AD	N_2, Ar, O_2, CH_4		[328]
$[Rh(bz\ derivatives)_2(pyz)_{0.5}]_n$	AD	N_2		[329]
$[Rh(bz)_2(pyz)_{0.5}]_n$			[k]	[330, 331]
	AD	CO_2	3rd-II-1	
	AD	N_2	[e,f]	
$\{[Pd(tib)]\cdot NO_3\}_n$	AE	I^-	[f]	[332]
$\{[Ag(3\text{-}pySO_3)]\cdot 0.5\,MeCN\}_n$			3rd-II-1	[333]
	Selective AD	MeCN over other nitriles		
$\{[Ag(4\text{-}teb)(CF_3SO_3)]\cdot 2\,benzene\}_n$			3rd-II-1	[132, 334]
	GE	aliphatic and aromatic guests (2nd), alcoholic aromatic guests (3rd)	2nd, 3rd-II-2	
$\{[Ag(hat)]\cdot ClO_4\cdot 2\,MeNO_2\}_n$			[d]	[335]
	GE	H_2O	3rd[L]	
$\{[Ag_3(NO_3)(L8)_4]\cdot 2\,NO_3\cdot H_2O\}_n$	AE	NO_2^-	2nd[m]	[336]
$\{[Ag(edtpn)]\cdot anion\}_n$	AE	NO_3^-, $CF_3SO_3^-$, ClO_4^-	CCT[j] and 3rd-II-2	[337]
$\{[Ag(3,3'\text{-}Py_2S)]\cdot anion\}_n$	AE	BF_4^-, ClO_4^-, PF_6^-, NO_3^-	3rd-II-2	[338]
$\{[Ag(4,4'\text{-}bpy)]\cdot NO_3\}_n$	AE	PF_6^-, MoO_4^{2-}, BF_4^-, SO_4^{2-}	3rd-II-2	[339]
$\{[Ag(bptp)]\cdot CF_3CO_2\}_n$	AE	$CF_3CO_2^-$, ClO_4^-, PF_6^-	[m]	[340]

Table 3: (Continued)

Compound	Function[b]	Guests or reactants	Generation type[c]	References
$\{[\mathrm{Ag(bpp)}]\cdot\mathrm{ClO_4}\}_n$	AE	$\mathrm{PF_6^-}$	CCT[j]	[341]
$\{[\mathrm{Ag(4,4'\text{-}bpy)}]\cdot\mathrm{anion}\}_n$	AE	$\mathrm{BF_4^-}$, $\mathrm{NO_3^-}$	3rd-II-2	[342]
$\{[\mathrm{Ag(3,3'\text{-}Py_2O)}]\cdot\mathrm{anion}\}_n$	AE	$\mathrm{BF_4^-}$, $\mathrm{ClO_4^-}$, $\mathrm{PF_6^-}$, $\mathrm{NO_3^-}$	3rd-II-2	[343]
$\{[\mathrm{Ag(bpcah)}]\cdot\mathrm{anion}\}_n$	AE	$\mathrm{ClO_4^-}$, $\mathrm{CF_3SO_3^-}$, $\mathrm{NO_3^-}$	CCT[j]	[344]
$\{[\mathrm{Ag(2,4'\text{-}Py_2S)}]\cdot\mathrm{anion}\}_n$	AE	$\mathrm{BF_4^-}$, $\mathrm{ClO_4^-}$, $\mathrm{PF_6^-}$	2nd[j]	[345]
$\{[\mathrm{Ag_4(L9)_3}]\cdot 4\,\mathrm{CF_3SO_3}\cdot x\,\mathrm{MeNO_2}\cdot x\,\mathrm{EtOH}\}_n$				[346]
	GE	$\mathrm{Et_2O}$, $\mathrm{H_2O}$	2nd[e]	
$\{[\mathrm{Cd_2(azpy)_3(NO_3)_4}]\cdot 2\,\mathrm{Me_2CO}\}_n$			CCT	[145]
	AD	$\mathrm{CH_4}$		
$[\mathrm{Cd(1,5\text{-}nds)(H_2O)_2}]_n$				[247]
	AD	$\mathrm{NH_3}$ and alkylamines	3rd-II-1	
$\{[\mathrm{InH(1,4\text{-}bdc)_2}]\cdot 1.5\,\mathrm{dmf}\cdot 4\,\mathrm{H_2O}\}_n$			[d]	[230]
	AD	$\mathrm{N_2}$		
$\{[\mathrm{Tb_2(adb)_3(dmso)_4}]\cdot 16\,\mathrm{dmso}\}_n$			[d]	[164]
	GE	$\mathrm{CHCl_3}$, dmf	3rd[f]	
	AD	$\mathrm{CO_2}$		
$\{[\mathrm{Tb_2(1,4\text{-}bdc)_3}]\cdot 4\,\mathrm{H_2O}\}_n$			2nd	[49]
	AD	$\mathrm{H_2O}$, $\mathrm{NH_3}$	2nd	
$\{[\mathrm{Tb(1,4\text{-}bdc)(NO_3)}]\cdot 2\,\mathrm{dmf}\}_n$			3rd-I	[347]
	AD	$\mathrm{H_2O}$	CAT	
	AD	$\mathrm{CO_2}$, $\mathrm{CH_2Cl_2}$, MeOH, EtOH, *i*PrOH		
$\{[\mathrm{Ln_2(pda)_3(H_2O)}]\cdot 2\,\mathrm{H_2O}\}_n$			2nd	[48]
(Ln = La, Er)	AD	$\mathrm{CO_2}$		

[a] In this table, coordination polymers with 1D, 2D, and 3D motifs are described. Discrete molecules, which are linked by hydrogen bonds to create infinite network, are not included. L1 = anthracenebisresorcinol derivative. L2 = 4,4′-bis(4-pyridyl)biphenyl. L3 = hexaazamacrocyclic ligand containing pendant pyridine groups. L4 = 1,8-dimethyl-1,3,6,8,10,13-hexaazacyclotetradecane. L5 = 1,1,1-trifluoro-5-methoxy-5,5-dimethylacetylacetonate. L6 = pseudorotaxane ligand, L7 is chiral organic ligands. L8 = bis(4-pyridyl)dimethylsilane. L9 = 1,3,5-tris(diphenylphosphanyl)benzene. dicarboxylate(1) = fumarate, 1,4-bdc, styrenedicarboxylate, and bpdc. dicarboxylate(2) = fumarate, 1,4-bdc, and *trans*-1,4-cyclohexanedicarboxylate. dicarboxylate(3) = fumarate, 1,4-bdc, *trans*,*trans*-muconate, pyridine-2,5-dicarboxylate, and *trans*-1,4-cyclohexanedicarboxylate. PLs (pillar ligands) are shown in Figure 20. [b] AD = adsorption, GE = guest exchange, AE = anion exchange, CE = cation exchange. [c] 1st = 1st generation compound, 2nd = 2nd generation compound, 3rd = 3rd generation compound, 3rd-I = crystal-to-amorphous transformation (CAT) type, 3rd-II-1 = crystal-to-crystal transformation (CCT) type accompanying a guest inclusion/removal, 3rd-II-2 = CCT type accompanying a guest exchange. Framework transformations, which are not checked for reversibility, are shown as CAT or CCT. [d] Framework information after the removal or exchange of guest molecules is not checked in detail. [e] Reversibility is not checked. [f] It is not known how the framework moves. [g] The phase generated by MeOH and EtOH solvation after 1 day of exposure has cubic symmetry, which is the same symmetry as that of the original framework. After 1 week, the structure relaxes to give the tetragonal form. [h] Empty framework after the removal of guests (the β-phase) is very slowly converted into an α-phase. [i] This transformation is not perfectly reversible: samples without guests left in thf at room temperature for a week gave XRPD patterns which can be ascribed to an approximately 1:1 mixture of compounds with and without guests. [j] Guest-adsorption/desorption or guest-exchange is not reversible. [k] As-synthesized coordination polymer has no effective vacant space in the framework. [l] First guest-exchange process accompanies CCT, but subsequent ones afford same crystal system (cubic). [m] Although information on exchanged materials is not known, reversibility is observed.

$\mathrm{CH_4}$ gas adsorption for porous coordination polymers was first reported for $\{[\mathrm{Co_2(4,4'\text{-}bpy)_3(NO_3)_4}]\cdot 4\,\mathrm{H_2O}\}_n$, which adsorbs an equivalent of about 52 $\mathrm{cm^3}$ (STP) $\mathrm{g^{-1}}$ (STP = standard temperature and pressure) of $\mathrm{CH_4}$ at a temperature of 298 K and a pressure of 30 atm (Figure 29c).[47] In 3D pillared-layer coordination polymers, CPL-1, CPL-2, and CPL-6, approximately 18, 56, and 65 $\mathrm{cm^3}$ (STP) $\mathrm{g^{-1}}$ of $\mathrm{CH_4}$ are adsorbed at 298 K and 31 atm. The triply interpenetrated framework of $\{[\mathrm{Cd_2(NO_3)_4(azpy)_3}]\cdot 2\,\mathrm{Me_2CO}\}_n$, which has microporous channels despite the interpenetration, also adsorbs a certain amount of $\mathrm{CH_4}$ (40 $\mathrm{cm^3}$ (STP) $\mathrm{g^{-1}}$ at 298 K and 36 atm).[145] This is the first case of gas adsorption by interpenetrated coordination polymers. The compounds, $\{[\mathrm{Cu(AF_6)(4,4'\text{-}bpy)_2}]\cdot 8\,\mathrm{H_2O}\}_n$ (A = Si and Ge), show a high $\mathrm{CH_4}$ adsorption activity at room temperature and relatively low pressure (134 and 146 $\mathrm{cm^3}$ (STP) $\mathrm{g^{-1}}$ for A = Si and Ge, respectively, at 298 K and 36 atm).[126,130] On the basis of the crystal structure, a grand canonical Monte Carlo (GCMC) simulation of the $\mathrm{CH_4}$ adsorption was performed which accurately reproduced the experimental results.[348]

Recently, other types of complexes with high methane capacity have been synthesized. IRMOF-6 (Section 3.3), affords a 3D cubic porous network and has a high surface area, 2630 $\mathrm{m^2\,g^{-1}}$, estimated by applying the Langmuir equation.[276] The $\mathrm{CH_4}$ adsorption isotherm was found to have an uptake of 240 $\mathrm{cm^3}$ (STP) $\mathrm{g^{-1}}$ (156 $\mathrm{cm^3}$ (STP) $\mathrm{cm^{-1}}$) at 298 K and 36 atm (Figure 32). Based on volume, the amount of methane adsorbed by IRMOF-6 at 36 atm is about 70% of the amount stored in gas cylinders where much higher pressures (205 atm) are used. Another type of highly porous coordination polymer which has methane adsorption ability are the 2D carboxylate-bridged polymers of [Cu(OOC-L-

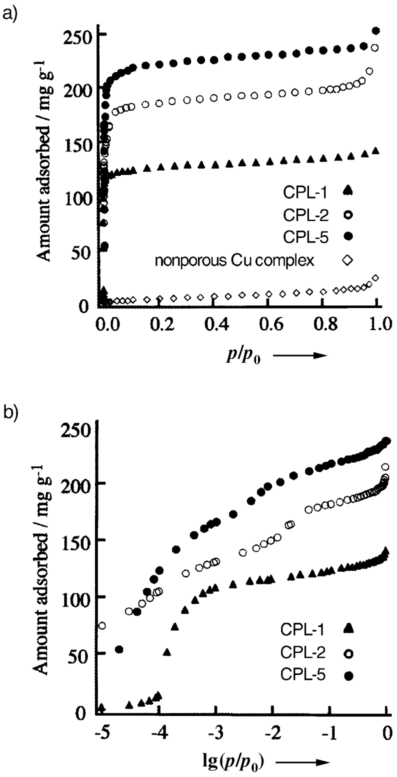

Figure 30. a) Adsorption isotherms and b) the logarithmic relative pressure expression of adsorption isotherms of N_2 on CPL-1, CPL-2, and CPL-5.[277]

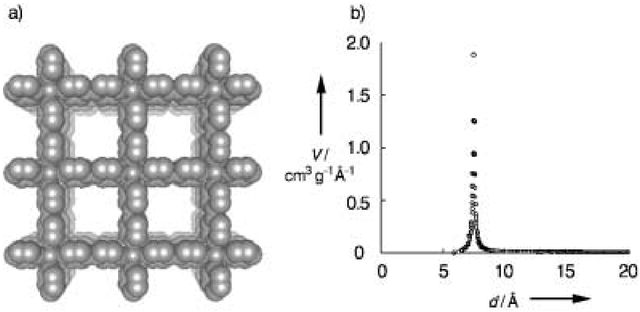

Figure 31. a) Microporous network along the c axis of $\{[Cu(SiF_6)(4,4'\text{-}bpy)_2]\cdot 8H_2O\}_n$, whose channel cross section is 8×8 A^2 based on the van der Waals radii. b) Pore size distribution calculated from the Ar adsorption.[130]

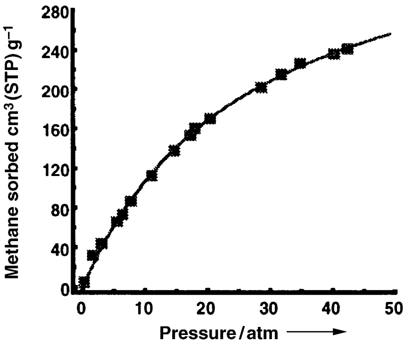

Figure 32. Adsorption isotherm of CH_4 gas in IRMOF-6 fitted at 298 K with the Langmuir equation.[276]

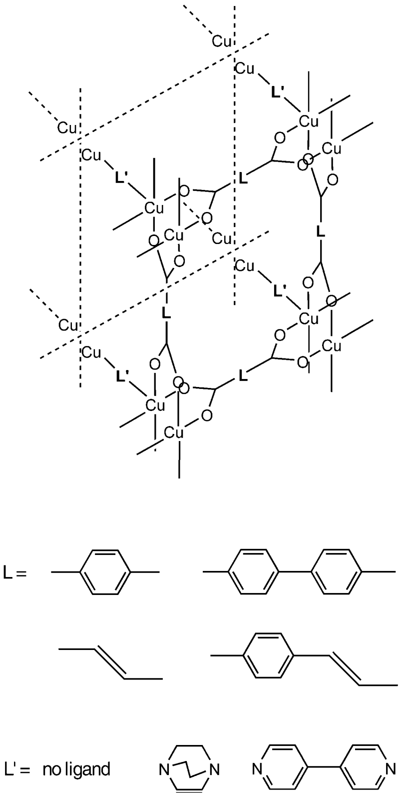

Figure 33. The 3D coordination polymer $[Cu(OOC\text{-}L\text{-}COO)(dabco)_{0.5}]_n$ which has methane adsorption properties.

$COO)]_n$ (L = Ph, CH=CH, Ph-Ph, Ph-CH=CH),[306] which in turn, are bridged by dabco to form more highly porous 3D networks of $[Cu(OOC\text{-}L\text{-}COO)(dabco)_{0.5}]_n$ with the topology of the B net in CaB_6 (Figure 33).[264–266] The polymers with L = Ph-Ph and Ph-CH=CH, adsorb 212 and 213 cm^3 (STP) g^{-1} methane (179 and 199 cm^3 (STP) cm^{-3}), respectively, at 298 K and 35 atm.[264,265] Analyses of high-resolution Ar adsorption isotherms at 87.3 K yield BET surface areas of 3265 (L = Ph-Ph) and 3129 (Ph-CH=CH) m^2 g^{-1}. The adsorption amount of CH_4 molecules around 35 atm appears to increase with the increase of cross-sectional channel size, however, this is not the whole truth. There is probably an upper limit of the size of the square pore of about 12 × 12 Å^2. This size provides the optimal fit for CH_4 molecules and the potential is thus sufficiently deep for the storage of methane.

Hydrogen (H_2) has attracted a great deal of attention as an energy source. Once it is generated, its use as a fuel creates neither air pollution nor greenhouse-gas emissions. However, no practical means for H_2 storage and transportation have yet been developed. So, the development of H_2-fueled vehicles and portable electronics will require new materials that can store large amounts of H_2 at ambient temperature and relatively low pressures, with small volume, low weight, and fast kinetics for recharging. Metal hydride systems,[349] zeolites,[350] and various carbon-based adsorbents[351–363] have been intensely examined in this respect. Very recently, H_2 adsorption has been carried out with the microporous Zn^{II}-cluster–dicarboxylate coordination polymers, MOF-5, IRMOF-6, and IRMOF-8[320] as well as nickel(II) phosphates.[364] The data from temperature programmed desorption (TPD) and inelastic neutron scattering (INS) measurements strongly suggest that nickel(II) phosphate has coordinatively unsaturated Ni^{II} sites accessible to H_2 molecules in the pores.[364] MOF-5 adsorbs up to 4.5 weight % of H_2 (17.2 H_2 molecules per formula unit) at 78 K and 1.0 weight % at room temperature and a pressure of 20 atm.[320]

4.2.2. *Exchange*

Porous zeolites have cation-exchange properties as a result of their anionic frameworks. Porous coordination polymers in contrast to zeolites tend to have cationic frameworks, which are constructed from cationic metal ions and neutral bridging ligands, and accommodate counteranions in the cavities, and therefore have anion-exchange properties.[43,116,126,141,301,319,332,336–338,340–343] Anion-exchange, which happens at a solid–liquid interface, was first reported in 1990.[43] $\{[Cu(4,4',4'',4'''\text{-tetracyanotetraphenylmethane})]\cdot BF_4\cdot x\,C_6H_5NO_2\}_n$ contains a diamond-like cationic framework with large admanantane-like cavities occupied by disordered $C_6H_5NO_2$ molecules together with BF_4^- ions. This crystal readily undergoes anion-exchange with PF_6^- ions. The partially dehydrated solid of $\{[Ni(4,4'\text{-bpy})_{2.5}(H_2O)_2]\cdot 2\,ClO_4\cdot 1.5(4,4'\text{-bpy})\cdot 2\,H_2O\}_n$, which has a railroad 1D motif, undergoes anion exchange with the PF_6^- ion.[301] $\{[Ag_3L_4]\cdot 3\,NO_3\cdot H_2O\}_n$ (L = bis(4-pyridyl)dimethylsilane) affords a nanotubular sheet constructed by interweaving of two independent undulating networks and smoothly exchanges NO_3^- for NO_2^- ions.[336] The reverse exchange of $\{[Ag_3(L)_4]\cdot 3\,NO_2\}_n$ with NO_3^- ions is slow, indicative of the stronger coordinating ability of NO_2^- than NO_3^- ions. Recently, structural transformations in the crystalline state were observed concomitant with anion exchange (see Section 4.3.3).[126,337,338,341–343,365]

4.2.3. *Conversion*

Metal ions play key roles in organic transformations, which are usually carried out with soluble species in a homogeneous solution. An advantage of heterogeneous catalysts is their ready recoverability; they are important in industry applications. However, to date, solid catalysts have been almost exclusively inorganic materials. Especially useful are microporous inorganic zeolites.[366] Despite recent interest in metal–organic solids with zeolitic guest-binding properties, their catalytic activities are largely unexplored.[44,141,142,283,284,292,367–373] Table 4 gives a list of porous coordination polymers with heterogeneous catalytic activities.[44,141,142,283,284,292,367–373] $[Cd(NO_3)_2(4,4'\text{-bpy})_2]_n$, which consists of 2D networks with cavities surrounded by 4,4′-bpy units, shows shape-specific catalytic activity for the cyanosilylation of aldehydes.[44] This reaction is apparently promoted by the heterogeneous polymer since no reaction takes place with powdered $Cd(NO_3)_2$ or 4,4′-bpy alone, or with the supernatant liquid from a CH_2Cl_2 suspension of the coordination polymer. 2D microporous polymers of $[Rh(OOC\text{-}L\text{-}COO)]_n$ (L = CH=CH and Ph) exhibit high catalytic activity for hydrogen exchange and hydrogenation of olefins at 200 K.[372] The hydrogen-exchange reaction takes place without complete scission of C–H bond of the olefin molecule and only occurs inside the nanopores of the complexes. A homochiral open-framework solid, $\{[Zn_3O(L)_6]\cdot 2\,H_3O\cdot 12\,H_2O\}_n$ (L = chiral organic ligand), has enantioselective catalytic activity for transesterification.[141] The observed size selectivity suggests that the catalysis mainly occurs in the channels. Zr and Ti coordination polymers $[Zr(OtBu)_2(L)]_n$ and $[Ti(OiPr)Cl(L)]_n$ (L = anthracenebisresorcinol deriva-

Table 4: Microporous coordination polymers capable of catalytic activity.

Compound [a]	Catalytic function	Guests or reactants	Ref.
Ti^{IV} aryldioxide coordination polymers[b,c]	Ziegler–Natta polymerization	ethene and propene	[367]
$[Ti_2Cl_2(iPrO)_2L1]_n$ and $[Zr_2(tBuO)_4L1]_n$[d]	Diels–Alder reaction	acrolein and 1,3-cyclohexadiene	[283,284]
$\{[Co_3(bpbc)_3(4,4'\text{-bpy})]\cdot 4\,dmf\cdot H_2O\}_n$	photoreaction	dibenzylketone derivatives	[292]
$\{[[Zn_3O(L2)_6]\cdot 2\,H_3O\cdot 12\,H_2O]_n$	transesterification	esters and alcohols	[141]
$[Cd(NO_3)_2(4,4'\text{-bpy})_2]_n$	cyanosilylation of aldehydes	aldehydes and cyanotri-methylsilane	[44]
$[In_2(OH)_3(1,4\text{-bdc})_{1.5}]_n$[e]	hydrogenation of nitroaromatics and oxidation of sulfides	nitrobenzene, 2-methyl-1-nitronaphthalene, methylphenylsulfide, and (2-ethylbutyl)phenylsulfide	[368]
$\{[Ru(1,4\text{-diisocyanobenzene})_2]\cdot 2Cl\}_n$[d]	hydrogenation and isomerization	1-hexene	[369,370]
$\{[Rh(4,4'\text{-diisocyanobiphenyl})_2]\cdot Cl\cdot 2.53\text{-}H_2O\}_n$[d]	hydrogenation and isomerization	1-hexene	[371]
$[RhL]_n$ (L = fumarate and 1,4-bdc)	hydrogen exchange	ethene, propene, butene, and hydrogenation	[372]
Pd^{II} coordination polymer gels[d]	oxidation of benzylalcohol	benzylalcohol	[373]
$\{[Ln(H_2L3)(H_3L3)(H_2O)_4]\cdot x\,H_2O\}_n$ (Ln = La, Ce, Pr, Nd, Sm, Tb; x = 9–14)	cyanosilylation of aldehydes and ring opening of *meso*-carboxylic anhydrides	aldehydes and cyanotri-methylsilane, *meso*-2,3-dimethylsuccinic anhydride	[142]

[a] L1 = anthracenebisresorcinol derivative. L2 is chiral organic ligands. H_4L3 = 2,2′-diethoxy-1,1′-binaphthalene-6,6′-bisphosphonic acid. [b] Methylalumoxane (MAO) as cocatalyst. [c] aryldioxide = *p*-benzenedioxide, 2,7- naphthalenedioxide, and 4,4′-biphenyldioxide. [d] Exact crystal structures are not determined. [e] Nonporous materials.

tives) catalyze the Diels–Alder reaction of acrolein with 1,3-cyclohexadiene in a remarkable manner.[283,284] The catalytic activity of these polymers is much higher than those of their components, L and M^{4+}. Homochiral lanthanide bisphosphonates with the general formula $\{[Ln(L\text{-}H_2)(L\text{-}H_3)(H_2O)_4]\cdot x\,H_2O\}_n$ (Ln = La, Ce, Pr, Nd, Sm, Gd, Tb; x = 9–14; L = 2,2′-diethoxy-1,1′-binaphthalene-6,6′-bisphosphonic acid (L-H_4)) catalyze the cyanosilylation of aldehydes and the ring opening of *meso*-carboxylic anhydrides.[142] $\{[Co_3(bpdc)_3(4,4'\text{-}bpy)]\cdot 4\,dmf\cdot H_2O\}_n$ which has a twofold interpenetrating 3D pillared structure carries out the ship-in-bottle photochemical reaction of *o*-methyldibenzylketone, in which the yield and selectivity are much higher than the values found in other zeolites.[292] 1D, 2D, and 3D Ti^{IV} aryldioxide coordination polymers have been used in the Ziegler–Natta polymerization of ethene or propene with methylalumoxane (MAO) as a cocatalyst.[367] However, fragmentation of the coordination frameworks readily occurs. The nonporous polymer, $[In_2(OH)_3(1,4\text{-}bdc)_{1.5}]_n$,[368] and 3D Pd^{II} coordination-polymer gels[373] are found to be active for the hydrogenation of nitroaromatics and the oxidation of alkylphenylsulfides (In^{III} coordination polymer), and the oxidation of benzyl alcohol by air into benzaldehyde (Pd^{II} coordination polymers). Using a metalloligand as a building unit could provide a novel porous coordination polymer with high catalytic activity because coordinatively unsaturated metal centers (UMCs) functioning as activation sites in the heterogeneous catalyst can be located in the channel wall, a position which is more accessible to substrate molecules than the nodal positions.[189,201]

4.3. Dynamic Frameworks with Nanospace

4.3.1. Design and Functionalizing Dynamic Frameworks

A versatile architecture is one of the most striking features of coordination polymers, and results from the variety of the molecular building blocks and the interactions between them. Numerous compounds and a great number of frameworks have been synthesized, and as a result the structural chemistry of coordination polymers has reached a mature level. The next challenge in this field is to control the functional aspects of the frameworks, which result from their dynamic nature.

Dynamic structural transformation based on flexible frameworks is one of the most interesting and presumably characteristic phenomena of coordination polymers of the so-called 3rd generation (Figure 17),[11] which leads to novel porous functions. In just a few years, various guest-induced structural distortion phenomena have been found which can be categorized in the following way (Figure 34):

1) Guest-induced crystal-to-amorphous transformation (CAT, type 3rd-I): the framework collapses on removal of the guest molecules owing to the close-packing force; however, it regenerates under the initial conditions.
2) Guest-induced crystal-to-crystal transformation (CCT, type 3rd-II): removal or exchange of guest molecules results in a structural change in the network but the crystallinity is maintained.

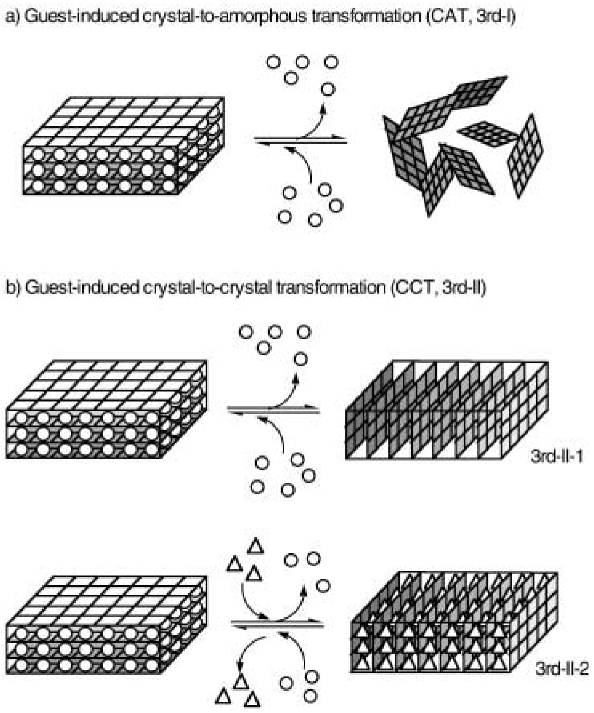

Figure 34. Classification of guest-induced structure transformations in coordination polymers.

The key to creating a flexible but durable framework is to utilize weak molecular interactions in addition to the strong covalent and coordination bonds. Actually, coordination bonds in coordination-polymer solids are frequently supported by hydrogen bonds, π–π stacking, and van der Waals forces and other weak interactions. Intermolecular links with these weaker interactions produce flexible parts in a framework, so that the system can exist in two or more solid phases. Depending on the external perturbations, the system will be in one of two solid phases. Interestingly, even for frameworks woven three-dimensionally by coordination bonds, a sort of flexibility could be created because a coordination polymer is an assembly of versatile metal-ion connectors and flexible organic ligand linkers. For instance, with Cu^{II} complex modules, a flexible coordination geometry is found at the apical positions as a result of the Jahn–Teller effect. In the case of a linking ligand, there is the flexibility of a ring rotation around the C–C bond of dipyridyl or an sp^3-hybridized ethylene group. The structural properties of coordination polymers, therefore, range from the robust to the flexible and dynamic.

The 3rd generation compounds have bistable states and can alter their frameworks in response to guest molecules, in that they reversibly change their channel structures to accommodate them (Figure 35). The ultimate example is the highly selective “induce-fit” found in proteins. Framework flexibility is a prerequisite for porous functionality, even if it is far more primitive than that of proteins. The 3rd generation compounds show characteristic sorption behavior, for exam-

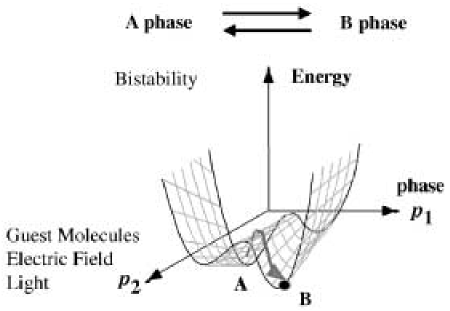

Figure 35. Structures in a bistable state could alter their frameworks in response to guest molecules, electric field, and light.

ple, high selectivity for guest inclusion, hysteretic sorption, and stepwise adsorption. Therefore, we can expect that this kind of coordination polymer will find applications for gas separations, sensors, and actuators.

Single-crystal-to-single-crystal structural transformations in coordination polymers can be directly monitored by X-ray diffraction analyses of single crystals.[297,331,374]

Because dynamic structures are associated with new porous function, it is of importance to seek principles or guidelines to establish a rational design and synthesis of them. Key ideas are "flexibility against robustness" and "bistability against single stability". One of the most useful ways is to design a building material (block or motif), which could be involved in a framework and also come into play for dynamic porous function. This building material is named a "function synthon" (or "function module") for functional engineering, in contrast to "supramolecular synthons" for crystal engineering.[375] The conceivable modules are listed in Table 5 and Figure 36, most of which are readily available and already used.

4.3.2. *Crystal Transformation by Guest Inclusion*

Structure transformations by guest molecules, in particular, of the crystal phase, are not common in zeolites. On the other hand, reversible structure transformations triggered by guest molecules have been found in coordination polymers. The phenomena are found to occur for various guest molecules, ranging from water, alcohols, ketones, ethers, to aromatic and aliphatic molecules. This transformation occurs when a guest-free host is immersed in the liquid phase of a guest compound and even when the host is exposed to a guest vapor.[45,126,132,153,156,162,167,203,285,287,288,290,295–297,299,310,311,314,315,318,322–324,333,334,372,376–379] Most striking is that supercritical gases (N_2, O_2, CH_4) can also be a stimulus for structural transformation.[152,161] These structure transformations are essentially related to "function synthons" (Table 5, Figure 36), which are composed of units linked by: 1) coordination bonds, 2) hydrogen bonds, and 3) other weak nonbonding interactions (π–π stacking and van der Waals forces). The structural flexibility of microporous coordination polymers is attributed to the combination of features (1)–(3). When the guest-induced structural variation of individual function synthons is cooperatively accumulated over a large part of the solid framework, a transformation of the macroscopic structure occurs but causes no wide-range degradation of the crystal phase, this is sufficient perturbation to cause a crystal transformation. Therefore, when we choose a relevant function synthon based on weak coordination and/or hydrogen bonds, a structural transformation is readily triggered by a low concentration of guest molecules, even in their vapor phase. On the other hand, when the frameworks are constructed by rigid covalent bonds, no structure transformation can occur. Furthermore, even supercritical gases can give rise to a structure transformation when frameworks are constructed by van der Waals interaction-based function synthons.

Table 5: Function synthons and modules

Site	Function synthons[a]	Chemical key	Examples
connector/ linker	symbol A	bond formation/cleavage	elongation site in Jahn–Teller distortion, semi-coordination
	symbol B	rotation around coordination bond	ligand with single bond
	symbol C	T_d–sp transformation[b]	Ni^{II}
connector/ linker	symbol D	spin crossover	Fe^{II}, Co^{II}
	symbol E	O_h–T_d or tbp transformation[c]	Co^{II}
linker	symbol F	hydrogen bond	coordinated water-carboxylate, coordinated water-pyridyl, and C-H···O interaction
		π–π stacking	interaction between aromatic rings
		photoactive bond	diarylethene
	symbol G	rotation and flip motion around single bond	C—C, C—O, and C—N bond etc
	symbol H	hinge	sp^3 bond
other module	symbol I	interdigitation	$[Cu_2(dhbc)_2(4,4'\text{-bpy})]_n$
	symbol J	interpenetration	$[Cu(1,4\text{-bdc})(dabco)_{0.5}]_n$
	symbol K	sliding of layers	$[Ni(NO_3)_2(L)_2]_n$[d]

[a] Schematic views of function synthons A–K are shown in Figure 36. [b] sp is square plane. [c] tbp is trigonal bipyramid. [d] L = 4,4′-bis(4-pyridyl)biphenyl.

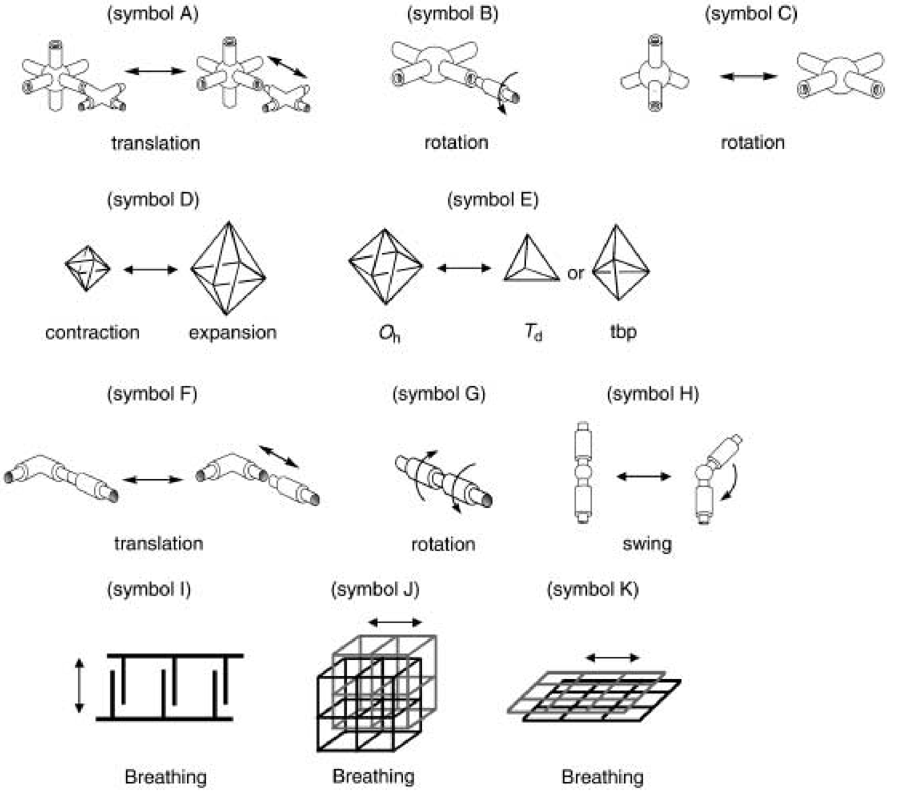

Figure 36. Schematic representations of function synthons (see also Table 5).

4.3.2.1. *Stretching*

A structure transformation ascribed to stretching motions around the connector and/or linker results from bond formation/cleavage. The key factor in realizing such stretchable frameworks is the utilization of weak interactions, such as hydrogen bonds, semicoordination, and the elongated coordination of Jahn–Teller distortions.

A hysteretic adsorption and desorption profile accompanied by a transformation of the crystal structure is observed for $\{[Cu_2(pzdc)_2(dpyg)]\cdot 8\,H_2O\}_n$, which has a 3D pillared-layer structure.[167] This compound shows reversible crystal-to-crystal transformation on adsorption and desorption of H_2O or MeOH molecules. A precise structure-determination study by high-resolution synchrotron powder X-ray diffraction reveals that contraction and re-expansion of the channels with the layer–layer separation varying between 9.6 Å and 13.2 Å is observed for the process of desorption/adsorption of the guest molecules; the unit cell volume decreases during the contraction by 27.9 % (Figure 37). This compound adsorbs MeOH and water but does not adsorb N_2 and CH_4 (Figure 38). This structure transformation is attributed to the cleavage/formation of the Cu^{II}–carboxylate bond. 3D frameworks of $\{[Cu(AF_6)(4,4'\text{-bpy})_2]\cdot x\,H_2O\}_n$ were transformed into 2D interpenetrating networks of $\{[Cu(4,4'\text{-bpy})_2(H_2O)_2]\cdot AF_6\}_n$ (A = Si, Ge, and Ti) on being immersed in H_2O solution.[126,380] To demonstrate the occurrence of this dynamic structural transformation in the solid state, 3D frameworks of $\{[Cu(AF_6)(4,4'\text{-bpy})_2]\cdot x\,H_2O\}_n$ were exposed to H_2O vapor for a few days. The same transformation into a 2D interpenetrating framework was observed, clearly indicating the solid-state conversion. This transformation causes not only the formation and cleavage of weak Cu–O (H_2O) and Cu–F (AF_6) bonds, but also the formation and cleavage of Cu–N (4,4'-bpy) bonds. An important role is often played by the elongated axial sites of Cu^{II} compounds. M^{II}–bis(acetylacetonato) (M = Cu, Zn, Ni) derivatives have characteristic inclusion phenomena.[310–312,379] The bis(1,1,1-trifluoro-5-methoxy-5,5-dimethylacetylacetonato)Cu^{II} coordination polymer forms two different crystal packings resulting in the dense and nonporous α-form and the porous β-form. In the β-form, oxygen atoms of methoxy groups occupy the axial sites of the Cu^{II} centers to form six-membered cyclic structures (Figure 39). The porous β-form has a strong affinity for guest molecules as is evident from the efficient α-to-β conversion on contact not only with liquid guests but also with organic vapors. The empty β-form undergoes slow crystal structure transformation to the dense α-form, this transformation is accelerated when the β-form is exposed to propane. Labile coordination between Cu^{II} and OMe is essential for this dynamic structure transformation.

Face-capped octahedral clusters of the type $[Re_6Q_8(CN)_6]^{4-}$ (Q = S, Se) react with Co^{II} to produce the coordination polymers, $\{[Co_2(H_2O)_4][Re_6Q_8(CN)_6]\cdot 10\,H_2O\}_n$ and $\{[Co(H_2O)_3]_4[Co_2(H_2O)_4][Re_6Q_8(CN)_6]\cdot 44\,H_2O\}$ (Figure 40a and b).[291] Upon exposure to diethyl ether vapor, the color of the compounds immediately changes from orange to an intense blue-violet or blue, and after allowing the diethyl ether to evaporate, the color changes back to orange. This reversible color change is attributed to a reversible structure transformation resulting from coordination bond cleavage and formation (octahedral $\{Co(NC)_3(H_2O)_3\}$ to

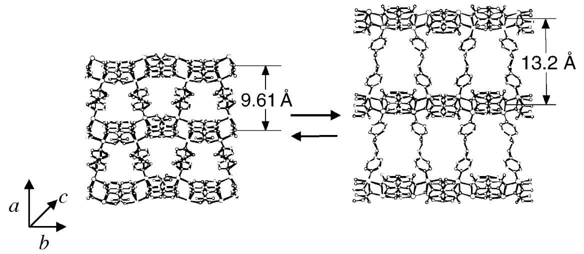

Figure 37. Reversible crystal-to-crystal structural transformation in $[Cu_2(pzdc)_2(dpyg)]_n$ involving the contraction and expansion of the channel by adsorption and desorption of H_2O or MeOH molecules.[167]

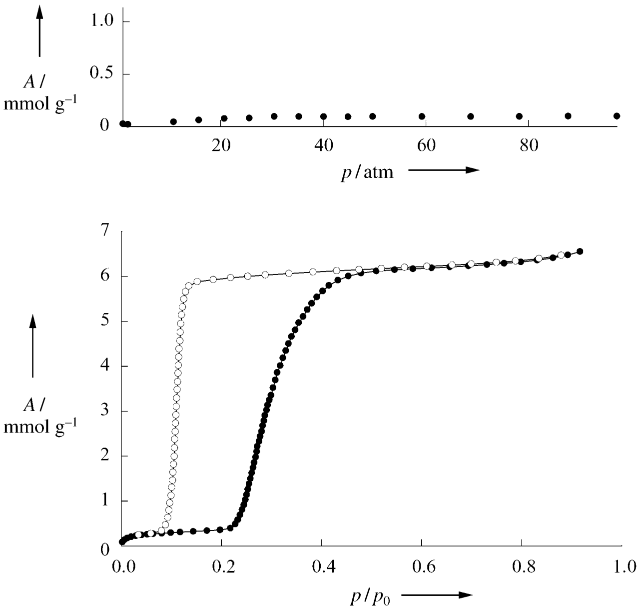

Figure 38. Adsorption isotherms of CH_4 (a) and MeOH (b) at 298 K in $[Cu_2(pzdc)_2(dpyg)]_n$.[167]

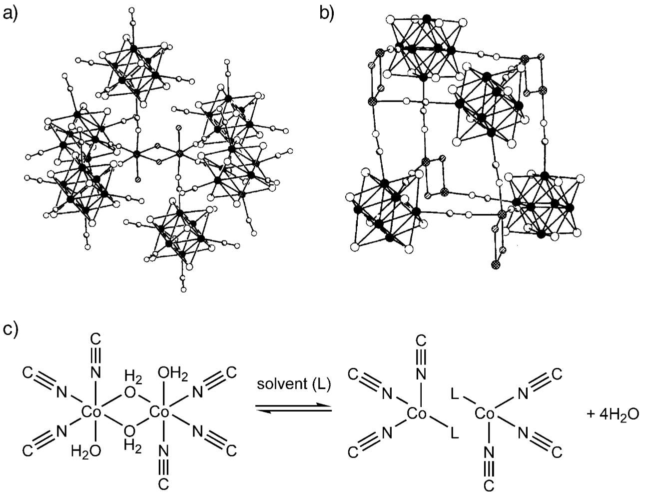

Figure 40. a) Local environment of $[Co_2(H_2O)_4]^{4+}$ clusters in the structure of $\{[Co_2(H_2O)_4][Re_6Q_8(CN)_6]\cdot 10\,H_2O\}_n$. The Co_2 and Re_6 clusters reside on crystallographic inversion centers. b) Cubelike cage unit defining the cavities in the structure of $\{[Co_2(H_2O)_4][Re_6Q_8(CN)_6]\cdot 10\,H_2O\}_n$. The small and large openings into the cavities correspond to the front and rear cage faces, respectively. c) Reversible structure transformation resulting from coordination bond cleavage and formation, conversion of octahedral $\{Co(NC)_3(H_2O)_3\}$ into $\{Co(NC)_3(L)\}$.[291]

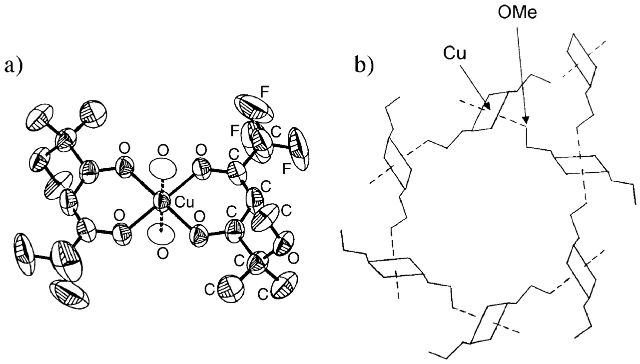

Figure 39. a) Cu^{II} complex as a building block in β-$\{[CuL_2]\cdot 2/3\,C_6H_6\}_n$ (L = 1,1,1-trifluoro-5-methoxy-5,5-dimethylacetylacetonate). b) Schematic representation showing how the Cu^{II} complexes are linked to form the channels. The dotted lines indicate a weak coordination interaction of Cu···O. The rectangles represent the roughly square-planar coordination environment around the Cu^{II} atoms located at the center of the rectangles.[310]

$\{Co(NC)_3(L)\}$; Figure 40c). Metal sulfonate based coordination networks exhibits a dynamic feature because of the flexible coordination properties of the weak Lewis base metal sulfonates. The 3D coordination network, $[Ag(3\text{-}pySO_3)]_n$, adsorbs MeCN selectively and change 3D structure from a tetragonal to a triclinic system.[333] In this example, for the network to rearrange, a weak Ag–O interaction is broken and a new Ag–O interaction is formed by rotation of the sulfonate group. An open framework, $\{[Cu_3(ptmtc)_2(py)_6(EtOH)_2(H_2O)]\}$ with a honeycomb arrangement of layers, has been synthesized (Figure 41 a and b).[317] In this framework, magnetic interactions exists between the Cu^{II} ions and the polychlorinated triphenylmethyl radicals, in which the central

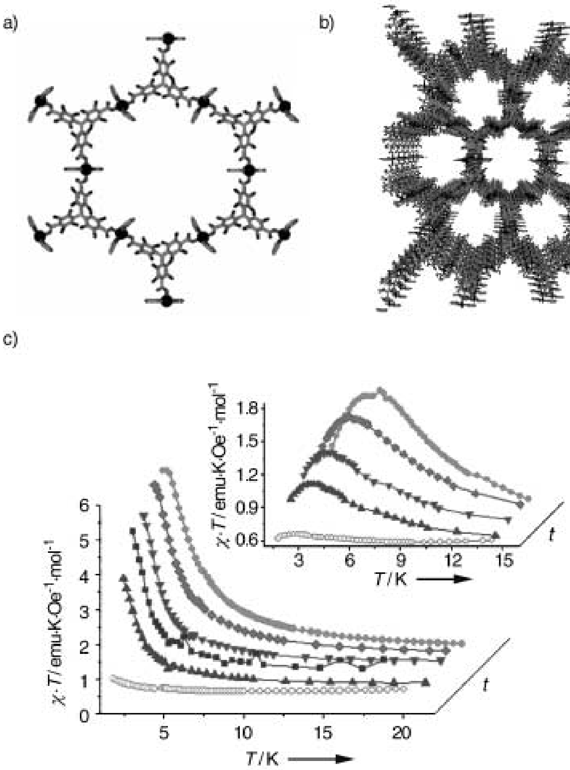

Figure 41. One hexagonal micropore (a) and a view of the distribution of the micropores of the open framework along the *c* axis (b) in $\{[Cu_3(ptmtc)_2(py)_6(EtOH)_2(H_2O)]\cdot 6\,H_2O\cdot 10\,EtOH\}_n$. c) Reversible magnetic behavior of the amorphous and evacuated phase in contact with EtOH liquid, as observed by plotting χT as a function of temperature *T* at a field of 1000 Oe. Inset: at 10000 Oe.[317]

carbon atom, where most of the spin density is localized, is sterically shielded by six bulky chlorine atoms. This framework shows a reversible and selective solvent-induced (MeOH or EtOH) structural transformation from the amorphous to the crystalline state that strongly influences the magnetic properties (Figure 41 c). This structural transformation may be due to the formation and cleavage of coordination bonds between the guest molecules and the Cu^{II} ions and of the hydrogen bonds between coordinated and included guest molecules.

Cleavage and formation of hydrogen bonds in coordination frameworks gives rise to changes in their overall structure. Typical hydrogen bonds found in coordination frameworks are listed in Table 5. Several 3rd generation compounds which have flexible channels as a result of hydrogen bonds have been prepared. Coordination networks constructed by Ni^{II} macrocyclic complex derivatives and carboxylate anions have been reported.[50,103,298,309,374,381,382] For instance, a 3D coordination network $[\{Ni(cyclam)(H_2O)\}_3(1,3,5\text{-btc})_2\cdot 24\,H_2O]_n$, (cyclam = 1,4,8,11-tetraazacyclotetradecane) which can be described as a molecular "floral lace", has been synthesized.[378] This framework is constructed by hydrogen bonds between btc^{3-} ions and water molecules binding to Ni^{II} cations, and has channels parallel to the *c* axis with dimensions of 10.3 Å in which guest water molecules are included (some of the guest water molecules are hydrogen bonded with the oxygen atoms of $1,3,5\text{-btc}^{3-}$). This framework undergoes a crystal-structure transformation on removal of guest water molecules. The original structure is regenerated when the dehydrated compound is immersed in water for a few minutes. In $\{[Ni_3(C_{20}H_{32}N_8)_3(ctc)_2]\cdot 16\,H_2O\}_n$ ($C_{20}H_{32}N_8$ = macrocyclic ligand: 1,8-(4-pyridylmethyl)-1,3,6,8,10,13-hexaazacyclotetradecane) each Ni^{II} macrocyclic unit binds two ctc^{3-} ions in the *trans* position and each ctc^{3-} ion coordinates to three Ni^{II} macrocyclic complexes. The result is a 2D honeycomb layer, in which pendant pyridine rings are involved in the herringbone π–π interaction and in N···O-H hydrogen bonds with carboxylic acids.[298,382] The XRPD pattern indicates that the framework deforms upon removal of H_2O guests but is restored upon rebinding of H_2O. This host solid binds $\{[Cu(NH_3)_4]\cdot 2\,ClO_4\}$ in MeCN. $\{[Cu(BF_4)_2(4,4'\text{-bpy})(H_2O)_2]\cdot 4,4'\text{-bpy}\}_n$ has 1D linear chains, which are linked by hydrogen bonds between metal-free 4,4′-bpy molecules and coordinated H_2O molecules, to form 2D noninterpenetrated sheets.[150] The adsorption of N_2, Ar, and CO_2 vapor begins suddenly at a certain relative pressure ("gate pressure"), there is almost no adsorption below the gate pressure.[314] Such a unique adsorption phenomenon is associated with the structure rearrangement involving the hydrogen bonds. $\{[Ni(NO_3)_2(4,4'\text{-bis(4-pyridyl)biphenyl})_2]\cdot 4(o\text{-xylene})\}_n$ has 2D square-grid layers of dimension 20 × 20 Å², which have a short interlayer separation of 4.1 Å. In this framework the layers stack on each other such that they overlap in one direction and are offset in the other direction which results in a channel dimension about 10 × 20 Å² (stacking mode A). Exchange of the adsorbed *o*-xylene molecules to mesitylene results in sliding of the stacking layers to give channel dimensions of approximately 15 × 20 Å² (stacking mode B).[297] In the stacking mode A, one of the C_6 rings of the bridging ligand forms C–H···O hydrogen bonds with NO_3 anions. However, in the stacking mode B, both of the C_6 rings form C–H···O hydrogen bonds, which means that cleavage and formation of hydrogen bonds occurs in this transformation.

Compound $[Co(H_2O)_6]H_2(tc\text{-ttf})\cdot H_2O$ has 1D channels, which are constructed by the 3D hydrogen-bonding network between $[Co(H_2O)_6]_2$, and $H_2(tc\text{-ttf})$ ions.[376] This compound shows a crystal-structure transformation on the removal of two water guest molecules (Figure 42). The breaking and formation of hydrogen bonds play an important role in this transformation. This change accompanies a reduction in the cross-sectional dimensions of the pseudo-rectangular channels within the framework: from about 9 × 7 to 8 × 5 Å. The anhydrous compound shows selective sorption for small polar molecules: water and methanol molecules can be incorporated, whereas ethanol, carbon disulfide, and acetonitrile are not. The frameworks of $\{[M_2(4,4'\text{-bpy})_3(NO_3)_4]\cdot x\,H_2O\}_n$ (M = Co, $x = 4$; Ni, $x = 4$; Zn, $x = 2$), which are best described as tongue-and-groove (bilayer) structures have been synthesized and their gas-adsorption properties investigated at ambient temperature under higher pressure.[47] In particular the detailed sorption properties and structural flexibility of $[Ni_2(4,4'\text{-bpy})_3(NO_3)_4]$, were investigated.[295,296] This structure has C–H···O hydrogen bonds between the nitrate anions bound directly to the metal ion and the bpy groups of every second bilayer, and breaking and formation of these C–H···O bonds gives this framework its flexible nature. The adsorption of EtOH results in the $[Ni_2(4,4'\text{-bpy})_3(NO_3)_4]$ structure undergoing a scissoring movement with a cell-dimension change of several percent; the isotherm is described by the Langmuir equation. This scissoring motion enables the framework to incorporate toluene molecules which are larger than the pore window. The MeOH adsorption isotherm has steps owing to the structural change of the adsorbent which allows adsorption on different surface sites after the complete occupation of the nitrate sites. Coordination networks constructed by Co^{II} and 3-pia have 2D structures made up of sheets of $[Co(NCS)_2(3\text{-pia})_2]$ which are stacked to form channels which have hydrogen-bonding groups lining their interiors.[153]. This compound shows a structure transformation, triggered by adsorption and desorption of guest molecules, which is attributable to a mutual sliding motion between the neighboring layers accompanied by an on/off

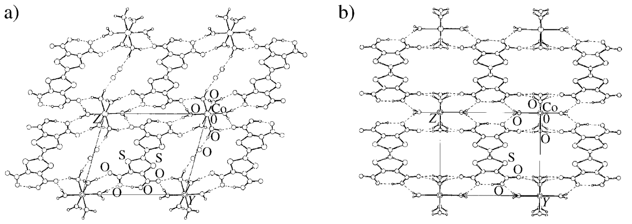

Figure 42. a) Projection of the structure of $[Co(H_2O)_6]H_2(tc\text{-ttf})\cdot H_2O$ down the *a* axis. For clarity, only one oxygen atom position of the disordered water molecule in the cavity is displayed. b) Projection of the structure of $[Co(H_2O)_6]H_2(tc\text{-ttf})$ (295 K) down the *a* axis.[376]

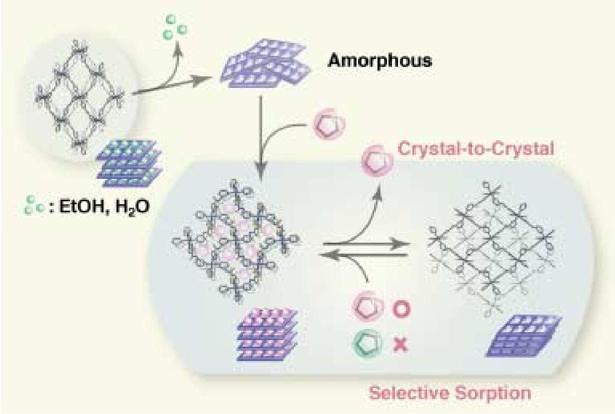

Figure 43. Crystal-to-crystal and amorphous-to-crystal transformations of $[Co(NCS)_2(3\text{-pia})_2]_n$ induced by thf guests.[153]

change of the hydrogen bond array of the amide groups (Figure 43).

4.3.2.2. *Rotation*

Rotation around a single bond provides structure flexibility (Table 5, Figure 36). A 3D coordination framework, $\{[Cu(in)]\cdot 2H_2O\}_n$ with an expandable structure responding to MeOH, EtOH and $CH_3(CH_2)_2OH$, has been synthesized.[318] This framework has a 1D channel, which selectively includes EtOH over pentane and $CH_3(CH_2)_2OH$. The springlike structure expansion along the channel on guest inclusion is probably due to rotation of the Cu–O or Cu–N bonds in the ligand. The X-ray crystal structure of $\{[Cu(pymo)_2]\cdot NH_4ClO_4\}_n$ reveals the square-planar coordination of the Cu^{II} ions which are linked together with bond angles of 120° by Hpymo units to generates a 3D porous framework with ammonium, ClO_4^-, and H_2O molecules included in the pores.[308] This complex reversibly and selectively sorbs $AClO_4$ salts (A = NH_4, Li, Na, K, and Rb) when exposed to $AClO_4$ aqueous solutions to give highly crystalline clathrates of $\{[Cu(pymo)_2]\cdot AClO_4\}_n$. Rotation of metal–nitrogen bonds plays an important role in this process.

A doubly interpenetrated (10,3)-b network is synthesized by using tpt and ZnI.[162] Despite this interlocking of the networks, 60 % of the unit-cell volume is occupied by the guest molecules, nitrobenzene. The unit-cell volume of this framework shrinks by 23 % when the guest molecules are removed and swells when they are returned (Figure 44). This springlike structure swelling and contraction are attributed to rotation of the Zn–N coordination bonds. The bilayer open framework structure $[Ni_2(C_{26}H_{52}N_{10})]_3(1,3,5\text{-btc})_4$, which is constructed from the dinickel(II) bismacrocyclic complex $[Ni_2(C_{26}H_{52}N_{10})]$ and 1,3,5-btc^{3-}, has 3D channels which are filled with 36 water and six pyridine guest molecules.[374] The channel walls created on the side of the bilayer are made of *p*-Xylyl pillars. By removal of all the pyridine and 32 water molecules, a sponge-like crystal structure transformation occurs which is due to the tilting of the pillars, which in turn is attributed to the rotation of the C–C bonds. The transformation takes place without breaking the single crystallinity.

4.3.2.3. *Breathing*

3D frameworks constructed by interpenetration and interdigitation are characteristic of coordination polymers. This kind of framework can have a dynamic nature which arises from the slip and glide motion of independent networks (Table 5). The crystal structure of $\{[Fe_2(NCS)_4(azpy)_4]\cdot EtOH\}_n$ reveals a double interpenetration of 2D rhombic grids that are constructed from Fe^{II} ions and azpy.[288] This framework provides 1D channels, parallel to the *c* axis, in which guest EtOH molecules are included. Adsorption and desorption of the guest molecules gives rise to structure transformation through the slipping motion of the interpenetrated layers which affects the compounds magnetic properties: the fully desorbed compound does not show spin crossover, whereas the EtOH and MeOH loaded compounds undergo a single-step spin crossover and the 1-propanol loaded compound undergoes a two-step crossover. The 3D coordination polymer, $\{[Cu_5(bpp)_8(SO_4)_4(EtOH)(H_2O)_5]\cdot SO_4\cdot EtOH\cdot 25.5H_2O\}_n$, has entangled 1D ribbons and 2D layers.[315] This framework undergoes reversible water adsorption and desorption accompanied by an amorphous to crystal transformation. A reversible spongelike structural change, which is probably due to variable ligand conformations and to the flexibility of the catenated architecture, was observed by atomic force microscopy (AFM).

Flexible and dynamic microporous coordination polymers based on interdigitation, $[Cu_2(dhbc)_2(4,4'\text{-bpy})]_n$ (CPL-p1), and interpenetration, $[Cu(1,4\text{-bdc})(4,4'\text{-bpy})_{0.5}]_n$ (CPL-v1), have been synthesized and characterized.[152,161] The structure of CPL-p1, contains a 2D interdigitated motif (Figure 45), and CPL-v1 gives a 3D interpenetrated motif (Figure 33). XRPD studies show that CPL-p1 undergoes a drastic crystal-struc-

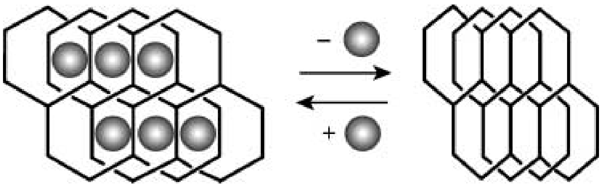

Figure 44. Schematic representation of the contraction and expansion of the 3D network of $\{[Zn_3I_6(tpt)_2]\cdot guests\}_n$ (guests = nitrobenzene and cyanobenzene), on removal and addition of guest molecules, respectively.[162]

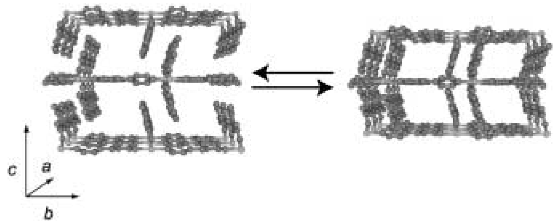

Figure 45. Reversible crystal-to-crystal structural transformation in $[Cu_2(dhbc)_2(4,4'\text{-bpy})]_n$ involving contraction and re-expansion of the channel on adsorption and desorption of supercritical gases.[152]

ture transformation triggered by desorption of included water and guest adsorption. A detailed structure investigation by synchrotron powder X-ray diffraction shows a cell-parameter change on dehydration from $a = 8.167(4)$, $b = 11.094(8)$, $c = 15.863(2)$ Å, and $\beta = 99.703(4)°$ to $a = 8.119(4)$, $b = 11.991(6)$, $c = 11.171\ (14)$ Å, and $\beta = 106.27(2)°$, which corresponds to a cell-volume contraction of 27%. This structure transformation of CPL-p1, especially the change of the length of the c axis, is accompanied by a shrinking of the layer gap, which is attributed to a glide motion of the two π-stack ring moieties, dhbc, which results in a decrease in the channel cross section (Figure 45). Interestingly, structure re-expansion was observed (confirmed by XRPD) when the compound is exposed to N_2 vapor below 160 K. This contraction and expansion behavior could be repeated many times. CPL-p1 shows characteristic hysteretic adsorption isotherms which have gate-opening and closing pressures for CO_2 vapor and various super critical gases (CH_4, O_2 and N_2; Figure 46 a). This behavior was observed on measuring the temperature dependence of the adsorption and desorption isotherms (Figure 46 b). This characteristic adsorption behavior should be attributed to crystal structure expansion and contraction triggered by gas adsorption and desorption, as confirmed by an XPRD study. CPL-v1 also shows similar adsorption isotherms, which result from a glide motion of interpenetrated networks. Note that only dynamic frameworks of the van - der Waals type can undergo a drastic structure transformation triggered by the adsorption and desorption of supercritical gases. This kind of coordination polymer could find application in gas separation and actuators.

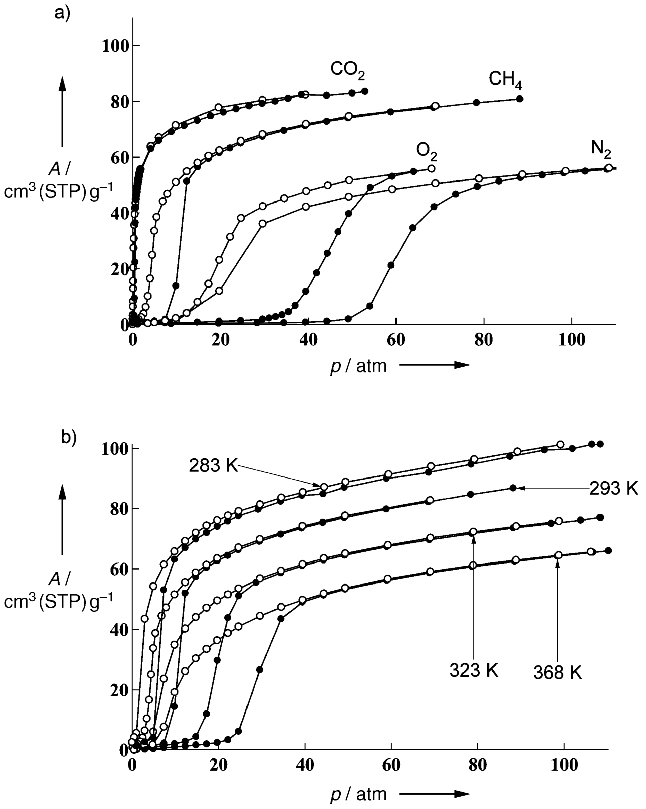

Figure 46. Porous properties of $[Cu_2(dhbc)_2(4,4'\text{-bpy})]_n$. a) Adsorption (filled circles) and desorption (open circles) isotherms of N_2, CH_4, CO_2, and O_2 at 298 K. b) Temperature dependence of adsorption (filled circles) and desorption (open circles) isotherms of CH_4 at 283, 293, 323, and 368 K.[152]

4.3.3. Crystal Transformation by Guest Exchange

Crystal transformation by guest exchange has been mainly observed in the case of anion-exchange processes. Reversible anion exchange accompanying a structural transformation was first reported in 1996.[339] The addition of a slight excess of $NaPF_6$ to a suspension of crystalline $[Ag(NO_3)(4,4'\text{-bpy})]_n$ in water at room temperature causes the exchange of NO_3^- for PF_6^- ions, which is 95% complete after 6 h. Inspection of the crystals under an optical microscope during the exchange process revealed that the crystals became opaque upon complete exchange; however, they still give a sharp X-ray powder diffraction pattern. On the other hand, upon the addition of KNO_3 to the exchanged solid, the transparency of the crystals is restored and their corresponding XRPD pattern is found to be indistinguishable from that of the original starting solid. $[Ag(edtpn)(NO_3)]_n$, which affords a 1D coordination polymer, undergoes anion-dependent rearrangement with recoordination of the Ag^I center.[337] During the anion exchange the supramolecular structural transformations between $[Ag(edtpn)(NO_3)]_n$, 2D-layer $\{[Ag(edtpn)]\cdot CF_3SO_3\}_n$, and boxlike 2D-network $\{[Ag(edtpn)]\cdot ClO_4\}_n$, are observed in the crystalline state (Figure 47). The infinite helices, $\{[Ag(Py_2O)]\cdot X\}_n$ ($X = NO_3$, BF_4, ClO_4, and PF_6), have counteranions arranged in two parallel columns inside the helix.[343] The four anions X can be exchanged for each other in an aqueous solution without destruction of the helical skeleton. The helical pitch is reversibly stretched by the anion-exchange and is proportional to the volume of the anion guest (Figure 48). On the other hand, Ag^I coordination polymers with the similar ligand, 3,3′-Py_2S, show slightly different phenomena.[338] The 2D network of $[Ag(3,3'\text{-}Py_2S)(NO_3)]_n$ is easily converted into the 1D helix $\{[Ag(3,3'\text{-}Py_2S)]\cdot PF_6\}_n$, but the reverse anion-exchange proceeds only slowly. The anions in $[Ag(L)(X)]_n$ (L = *N*,*N*′-bis(3-pyridinecarboxamide)-1,6-hexane; $X = NO_3^-$ and $CF_3SO_3^-$) with zigzag conformation can be replaced completely with ClO_4^- ions to produce a new crystalline phase of a twisted zigzag coordination polymer $\{[Ag(L)]\cdot ClO_4\}_n$.[344] However, the exchange is not reversible. In addition, interconversion between $[Ag(L)(NO_3)]_n$ and $[Ag(L)(CF_3SO_3)]_n$ by anion-exchange does not occur.

The exchange of neutral guest molecules is studied in the 3D $ThSi_2$-type network of $[Ag(4\text{-teb})(OTf)]_n$ (OTf = triflate),[334] which has 15 × 22 Å^2 channels. Guest exchange of non-functionalized aliphatic and aromatic molecules results in no structural changes in the original adduct of more than 0.4 Å per orthorhombic cell axis. However, crystals containing aromatic alcohol molecules can be indexed to the 2D rectangular analogue of an orthorhombic cell. $\{[Cd(CN)_2]\cdot 2/3\,H_2O\cdot t\text{BuOH}\}_n$, which forms a 3D network with honeycomb-

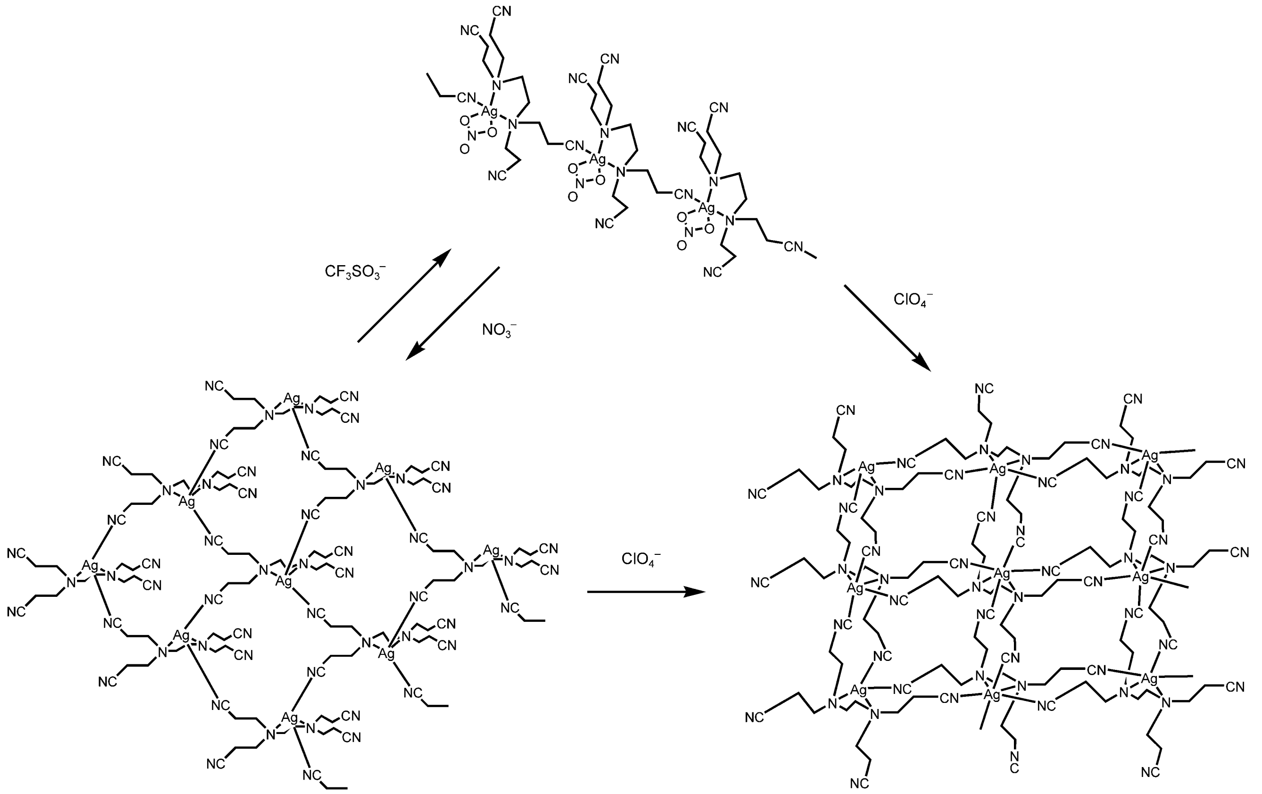

Figure 47. Structural rearrangement through anion exchange in [Ag(edtpn)(NO$_3$)]$_n$.

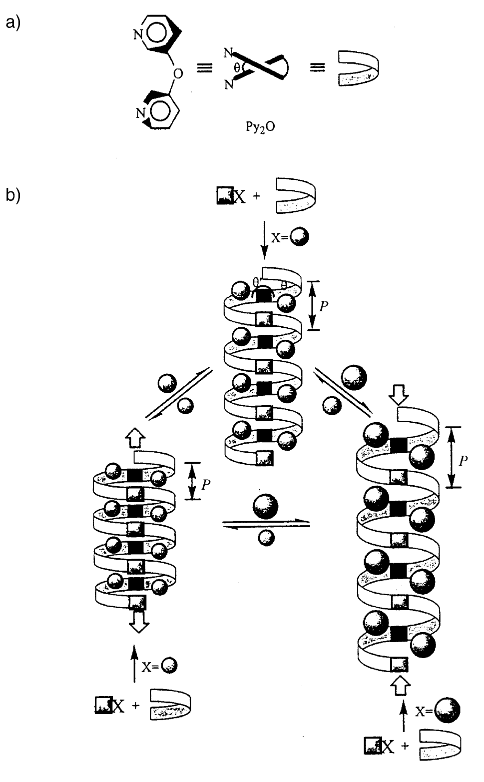

Figure 48. a) Schematic diagram of the stable skewed conformation of the Py$_2$O ligand. b) Design for the molecular spring from a combination of the linear Ag^I ion and the skewed Py$_2$O spacer, the pitch (*P*) is tuned through counteranion exchange.[343]

like channels, is transformed to the 3D diamond network $\{[Cd(CN)_2]\cdot CHCl_3\}_n$, when exposed to chloroform vapor.[383]

The mechanism of anion exchange in coordination polymers is not yet fully understood; however, there have been a number of attempts to rationalize the observations made during the exchange process. Thus, it has been proposed that anions diffuse from the solution into the framework without dissolution and recrystallization of the material, in other words, by a solid-state mechanism. However, macrosized single crystals of the initial phase rapidly lose their crystallinity turning opaque during the exchange reaction.[17,337,339] This observation indicates that a significant restructuring of the crystal occurs, as do changes in the crystallographic symmetry of the polymer. Such changes are inconsistent with the proposed solid-state mechanism. Therefore, it is important to show whether such guest exchanges occur by means of a solid-state or a solvent-mediated process, by using other measurements in addition to routinely utilized methods such as XRPD, IR, and elemental analysis. Interconversion of the chain coordination polymers $\{[Ag(4,4'\text{-}bpy)]\cdot X\}_n$ ($X = NO_3$ or BF_4) in aqueous media has been studied in detail by TEM and AFM which indicate a solvent-mediated rather than a solid-state mechanism for the exchange process.[342] The reversible anion exchange observed in 2D networks of $\{[Mn(L)_2(H_2O)_2]\cdot 2\,ClO_4\cdot 2\,H_2O\}_n$ and $\{[Mn(L)_2(H_2O)_2]\cdot 2\,NO_3\}_n$ (L = 1,3,5-tris(1-imidazolyl)benzene) is considered, on the basis of NMR and atomic adsorption spectroscopy, to be a solid-state phenomenon.[365]

4.3.4. *Crystal Transformation by Physical Stimulus*

Porous properties that respond to physical stimulus, such as light, magnetic and electric field besides heat, is another property of 3rd generation materials. Crystal-structure transformations of porous materials induced by physical stimulus have not been reported yet. In the case of inorganic mesoporous silica, several attempts to control the porous properties by light irradiation have been made. A periodic mesoporous organosilica MCM-41 containing *trans*-dpe incorporated in the silica walls has been synthesized.[384] UV radiation gives rise to the photochemical isomerization of the *trans*-dpe isomer (BET surface area : 350 $m^2 g^{-1}$, pore diameter : 39.8 Å) to the *cis*-dpe isomer (473 $m^2 g^{-1}$, 36.5 Å). Recently, the storage and release of organic molecules in mesoporous MCM-41 was successfully regulated by the photocontrolled and reversible intermolecular dimerization of coumarin derivatives attached to the pore outlets.[385] In this system, the cyclobutane coumarin dimers prevent passage through the pore outlets, thus capturing and releasing guest molecules, such as cholestane, pyrene, and phenanthrene. This kind of compound which responds to a physical stimulus is emerging in inorganic materials, whereas there are no examples of such behavior in coordination polymers at present. It is anticipated that 3rd generation materials which respond to physical stimuli will emerge in the near future and become a central topic in functional coordination polymers.

5. *Nanospace Laboratories*

5.1. *Low-Dimensional Molecular Arrays in Micropores*

Molecules confined in a channel form a specific assembly owing to the channel's restricting geometry and the adsorption enhancement by the overlapping of the interaction potentials from the opposing and neighboring channel walls. Figure 49 shows the potential profiles of CH_4 in a slit-shaped graphite pore as a function of the slit gap, *w*.[259] The molecular position in Figure 49 is expressed by a distance *z* from the central plane between two surfaces. The potential becomes deeper with decreasing *w* value, and reaches about −2700 K ($w = 5$ Å). Needless to say, a 1D rectangular channel surrounded by four pore walls provides a deeper potential than a slit-shaped pore. This kind of confinement effect can be considered as the stabilization effect of micropores that enables the preparation of an ordered array of specific molecules, which is not stable as a bulk fluid. Contemporary studies have focused on synthetic strategies to obtain regular, highly ordered pore or channel structures to control the orientation and/or conformational properties of confined guest molecules.[386] Formation of a low-dimensional assembly, such as a 1D chain or ladder, is one of the most attractive challenges because of the unusual quantum properties of such species and their potential use as nanowire materials for nanoconnectors and nanoscale devices.[387] Usually, the preparation of nanowire arrays needs rigorous reaction conditions and their structures are not very stable.[388,389] On the other hand, utilization of the 1D channels of microporous materials is an alternative method for the formation of stable 1D arrays.

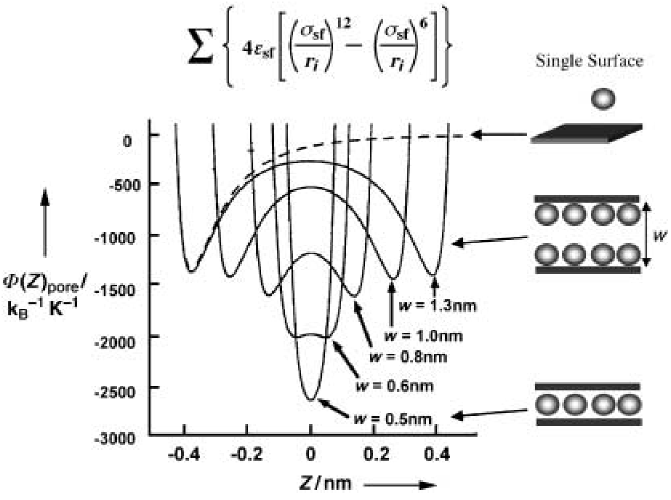

Figure 49. Potential profile of CH_4 with the graphitic slit-pore as a function of the pore width *w*.[259]

A 1D I_2-chain array was prepared by using a 1D channel of the molecular assembly of ttp, which has a quasi-cylindrical channel topology with the dimensions of 5 Å.[390] The inclusion of I_2 in this 1D channel gives a 1D I_2 chain array along the channel direction. There is a translational disorder of I_2 molecules along the channel direction owing to the incommensurate relationship between the I_2 (van der Waals length 5.8 Å) and host structure (10 Å). This I_2 chain exhibits electric conductivity: the $\sigma_{\parallel}$ values are in the order of 10^{-6}–10^{-8} $S\,m^{-1}$ for a potential of 50 V and are enhanced by a factor of 30–300 for 500–1000 V. The observed anisotropy factor ($\sigma_{\parallel}$, $\sigma_{\perp}$) of 30 is a result of the 1D chain structure.

Self-assembly of calix[4]hydroquione (chq) provides 1D rectangular pores of 6×6 $Å^2$ with redox active pore walls. Silver nanowires with 4 Å width and micrometer-scale length form inside the 1D pore of chq by electro- or photochemical redox reactions in an aqueous phase (Figure 50). The wires exist as coherently oriented 3D arrays.[391] The band structure obtained by theoretical calculations suggests that these silver nanowires have a metallic nature and three conducting channels for electronic transport.

The specific array of polar molecules is primarily associated with the second harmonic generation (SHG). Polar arrays with SHG activity are formed in 1D channel-like cavities of organic host frameworks.[392,393] For example, organic host frameworks, constructed by hydrogen bonds between guanidinium and organodisulfonate ions, have a pillared layer structure with 1D channels between the layers in which guest molecules are included during the crystallization.[394,395] Inclusion host compound {G_2tmbds·(*N*,*N*-dimethyl-4-nitroaniline)} (G = guanidinium) shows SHG activity 10-times higher than that of potassium dihydrogen phosphate (KDP).[393]

To date several metallic nanowires of transition metals, such as Pt, Ag, Au, and bimetallic Pt/Rh, have been synthesized by using inorganic mesoporous materials and carbon nanotubes. For example, Pt nanowires with diameter

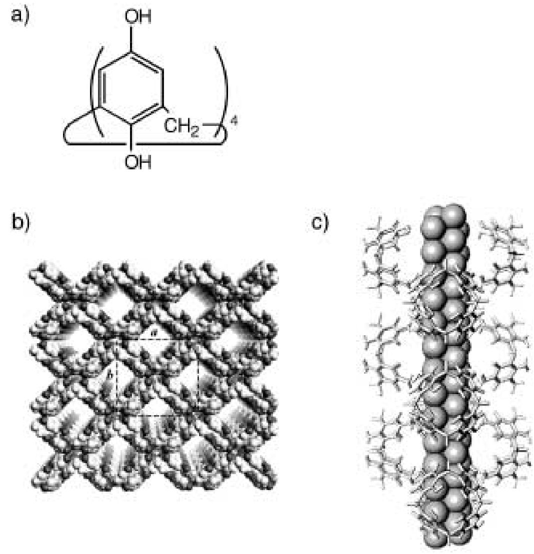

Figure 50. a) Molecular structure of chq. b) chq nanotube arrays with pores of 6×6 Å^2 (van der Waals volume excluded), The pores are separated by 1.7 nm from each other. c) Silver nanowires (space-filled model) inside the chq nanotubes (stick model).[391]

of 30 Å were synthesized using mesoporous silica, MCM-41, and their structures were characterized by transmission electron microscopy (TEM).[396] This nanowire is stable up to 500 °C in the channel. A Pt/Rh mixed-metal nanowire was synthesized by using mesoporous hybrid material, HMM-1, whose pore diameter is 31 Å. This Pt–Rh nanowire shows two- or three-times higher magnetization than expected from the simple sum of the values of bulk Pt and Rh, and is a result of the low dimensionality of the metal topology.[397]

Microporous coordination polymers are one of the most plausible candidates for the formation of specific molecular arrays because of their highly designable nature and pore homogeneity. 1D channels with cross-sectional sizes ranging from ultramicropore to mesopore range (Table 1) have been created with coordination polymers.[130,158,229,276] The principal purpose is to accommodate a large number of a certain molecule (storage) and/or a specific molecule from a number of others (separation and exchange) in their pores. Sometimes, 1D arrays of solvent molecules result from the crystallization process.[124,128,229,292,310,318,398] O_2 and NO are among the smallest stable paramagnetic molecules under ambient conditions and have the potential to form new molecular-based magnetic and dielectric materials. However, many attempts to form 1D arrays of these paramagnetic gas molecules through confinement of the molecules in porous coordination polymers[399] as well as carbon materials[400,401] were not successful. Unlike aromatic and polar molecules which can take part in intermolecular interactions, such as π–π stacking and hydrogen bonding, these simple molecules can only enter into weak van der Waals force interactions which are not strong enough to form 1D assemblies. To form a regular assembly of the simple molecules, utilization of a uniform ultramicropore, which can induce a strong confinement effect, is a key idea. Very recently, a 1D ladder structure of O_2 was successfully formed in a copper coordination polymer, $[Cu_2(pzdc)_2(pyz)]_n$ (CPL-1) whose pore size is 4×6 Å^2.[303] The 1D ordered array of O_2 molecules was characterized by high-resolution synchrotron X-ray diffraction (Figure 51 a). The X-ray structure analysis reveals that O_2 molecules are in the a solid state rather than the liquid state even at 130 K under 80 kPa (0.79 atm), which is much higher than the boiling point of bulk O_2 under atmospheric pressure, 54.4 K. This result is ascribed to the strong confinement effect of CPL-1. The magnetic susceptibility for adsorbed O_2 molecules approaches zero with decreasing temperature,

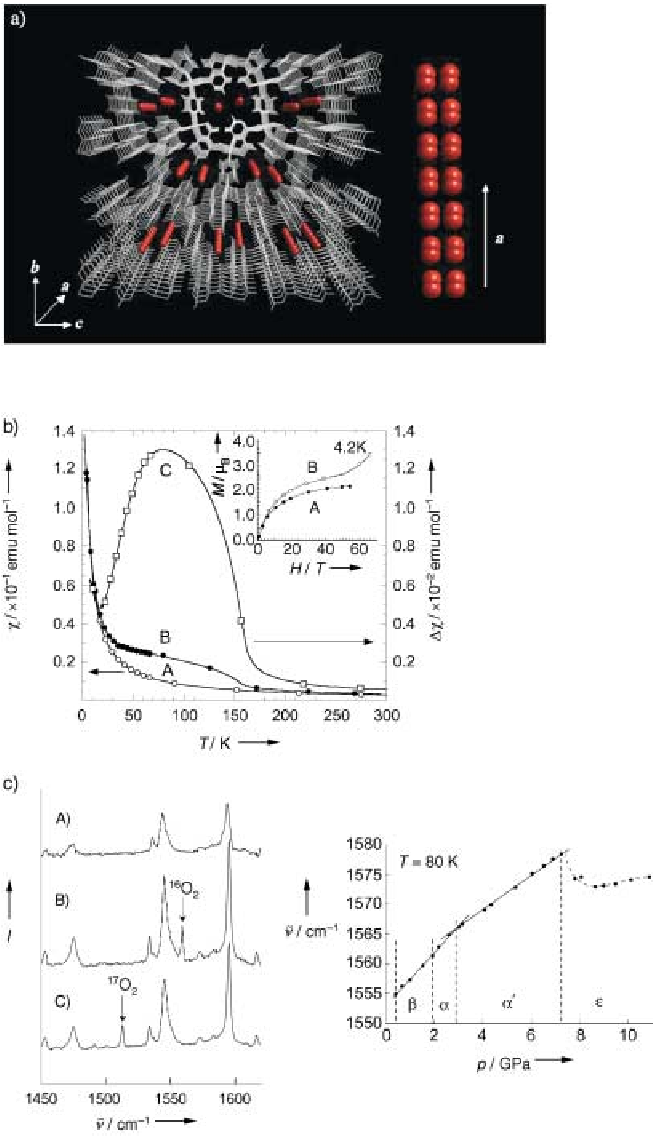

Figure 51. a) A perspective view of CPL-1 down the *a* axis with adsorbed O_2 (left) and the O_2 ladder structure (right) at 90 K. b) Temperature dependence of the susceptibility of A) CPL-1 and B) CPL-1 with O_2 molecules, and C) the difference curve. Inset: high-field magnetization of (A) and (B). c) Left: Raman spectra at 90 K of A) CPL-1, B) CPL-1 with 80 kPa of $^{16}O_2$, and C) 80 kPa of $^{17}O_2$ molecules. A peak due to the stretching of adsorbed O_2 molecules is marked by an arrow. The abscissas were calibrated using the standard lines form a neon lamp, and the resolution of the data is 0.6 cm^{-1}. Right: Pressure dependence of the vibrational energies of solid oxygen at 80 K.[303]

which indicates a nonmagnetic ground state of the antiferromagnetic dimer $(O_2)_2$ (Figure 51 b). The antiferromagnetic interaction is estimated to be $J/k_B \approx -50$ K which is larger than that of α-phase of $J/k_B \approx -30$ K ($H = -2J\boldsymbol{S}_1\boldsymbol{S}_2$).[402] The Raman spectrum the O_2 stretching-vibration mode appears as a sharp peak at a higher energy than that of solid α-O_2 under atmospheric pressure and comparable to that of α-O_2 under 2 GPa (2.0×10^4 atm; Figure 51 c).[403]

Importantly, a porous host promotes the formation of a specific assembly of guest molecules, which can not be obtained under other conditions, actually stabilizing it through the effective deep attractive potential of micropores. The micropore can thus be regarded as a so-called "nanospace laboratory". The word "nanoreactor" has a similar definition to nanospace laboratory and has been known for several years. Nanoreactor means a series of nanosized reaction vessels for syntheses of new compounds with the aid of their specific nanospace. On the other hand, the nanospace laboratory contains not only the nanoreactor but also specific arrangement of molecules and functions, such as nonlinear optical and magnetic properties.

5.2. Molecules and Atoms Confined in Nanospace

Molecules and atoms confined and ordered in a nanospace have properties characteristic of low-dimensional and nanosized assemblies. In addition, a nanospace could exert a pressure effect on guest molecules, for instance a spin crossover in accommodated transition-metal complexes.[228] [Co(2,2′-bpy)$_3$][NaCr(ox)$_3$] has a honeycomb framework of [NaCr(ox)$_3$], whose hexagonal cavities incorporate a guest [Co(2,2′-bpy)$_3$]$^{2+}$ ion. In this system, the cation has a high-spin state of $^4T_1(t_{2g}{}^5e_g{}^2)$, as in the corresponding bulk solid. When Na^+ is replaced by the smaller Li^+ ion, the cavity size of the framework becomes smaller. The resulting steric pressure leads to a shortening of the Co–N(2,2′-bpy) bond length, and the low-spin ground state, $^2E(t_{2g}{}^6e_g{}^1)$. Thus [Co(2,2′-bpy)$_3$][LiCr(ox)$_3$] can be converted into a spin-crossover system by a nanosized pore, (see the temperature-dependent magnetic susceptibility measurement Figure 52).

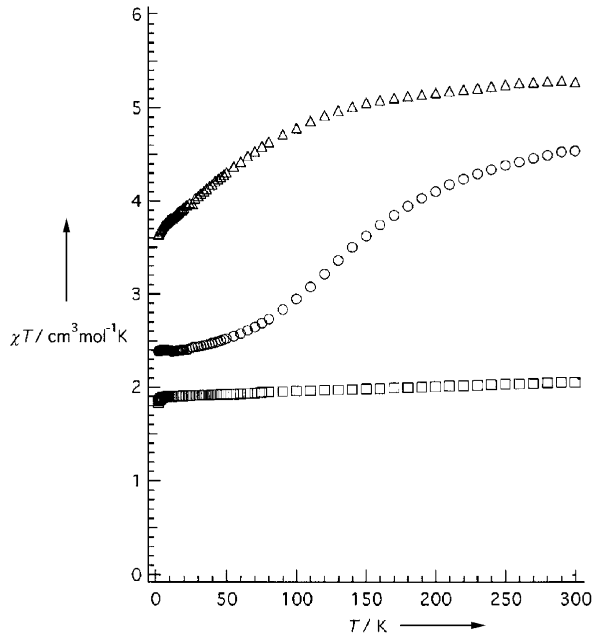

Figure 52. Magnetic susceptibilities of polycrystalline samples of [Co(2,2′-bpy)$_3$][NaCr(ox)$_3$] (open triangle), [Co(2,2′-bpy)$_3$][LiCr(ox)$_3$] (-open circle), and [Zn(2,2′-bpy)3][NaCr(ox)$_3$] (open square) plotted as χ*T* versus temperature.[228]

An isolated metal cluster of a nonmagnetic element is expected to exhibit a magnetic moment when it has an odd number of electrons. When such clusters are arranged periodically and their magnetic moments interact mutually, the magnetic properties of the resulting materials are expected to be significantly different from the isolated clusters but also from the original bulk material. Periodically arranged potassium clusters were prepared from zeolite LTA by the vapor diffusion of potassium. This K-LTA system shows ferromagnetism below about 4 K.[404] The properties of the low-dimensional quantum fluids, ^{3}He and ^{4}He, have attracted physicists. ^{4}He molecules confined in the mesoporous silica, FSM-16 (1D pore with dimensions of 18 Å), shows a rise of on-set temperature, T_o, for the superfluid state.[405] The smaller the pore size becomes, the higher the T_o value observed: in the case of FSM-16-^{4}He, the T_o value is more than 10-times higher than that of a 2D fluid of ^{4}He on a mylar film. This T_o-rise effect is associated with a strong confinement effect. These types of physical properties of confined guests, or cooperative phenomena of both guests and frameworks would be expected for porous coordination polymers because of the designable flexibility of their frameworks, and the possibility of incorporating redox- and photoactive building blocks. Coordination polymers with these properties will certainly appear in the next decade.

6. Perspectives

As shown above, molecules and atoms confined in nanospaces exhibit interesting properties, which are not observed in the corresponding bulk state. To develop the chemistry and physics of confined molecules and atoms in the low-dimensional nanospace, the precise controlling and tuning of the pore size, shape, and periodicity of a unit are of great importance. For this purpose, possible candidates are mesoporous silicas (for mesopores) and coordination polymers (for micropores). For di- and tri-atomic molecules, microporous compounds are the most relevant because their frames are well-suited for trapping and arranging such molecules in a channel. In particular coordination polymers can play an important role in the "gas molecule-accumulation science" of gases such as H_2, O_2, CO, NO, CO_2, and CH_4 which are associated with important environmental and energy issues.

A great number of coordination polymers have been reported (see Figure 1). The data on these compounds should be categorized into 1) structure and 2) function. On this basis, we can then search for the porous structure most suitable for

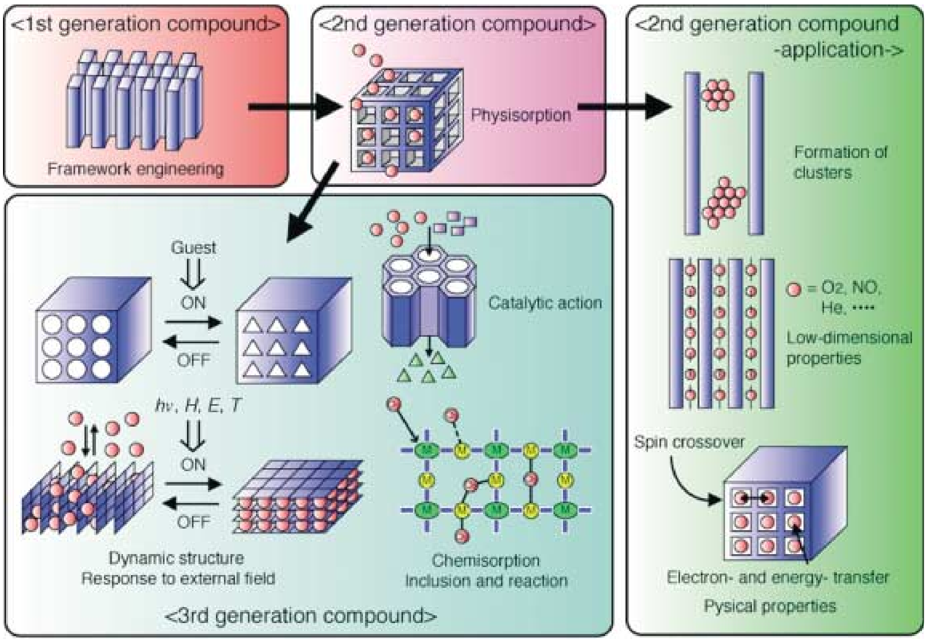

Figure 53. A selection of porous functions created by porous coordination polymers ("nanospace laboratory").

the properties demanded. The porous functions catalogued in Tables 3 and 4 are shown in Figure 53; some of them have already been realized and others are yet to be created.[386] In addition to these functions, form (shape, and size of crystals) needs to be considered.

The followings are categories for future porous coordination polymers:

1) Cooperative properties with functional frameworks and guests: porous coordination polymers, whatever their structural dimensionality is, possess two inherent components, the porous framework and the guest molecule. The properties of functional guests and those of porous frameworks (nonlinear optical, conductivity, magnetism, spin crossover, chromism, fluorescent) have been studied independently to date. Several examples have been reported of framework properties that change on inclusion and removal of guest molecules, and which induce a change in the environment of the metal centers. In these systems, the guest molecules have no function. Next step is to research the cooperative properties of functional frameworks and functional guest molecules. In the restricted micropore, unprecedented cooperative properties are expected.
2) Thin layer compounds: controlling the size, shape, and distribution of pores is one thing, however, even when they have nano-sized channels or cavities, the crystals of the compounds themselves are at least μm-sized, and insoluble in any solvents, and therefore, the preparation of a thin-layer form is not possible. A method to prepare a 2D sample is not yet available.
3) Mesoscale compounds: The next challenge in this field is at the mesoscale, with the aim of closing the gap between so-called top-down and bottom-up approaches to materials assembly. The ultimate goal is the ability to control the arrangement of channels, which means the formation of porous modules for various nanodevices. For this development small nanocrystals are required, which are wells, wires, rods, and dots.[406]

Abbreviations

adb	4,4′-azodibenzoate
atc	11,3,5,7-adamantanetetracarboxylate
azpy	4,4′-azopyridine
bdc	benzenedicarboxylate
bz	benzoate
bedt-ttf	bis(ethylenedithio)tetrathiafulvalene
ben	benzene
bpcah	*N*,*N*′-bis(3-pyridinecarboxamide)1,6-hexane
bpdc	4,4′-biphenyldicarboxylate
bpm	2,2′-bipyrimidine
bpp	1,3-bis(4-pyridyl)propane
bptp	4,6-bis(2′-pyridylthio)pyrimidine
bpy	bipyridine
btb	4,4′,4′′-benzen-1,3,5-triyl-tribenzoate
btc	benzenetricarboxylate
ca	chloranilate
chq	calix[4]hydroquinone
ctc	*cis*,*cis*-1,3,5-cyclohexanetricarboxylate
dabco	1,4-diazabicyclo[2.2.2]octane
def	*N*,*N*′-diethylformamide
dma	*N*,*N*-dimethylacetamide
dmf	dimethylformamide
dmpyz	2,5-dimethylpyrazine
dmso	dimethylsulfoxide

dpe	1,2-di(4-pyridyl)ethylene
dpyg	1,2-di(4-pyridyl)glycol
edtpn	ethylendiaminetetrapropionitrile
eg	ethylenglycol
hat	1,4,5,8,9,12-hexaazatriphenylene
Hbpca	bis(2-pyridylcarbonyl)amine
Hdhbc	,5-dihydroxybenzoic acid
Hdimto	4,6-di(1-imidazolyl)-1,3,5-triazine-2-one
Hpymo	2-hydroxypyrimidine
H_6tta	4,4′,4″-tris(*N*,*N*-bis(4-carboxyphenyl)amino)triphenylamine
im	imidazole
in	isonicotinate
ndc	2,6-naphthalenedicarboxylate
1,5-nds	1,5-naphthalenedisulfonate
ohphz	1,2,3,4,6,7,8,9-octahydrophenazine
ox	oxalate
pbaOH	2-hydroxy-1,3-propylenebis(oxamato)
1,2-pd	1,2-propandiol
pda	1,4-phenylendiacetate
phz	phenazine
pia	*N*-pyridylisonicotinamide
pna	*N*-pyridylnicotinamide
ptmtc	tris(2,3,5,6-tetrachloro-4-carboxyphenyl)methyl radical
py	pyridine
pyre	diazapyrene
Py_2O	oxybispyridine
Py_2S	thiobispyridine
3-$pySO_3$	3-pyridinesulfonate
pyz	pyrazine
pzdc	pyrazine-2,3-dicarboxylate
salphdc	*N*,*N*′-phenylenebis(salicylideneiminedicarboxylate)
suc	succinate
tcnb	1,2,4,5-tetracyanobenzene
tcpp	tetra(4-carboxyphenyl)porphyrin
tc-ttf	tetra(carbonyl)tetrathiafulvalene
4-teb	1,3,5-tirs(4-ethynylbenzonitrile)benzene
thf	tetrahydrofurane
tib	tetrakis(imidazolyl)borate
tol	toluene
tpt	2,4,6-tri(4-pyridyl)-1,3,5-triazine
ttp	tris(*o*-phenylenedioxy)cyclotriphosphazene

Our research has been supported by a Grant-in-Aid for Creative Scientific Research (No. 13GS0024) from the Japanese Ministry of Education, Culture, Sport, Science and Technology.

Received: May 26, 2003 [A610]

---

[1] C. Janiak, *Angew. Chem.* **1997**, *109*, 1499–1502; *Angew. Chem. Int. Ed. Engl.* **1997**, *36*, 1431–1434.

[2] S. R. Batten, R. Robson, *Angew. Chem.* **1998**, *110*, 1558–1595; *Angew. Chem. Int. Ed.* **1998**, *37*, 1460–1494.

[3] A. J. Blake, N. R. Champness, P. Hubberstey, W.-S. Li, M. A. Withersby, M. Schröder, *Coord. Chem. Rev.* **1999**, *183*, 117–138.

[4] M. Eddaoudi, D. B. Moler, H. Li, B. Chen, T. M. Reineke, M. O'Keeffe, O. M. Yaghi, *Acc. Chem. Res.* **2001**, *34*, 319–330.

[5] O. R. Evans, W. Lin, *Acc. Chem. Res.* **2002**, *35*, 511–522.

[6] I. Goldberg, *Chem. Eur. J.* **2000**, *6*, 3863–3870.

[7] P. J. Hagrman, D. Hagrman, J. Zubieta, *Angew. Chem.* **1999**, *111*, 2798–2848; *Angew. Chem. Int. Ed.* **1999**, *38*, 2638–2684.

[8] A. N. Khlobystov, A. J. Blake, N. R. Champness, D. A. Lemenovskii, A. G. Majouga, N. V. Zyk, M. Schröder, *Coord. Chem. Rev.* **2001**, *222*, 155–192.

[9] K. Kim, *Chem. Soc. Rev.* **2002**, *31*, 96–107.

[10] S. Kitagawa, M. Munakata, *Trends Inorg. Chem.* **1993**, *3*, 437–462.

[11] S. Kitagawa, M. Kondo, *Bull. Chem. Soc. Jpn.* **1998**, *71*, 1739–1753.

[12] S. Kitagawa, R. Kitaura, *Comments Inorg. Chem.* **2002**, *23*, 101–126.

[13] S. Kitagawa, S. Kawata, *Coord. Chem. Rev.* **2002**, *224*, 11–34.

[14] B. Moulton, M. J. Zaworotko, *Chem. Rev.* **2001**, *101*, 1629–1658.

[15] M. Munakata, *Adv. Inorg. Chem.* **1998**, *46*, 173–303.

[16] H. Okawa, M. Ohba, *Bull. Chem. Soc. Jpn.* **2002**, *75*, 1191–1203.

[17] O. M. Yaghi, H. Li, C. Davis, D. Richardson, T. L. Groy, *Acc. Chem. Res.* **1998**, *31*, 474–484.

[18] M. J. Zaworotko, *Chem. Soc. Rev.* **1994**, *23*, 283–288.

[19] M. J. Zaworotko, *Chem. Commun.* **2001**, 1–9.

[20] C. Janiak, *J. Chem. Soc. Dalton Trans.* **2003**, 2781–2804.

[21] O. M. Yaghi, M. O'Keeffe, N. W. Ockwig, H. K. Chae, M. Eddaoudi, J. Kim, *Nature* **2003**, *423*, 705–714.

[22] S. L. James, *Chem. Soc. Rev.* **2003**, *32*, 276–288.

[23] "Coordination Polymers": J. C. Bailar, Jr., *Prep. Inorg. React.* **1964**, *1*.

[24] D. W. Breck, *Zeolite Molecular Sieves*: *Structure*, *Chemistry*, *and Use*, Wiley, New York, **1974**.

[25] W. M. Meier, D. H. Olsen, C. Baerlocher, *Atlas of Zeolite Structure Types*, Elsevier, London, **1996**.

[26] P. B. Venuto, *Microporous Mater.* **1994**, *2*, 297–411.

[27] H. de Sainte Claire Deville, *C. R. Hebd. Seances Acad. Sci.* **1862**, *54*, 324.

[28] J. V. Smith, *Chem. Rev.* **1988**, *88*, 149–182.

[29] S. T. Wilson, B. M. Lok, C. A. Messina, T. R. Cannan, E. M. Flanigen, *J. Am. Chem. Soc.* **1982**, *104*, 1146–1147.

[30] B. M. Weckhuysen, R. R. Rao, J. A. Martens, R. A. Schoonheydt, *Eur. J. Inorg. Chem.* **1999**, 565–577.

[31] A. K. Cheetham, G. Ferey, T. Loiseau, *Angew. Chem.* **1999**, *111*, 3466–3492; *Angew. Chem. Int. Ed.* **1999**, *38*, 3268–3292.

[32] C. T. Kresge, M. E. Leonowicz, W. J. Roth, J. C. Vartuli, J. S. Beck, *Nature* **1992**, *359*, 710–712.

[33] A. Corma, *Chem. Rev.* **1997**, *97*, 2373–2419.

[34] J. Y. Ying, C. P. Mehnert, M. S. Wong, *Angew. Chem.* **1999**, *111*, 58–82; *Angew. Chem. Int. Ed.* **1999**, *38*, 56–77.

[35] S. Inagaki, S. Guan, T. Ohsuna, O. Terasaki, *Nature* **2002**, *416*, 304–307.

[36] R. M. Barrer, *Molecular Sieves*, American Chemical Society, Washington, **1974**.

[37] R. E. Wilde, S. N. Ghosh, B. J. Marshall, *Inorg. Chem.* **1970**, *9*, 2512–2516.

[38] H. J. Buser, D. Schwarzenbach, W. Petter, A. Ludi, *Inorg. Chem.* **1977**, *16*, 2704–2710.

[39] K. R. Dunbar, R. A. Heintz, *Prog. Inorg. Chem.* **1997**, *45*, 283–391.

[40] T. Iwamoto, *Inclusion Compd.* **1984**, *1*, 29–57.

[41] T. Iwamoto, *Inclusion Compd.* **1991**, *5*, 172–212.

[42] Y. Kinoshita, I. Matsubara, T. Higuchi, Y. Saito, *Bull. Chem. Soc. Jpn.* **1959**, *32*, 1221–1226.

[43] B. F. Hoskins, R. Robson, *J. Am. Chem. Soc.* **1990**, *112*, 1546–1554.

[44] M. Fujita, Y. J. Kwon, S. Washizu, K. Ogura, *J. Am. Chem. Soc.* **1994**, *116*, 1151 – 1152.
[45] O. M. Yaghi, G. Li, H. Li, *Nature* **1995**, *378*, 703 – 706.
[46] D. Venkataraman, G. B. Gardner, S. Lee, J. S. Moore, *J. Am. Chem. Soc.* **1995**, *117*, 11 600 – 11 601.
[47] M. Kondo, T. Yoshitomi, K. Seki, H. Matsuzaka, S. Kitagawa, *Angew. Chem.* **1997**, *109*, 1844 – 1846; *Angew. Chem. Int. Ed. Engl.* **1997**, *36*, 1725 – 1727.
[48] L. Pan, K. M. Adams, H. E. Hernandez, X. Wang, C. Zheng, Y. Hattori, K. Kaneko, *J. Am. Chem. Soc.* **2003**, *125*, 3062 – 3067.
[49] T. M. Reineke, M. Eddaoudi, M. Fehr, D. Kelley, O. M. Yaghi, *J. Am. Chem. Soc.* **1999**, *121*, 1651 – 1657.
[50] H. J. Choi, M. P. Suh, *Inorg. Chem.* **1999**, *38*, 6309 – 6312.
[51] H. Okamoto, M. Yamashita, *Bull. Chem. Soc. Jpn.* **1998**, *71*, 2023 – 2039.
[52] R. J. H. Clark, *Chem. Soc. Rev.* **1990**, *19*, 107 – 131.
[53] B. Scott, R. Willett, L. Porter, J. Williams, *Inorg. Chem.* **1992**, *31*, 2483 – 2492.
[54] O. M. Yaghi, G. Li, *Angew. Chem.* **1995**, *107*, 232 – 234; *Angew. Chem. Int. Ed. Engl.* **1995**, *34*, 207 – 209.
[55] S. Kawata, S. Kitagawa, H. Kumagai, S. Iwabuchi, M. Katada, *Inorg. Chim. Acta* **1998**, *267*, 143 – 145.
[56] A. J. Blake, N. R. Brooks, N. R. Champness, P. A. Cooke, A. M. Deveson, D. Fenske, P. Hubberstey, W.-S. Li, M. Schröder, *J. Chem. Soc. Dalton Trans.* **1999**, 2103 – 2110.
[57] D. J. Chesnut, A. Kusnetzow, R. R. Birge, J. Zubieta, *Inorg. Chem.* **1999**, *38*, 2663 – 2671.
[58] A. M. A. Ibrahim, E. Siebel, R. D. Fischer, *Inorg. Chem.* **1998**, *37*, 3521 – 3525.
[59] D. J. Chesnut, D. Plewak, J. Zubieta, *J. Chem. Soc. Dalton Trans.* **2001**, 2567 – 2580.
[60] P. C. Healy, C. P. Pakawatchai, R. I. Papasergio, V. A. Patrick, A. H. White, *Inorg. Chem.* **1984**, *23*, 3769 – 3776.
[61] A. J. Blake, N. R. Brooks, N. R. Champness, M. Crew, L. R. Hanton, P. Hubberstey, S. Parsons, M. Schröder, *J. Chem. Soc. Dalton Trans.* **1999**, 2813 – 2817.
[62] D. B. Leznoff, B.-Y. Xue, R. J. Batchelor, F. W. B. Einstein, B. O. Patrick, *Inorg. Chem.* **2001**, *40*, 6026 – 6034.
[63] W.-F. Yeung, W.-T. Wong, J.-L. Zuo, T.-C. Lau, *J. Chem. Soc. Dalton Trans.* **2000**, 629 – 631.
[64] V. Niel, M. C. Muñoz, A. B. Gaspar, A. Galet, G. Levchenko, J. A. Real, *Chem. Eur. J.* **2002**, *8*, 2446 – 2453.
[65] T. Iwamoto, T. Soma, *Inorg. Chem.* **1996**, *35*, 1849 – 1856.
[66] G. A. Bowmaker, Effendy, J. C. Reid, C. E. F. Rickard, B. W. Skelton, A. H. White, *J. Chem. Soc. Dalton Trans.* **1998**, 2139 – 2146.
[67] S. Nishikiori, *J. Coord. Chem.* **1996**, *37*, 23 – 38.
[68] S.-S. Yun, Y.-P. Kim, C.-H. Kim, *Acta Crystallogr. Sect. C* **1999**, *55*, 2026 – 2028.
[69] T. Kitazawa, T. Kikuyama, H. Ugajin, M. Takahashi, M. Takeda, *J. Coord. Chem.* **1996**, *37*, 17 – 22.
[70] H. Yuge, C.-H. Kim, T. Iwamoto, T. Kitazawa, *Inorg. Chim. Acta* **1997**, *257*, 217 – 224.
[71] S. Nishikiori, T. Iwamoto, *J. Inclusion Phenom.* **1985**, *3*, 283 – 295.
[72] D. W. Knoeppel, J. Liu, E. A. Meyers, S. G. Shore, *Inorg. Chem.* **1998**, *37*, 4828 – 4837.
[73] J. Liu, E. A. Meyers, S. G. Shore, *Inorg. Chem.* **1998**, *37*, 5410 – 5411.
[74] M. Munakata, J. C. Zhong, I. Ino, T. Kuroda-Sowa, M. Maekawa, Y. Suenaga, N. Oiji, *Inorg. Chim. Acta* **2001**, *317*, 268 – 275.
[75] B. Du, E. A. Meyers, S. G. Shore, *Inorg. Chem.* **2001**, *40*, 4353 – 4360.
[76] J. O. Eriksen, A. Hazell, A. Jensen, J. Jepsen, R. D. Poulsen, *Acta Crystallogr. Sect. C* **2000**, *56*, 551 – 553.
[77] B. Yan, H.-D. Wang, Z.-D. Chen, *Polyhedron* **2001**, *20*, 591 – 597.
[78] H. Miyasaka, N. Matsumoto, H. Okawa, N. Re, E. Gallo, C. Floriani, *J. Am. Chem. Soc.* **1996**, *118*, 981 – 994.
[79] E. Colacio, J. M. Domínguez-Vera, M. Chazi, R. Kivekäs, M. Klinga, J. M. Moreno, *Chem. Commun.* **1998**, 1071 – 1072.
[80] H.-Z. Kou, W.-M. Bu, D.-Z. Liao, Z.-H. Jiang, S.-P. Yan, Y.-G. Fan, G.-L. Wang, *J. Chem. Soc. Dalton Trans.* **1998**, 4161 – 4164.
[81] M. Ferbinteanu, S. Tanase, M. Andruh, Y. Journaux, F. Cimpoesu, I. Strenger, E. Riviere, *Polyhedron* **1999**, *18*, 3019 – 3025.
[82] N. Mondal, D. K. Dey, S. Mitra, V. Gramlich, *Polyhedron* **2001**, *20*, 607 – 613.
[83] A. Marvilliers, S. Parsons, E. Rivière, J.-P. Audière, M. Kurmoo, T. Mallah, *Eur. J. Inorg. Chem.* **2001**, 1287 – 1293.
[84] A. Figuerola, C. Diaz, M. S. E. Fallah, J. Ribas, M. Maestro, J. Mahía, *Chem. Commun.* **2001**, 1204 – 1205.
[85] H.-Z. Kou, S. Gao, O. Bai, Z.-M. Wang, *Inorg. Chem.* **2001**, *40*, 6287 – 6294.
[86] B. Ziegler, M. Witzel, M. Schwarten, D. Babel, *Z. Naturforsch. B* **1999**, *54*, 870 – 876.
[87] D. Babel, W. Kurtz, *Stud. Inorg. Chem.* **1982**, *3*, 593 – 596.
[88] J. Larionova, O. Kahn, S. Golhen, L. Ouahab, R. Clérac, *Inorg. Chem.* **1999**, *38*, 3621 – 3627.
[89] O. Kahn, J. Larionova, L. Ouahab, *Chem. Commun.* **1999**, 945 – 952.
[90] J. Larionova, O. Kahn, S. Gohlen, L. Ouahab, R. Clérac, *J. Am. Chem. Soc.* **1999**, *121*, 3349 – 3356.
[91] A. K. Sra, G. Rombaut, F. Lahitête, S. Golhen, L. Ouahab, C. Mathonière, J. V. Yakhmi, O. Kahn, *New J. Chem.* **2000**, *24*, 871 – 876.
[92] Z. J. Zhong, H. Seino, Y. Mizobe, M. Hidai, M. Verdaguer, S. Ohkoshi, K. Hashimoto, *Inorg. Chem.* **2000**, *39*, 5095 – 5101.
[93] G. Rombaut, S. Golhen, L. Ouahab, C. Mathonière, O. Kahn, *J. Chem. Soc. Dalton Trans.* **2000**, 3609 – 3614.
[94] J. Lu, T. Paliwala, S. C. Lim, C. Yu, T. Niu, A. J. Jacobson, *Inorg. Chem.* **1997**, *36*, 923 – 929.
[95] S. Banfi, L. Carlucci, E. Caruso, G. Ciani, D. M. Proserpio, *J. Chem. Soc. Dalton Trans.* **2002**, 2714 – 2721.
[96] K. Biradha, M. Fujita, *Chem. Commun.* **2001**, 15 – 16.
[97] M. A. Withersby, A. J. Blake, N. R. Champness, P. A. Cooke, P. Hubberstey, M. Schröder, *J. Am. Chem. Soc.* **2000**, *122*, 4044 – 4046.
[98] B. F. Abrahams, M. J. Hardie, B. F. Hoskins, R. Robson, E. E. Sutherland, *J. Chem. Soc. Chem. Commun.* **1994**, 1049 – 1050.
[99] M. Fujita, Y. J. Kwon, O. Sasaki, K. Yamaguti, K. Ogura, *J. Am. Chem. Soc.* **1995**, *117*, 7287 – 7288.
[100] N. G. Pschirer, D. M. Ciurtin, M. D. Smith, U. H. Bunz, H.-C. zur Loye, *Angew. Chem.* **2002**, *114*, 603 – 605; *Angew. Chem. Int. Ed.* **2002**, *41*, 583 – 585.
[101] H.-X. Zhang, B.-S. Kang, A.-W. Xu, Z.-N. Chen, Z.-Y. Zhou, A. S. C. Chan, K.-B. Yu, C. Ren, *J. Chem. Soc. Dalton Trans.* **2001**, 2559 – 2566.
[102] A. D. Burrows, R. W. Harrington, M. F. Mahon, C. E. Price, *J. Chem. Soc. Dalton Trans.* **2000**, 3845 – 3854.
[103] H. J. Choi, T. S. Lee, M. P. Suh, *J. Inclusion Phenom. Macrocyclic Chem.* **2001**, *41*, 155 – 162.
[104] S. O. H. Gutschke, D. J. Price, A. K. Powell, P. T. Wood, *Angew. Chem.* **2001**, *113*, 1974 – 1977; *Angew. Chem. Int. Ed.* **2001**, *40*, 1920 – 1923.
[105] T. J. Prior, M. J. Rosseinsky, *Chem. Commun.* **2001**, 495 – 496.
[106] O. M. Yaghi, H. Li, T. L. Groy, *J. Am. Chem. Soc.* **1996**, *118*, 9096 – 9101.
[107] R. Murugavel, D. Krishnamurthy, M. Sathiyendiran, *J. Chem. Soc. Dalton Trans.* **2002**, 34 – 39.
[108] H. Kumagai, C. J. Kepert, M. Kurmoo, *Inorg. Chem.* **2002**, *41*, 3410 – 3422.

[109] H. Endres, A. Knieszner, *Acta Crystallogr. Sect. C* **1984**, *40*, 770–772.

[110] S. S.-Y. Chui, A. Siu, X. Feng, Z. Y. Zhang, T. C. W. Mak, I. D. Williams, *Inorg. Chem. Commun.* **2001**, *4*, 467–470.

[111] S. Kawata, S. Kitagawa, M. Kondo, I. Furuchi, M. Munakata, *Angew. Chem.* **1994**, *106*, 1851–1854; *Angew. Chem. Int. Ed. Engl.* **1994**, *33*, 1759–1761.

[112] J. Zhang, M. M. Matsushita, X. X. Kong, J. Abe, T. Iyoda, *J. Am. Chem. Soc.* **2001**, *123*, 12105–12106.

[113] M. M. Matsushita, M. Morikawa, T. Kawai, T. Iyoda, *Mol. Cryst. Liq. Cryst.* **2000**, *343*, 87–96.

[114] G. J. E. Davidson, S. J. Loeb, *Angew. Chem.* **2003**, *115*, 78–81; *Angew. Chem. Int. Ed.* **2003**, *42*, 74–77.

[115] E. Lee, J. Heo, K. Kim, *Angew. Chem.* **2000**, *112*, 2811–2813; *Angew. Chem. Int. Ed.* **2000**, *39*, 2699–2701.

[116] E. Lee, J. Kim, J. Heo, D. Whang, K. Kim, *Angew. Chem.* **2001**, *113*, 413–416; *Angew. Chem. Int. Ed.* **2001**, *40*, 399–402.

[117] A. F. Wells, *Three Dimensional Nets and Polyhedra*, Wiley, New York, **1977**.

[118] "Further Studies of Three-Dimensional Nets": A. F. Wells, *Trans. Am. Crystallogr. Assoc.* **1979**, *8*.

[119] S. T. Hyde, S. Andersson, *Z. Kristallogr.* **1984**, *168*, 221–254.

[120] M. O'Keeffe, B. G. Hyde, *Crystal Structure I*: *Patterns and Symmetry*, American Mineralogical Association, Washington, **1996**.

[121] S. Han, J. V. Smith, *Acta Crystallogr. Sect. A* **1999**, *55*, 332–341.

[122] M. O'Keeffe, M. Eddaoudi, H. Li, T. Reineke, O. M. Yaghi, *J. Solid State Chem.* **2000**, *152*, 3–20.

[123] G. Férey, *J. Solid State Chem.* **2000**, *152*, 37–48.

[124] K. Biradha, M. Fujita, *J. Chem. Soc. Dalton Trans.* **2000**, 3805–3810.

[125] M. A. Withersby, A. J. Blake, N. R. Champness, P. A. Cooke, P. Hubberstey, M. Schröder, *New J. Chem.* **1999**, *23*, 573–575.

[126] S. Noro, R. Kitaura, M. Kondo, S. Kitagawa, T. Ishii, H. Matsuzaka, M. Yamashita, *J. Am. Chem. Soc.* **2002**, *124*, 2568–2583.

[127] T. Otieno, S. J. Rettig, R. C. Thompson, J. Trotter, *Inorg. Chem.* **1993**, *32*, 1607–1611.

[128] L. Carlucci, G. Ciani, D. M. Proserpio, A. Sironi, *Angew. Chem.* **1995**, *107*, 2037–2040; *Angew. Chem. Int. Ed. Engl.* **1995**, *34*, 1895–1898.

[129] S. Subramanian, M. J. Zaworotko, *Angew. Chem.* **1995**, *107*, 2295; *Angew. Chem. Int. Ed. Engl.* **1995**, *34*, 2127–2129.

[130] S.-i. Noro, S. Kitagawa, M. Kondo, K. Seki, *Angew. Chem.* **2000**, *112*, 2161–2164; *Angew. Chem. Int. Ed.* **2000**, *39*, 2081–2084.

[131] H. Li, M. Eddaoudi, M. O'Keeffe, O. M. Yaghi, *Nature* **1999**, *402*, 276–279.

[132] G. B. Gardner, D. Venkataraman, J. S. Moore, S. Lee, *Nature* **1995**, *374*, 792–795.

[133] K. N. Power, T. L. Hennigar, M. J. Zaworotko, *Chem. Commun.* **1998**, 595–596.

[134] L. Carlucci, N. Cozzi, G. Ciani, M. Moret, D. M. Proserpio, S. Rizzato, *Chem. Commun.* **2002**, 1354–1355.

[135] B. Rather, B. Moulton, R. D. B. Walsh, M. J. Zaworotko, *Chem. Commun.* **2002**, 694–695.

[136] H. Gudbjartson, K. Biradha, K. M. Poirier, M. J. Zaworotko, *J. Am. Chem. Soc.* **1999**, *121*, 2599–2600.

[137] B. Chen, M. Eddaoudi, T. M. Reineke, J. W. Kampf, M. O'Keeffe, O. M. Yaghi, *J. Am. Chem. Soc.* **2000**, *122*, 11559–11560.

[138] M. Eddaoudi, J. Kim, M. O'Keeffe, O. M. Yaghi, *J. Am. Chem. Soc.* **2002**, *124*, 376–377.

[139] A. F. Wells, *Structural Inorganic Chemistry*, Oxford University Press, New York, **1984**.

[140] Y. Cui, H. L. Ngo, P. S. White, W. Lin, *Chem. Commun.* **2002**, 1666–1667.

[141] J. S. Seo, D. Whang, H. Lee, S. I. Jun, J. Oh, Y. J. Jeon, K. Kim, *Nature* **2000**, *404*, 982–986.

[142] O. R. Evans, H. L. Ngo, W. Lin, *J. Am. Chem. Soc.* **2001**, *123*, 10395–10396.

[143] K. Biradha, C. Seward, M. J. Zaworotko, *Angew. Chem.* **1999**, *111*, 584–587; *Angew. Chem. Int. Ed.* **1999**, *38*, 492–495.

[144] D. Hagrman, C. Zubieta, D. J. Rose, J. Zubieta, R. C. Harshalter, *Angew. Chem.* **1997**, *109*, 904–907; *Angew. Chem. Int. Ed. Engl.* **1997**, *36*, 873–876.

[145] M. Kondo, M. Shimamura, S. Noro, S. Minakoshi, A. Asami, K. Seki, S. Kitagawa, *Chem. Mater.* **2000**, *12*, 1288–1299.

[146] M.-X. Li, G.-Y. Xie, Y.-D. Gu, J. Chen, P.-J. Zheng, *Polyhedron* **1995**, *14*, 1235–1239.

[147] N. Moliner, M. C. Muñoz, J. A. Real, *Inorg. Chem. Commun.* **1999**, *2*, 25–27.

[148] S. Noro, M. Kondo, T. Ishii, S. Kitagawa, H. Matsuzaka, *J. Chem. Soc. Dalton Trans.* **1999**, 1569–1574.

[149] X. M. Chen, M. L. Tong, Y. J. Luo, Z. N. Chen, *Aust. J. Chem.* **1996**, *49*, 835–838.

[150] A. J. Blake, S. J. Hill, P. Hubberstey, W.-S. Li, *J. Chem. Soc. Dalton Trans.* **1997**, 913–914.

[151] M.-L. Tong, X.-M. Chen, B.-H. Ye, S. W. Ng, *Inorg. Chem.* **1998**, *37*, 5278–5281.

[152] R. Kitaura, K. Seki, G. Akiyama, S. Kitagawa, *Angew. Chem.* **2003**, *115*, 444–447; *Angew. Chem. Int. Ed.* **2003**, *42*, 428–431.

[153] K. Uemura, S. Kitagawa, M. Kondo, K. Fukui, R. Kitaura, H.-C. Chang, T. Mizutani, *Chem. Eur. J.* **2002**, *8*, 3587–3600.

[154] M.-L. Tong, Y.-M. Wu, X.-M. Chen, H.-C. Chang, S. Kitagawa, *Inorg. Chem.* **2002**, *41*, 4846–4848.

[155] L. Carlucci, G. Ciani, D. M. Proserpio, S. Rizzato, *Chem. Eur. J.* **2002**, *8*, 1520–1526.

[156] N. Rosi, M. Eddaoudi, J. Kim, M. O'Keeffe, O. M. Yaghi, *Angew. Chem.* **2002**, *114*, 294–297; *Angew. Chem. Int. Ed.* **2002**, *41*, 284–287.

[157] K. Kasai, M. Aoyagi, M. Fujita, *J. Am. Chem. Soc.* **2000**, *122*, 2140–2141.

[158] M. Kondo, T. Okubo, A. Asami, S. Noro, T. Yoshitomi, S. Kitagawa, T. Ishii, H. Matsuzaka, K. Seki, *Angew. Chem.* **1999**, *111*, 190–193; *Angew. Chem. Int. Ed.* **1999**, *38*, 140–143.

[159] R. Kitaura, S. Noro, S. Kitagawa, unpublished results.

[160] B. Chen, M. Eddaoudi, S. T. Hyde, M. O'Keeffe, O. M. Yaghi, *Science* **2001**, *291*, 1021–1023.

[161] K. Seki, *Phys. Chem. Chem. Phys.* **2002**, *4*, 1968–1971.

[162] K. Biradha, M. Fujita, *Angew. Chem.* **2002**, *114*, 3542–3545; *Angew. Chem. Int. Ed.* **2002**, *41*, 3392–3395.

[163] O. R. Evans, W. Lin, *Chem. Mater.* **2001**, *13*, 2705–2712.

[164] T. M. Reineke, M. Eddaoudi, D. Moler, M. O'Keeffe, O. M. Yaghi, *J. Am. Chem. Soc.* **2000**, *122*, 4843–4844.

[165] M.-L. Tong, X.-M. Chen, X. L. Yu, T. C. W. Mak, *J. Chem. Soc. Dalton Trans.* **1998**, 5–6.

[166] S. Kawata, S. Kitagawa, M. Enomoto, H. Kumagai, M. Katada, *Inorg. Chim. Acta* **1998**, *283*, 80–90.

[167] R. Kitaura, K. Fujimoto, S. Noro, M. Kondo, S. Kitagawa, *Angew. Chem.* **2002**, *114*, 141–143; *Angew. Chem. Int. Ed.* **2002**, *41*, 133–135.

[168] S. Kitagawa, T. Okubo, S. Kawata, M. Kondo, M. Katada, H. Kobayashi, *Inorg. Chem.* **1995**, *34*, 4790–4796.

[169] S. M.-F. Lo, S. S.-Y. Chui, L.-Y. Shek, Z. Lin, X. X. Zhang, G.-H. Wen, I. D. Williams, *J. Am. Chem. Soc.* **2000**, *122*, 6293–6294.

[170] Z. Shi, L. Zhang, S. Gao, G. Yang, J. Hua, L. Gao, S. Feng, *Inorg. Chem.* **2000**, *39*, 1990–1993.

[171] M. Moon, I. Kim, M. S. Lah, *Inorg. Chem.* **2000**, *39*, 2710–2711.

[172] L. R. MacGillivray, R. H. Groeneman, J. L. Atwood, *J. Am. Chem. Soc.* **1998**, *120*, 2676–2677.

[173] S. Dalai, P. S. Mukherjee, E. Zangrando, F. Lloret, N. R. Chaudhuri, *J. Chem. Soc. Dalton Trans.* **2002**, 822–823.

[174] J. Tao, M.-L. Tong, J.-X. Shi, X.-M. Chen, S. W. Ng, *Chem. Commun.* **2000**, 2043 – 2044.

[175] R. H. Groeneman, L. R. MacGillivray, J. L. Atwood, *Chem. Commun.* **1998**, 2735 – 2736.

[176] S. Decurtins, H. W. Schmalle, P. Schneuwly, L.-M. Zheng, J. Ensling, A. Hauser, *Inorg. Chem.* **1995**, *34*, 5501 – 5506.

[177] J. Tao, Y. Zhang, M.-L. Tong, X.-M. Chen, T. Yuen, C. L. Lin, X. Huang, J. Li, *Chem. Commun.* **2002**, 1342 – 1343.

[178] P. Lightfoot, A. Snedden, *J. Chem. Soc. Dalton Trans.* **1999**, 3549 – 3551.

[179] L.-M. Zheng, X. Fang, K.-H. Lii, H.-H. Song, X.-Q. Xin, H.-K. Fun, K. Chinnakali, I. A. Razak, *J. Chem. Soc. Dalton Trans.* **1999**, 2311 – 2316.

[180] J. Tao, M.-L. Tong, X.-M. Chen, *J. Chem. Soc. Dalton Trans.* **2000**, 3669 – 3674.

[181] C. S. Hong, S.-K. Son, Y. S. Lee, M.-J. Jun, Y. Do, *Inorg. Chem.* **1999**, *38*, 5602 – 5610.

[182] Y. Pei, O. Kahn, J. Sletten, J.-P. Renard, R. Georges, J.-C. Gianduzzo, J. Curely, Q. Xu, *Inorg. Chem.* **1988**, *27*, 47 – 53.

[183] V. Baron, B. Gillon, A. Cousson, C. Mathonière, O. Kahn, A. Grand, L. Öhrström, B. Delley, M. Bonnet, J.-X. Boucherle, *J. Am. Chem. Soc.* **1997**, *119*, 3500 – 3506.

[184] H. O. Stumpf, L. Ouahab, Y. Pei, P. Bergerat, O. Kahn, *J. Am. Chem. Soc.* **1994**, *116*, 3866 – 3874.

[185] D. M. Ciurtin, M. D. Smith, H.-C. zur Loye, *Chem. Commun.* **2002**, 74 – 75.

[186] Y.-B. Dong, M. D. Smith, H.-C. zur Loye, *Inorg. Chem.* **2000**, *39*, 1943 – 1949.

[187] R. Horikoshi, T. Mochida, H. Moriyama, *Inorg. Chem.* **2002**, *41*, 3017 – 3024.

[188] G. Dong, M. Hong, D. Chun-ying, L. Feng, M. Qing-jin, *J. Chem. Soc. Dalton Trans.* **2002**, 2593 – 2594.

[189] S. Noro, S. Kitagawa, M. Yamashita, T. Wada, *Chem. Commun.* **2002**, 222 – 223.

[190] S. Noro, S. Kitagawa, M. Yamashita, T. Wada, *CrystEngComm* **2002**, *4*, 162 – 164.

[191] L. Carlucci, G. Ciani, F. Porta, D. M. Proserpio, L. Santagostini, *Angew. Chem.* **2002**, *114*, 1987 – 1991; *Angew. Chem. Int. Ed.* **2002**, *41*, 1907 – 1911.

[192] B. F. Abrahams, B. F. Hoskins, D. M. Michail, R. Robson, *Nature* **1994**, *369*, 727 – 729.

[193] C. V. K. Sharma, G. A. Broker, J. G. Huddleston, J. W. Baldwin, R. M. Metzger, R. D. Rogers, *J. Am. Chem. Soc.* **1999**, *121*, 1137 – 1144.

[194] Y. Diskin-Posner, G. K. Patra, I. Goldberg, *Eur. J. Inorg. Chem.* **2001**, 2515 – 2523.

[195] Z.-J. Zhong, H. Matsumoto, H. Okawa, S. Kida, *Chem. Lett.* **1990**, 87 – 90.

[196] J. Tamaki, Z. J. Zhong, N. Matsumoto, S. Kida, M. Koikawa, N. Achiwa, Y. Hashimoto, H. Okawa, *J. Am. Chem. Soc.* **1992**, *114*, 6974 – 6979.

[197] S. Decurtins, H. W. Schmalle, H. R. Oswald, A. Linden, J. Ensling, P. Gütlich, A. Hauser, *Inorg. Chim. Acta* **1994**, *216*, 65 – 73.

[198] S. G. Carling, C. Mathonière, P. Day, K. M. Abdul Malik, S. J. Coles, M. B. Hursthouse, *J. Chem. Soc. Dalton Trans.* **1996**, 1839 – 1843.

[199] J. Larionova, B. Mombelli, J. Sanchiz, O. Kahn, *Inorg. Chem.* **1998**, *37*, 679 – 684.

[200] H. Okawa, M. Mitsumi, M. Ohba, M. Kodera, N. Matsumoto, *Bull. Chem. Soc. Jpn.* **1994**, *67*, 2139 – 2144.

[201] R. Kitaura, G. Onoyama, H. Sakamoto, R. Matsuda, S. Noro, S. Kitagawa, *Angew. Chem./Angew. Chem. Int. Ed.*, in press.

[202] O. Kahn, Y. Pei, M. Verdaguer, J. P. Renard, J. Sletten, *J. Am. Chem. Soc.* **1988**, *110*, 782 – 789.

[203] M. E. Kosal, J.-H. Chou, S. R. Wilson, K. S. Suslick, *Nat. Mater.* **2002**, *1*, 118 – 121.

[204] G. A. Ozin, C. Gil, *Chem. Rev.* **1989**, *89*, 1749 – 1764.

[205] R. A. Sheldon, J. K. Kochi, *Metal-Catalyzed Oxidations of Organic Compounds*, Academic Press, New York, **1981**.

[206] L. Canali, D. C. Sherrington, *Coord. Chem. Rev.* **1999**, *28*, 85 – 93.

[207] Y. N. Ito, T. Katsuki, *Bull. Chem. Soc. Jpn.* **1999**, *72*, 603 – 619.

[208] H. Li, A. Laine, M. O'Keeffe, O. M. Yaghi, *Science* **1999**, *283*, 1145 – 1147.

[209] G.-Y. Yang, S. C. Sevov, *J. Am. Chem. Soc.* **1999**, *121*, 8389 – 8390.

[210] Y. Zhou, H. Zhu, Z. Chen, M. Chen, Y. Xu, H. Zhang, D. Zhao, *Angew. Chem.* **2001**, *113*, 2224 – 2226; *Angew. Chem. Int. Ed.* **2001**, *40*, 2166 – 2168.

[211] J. Plévert, T. M. Gentz, A. Laine, H. Li, V. G. Young, O. M. Yaghi, M. O'Keeffe, *J. Am. Chem. Soc.* **2001**, *123*, 12706 – 12707.

[212] N. Guillou, Q. Gao, P. M. Forster, J.-S. Chang, M. Noguès, S.-E. Park, G. Férey, A. K. Cheetham, *Angew. Chem.* **2001**, *113*, 2913 – 2916; *Angew. Chem. Int. Ed.* **2001**, *40*, 2831 – 2834.

[213] N. Zheng, X. Bu, P. Feng, *J. Am. Chem. Soc.* **2003**, *125*, 1138 – 1139.

[214] X. Bu, N. Zheng, Y. Li, P. Feng, *J. Am. Chem. Soc.* **2003**, *125*, 6024 – 6025.

[215] X. Wang, M. Simard, J. D. Wuest, *J. Am. Chem. Soc.* **1994**, *116*, 12119 – 12120.

[216] K. Endo, T. Sawaki, M. Koyanagi, K. Kobayashi, H. Masuda, Y. Aoyama, *J. Am. Chem. Soc.* **1995**, *117*, 8341 – 8352.

[217] Y. Aoyama, K. Endo, T. Anzai, Y. Yamaguchi, T. Sawaki, K. Kobayashi, N. Kanehisa, H. Hashimoto, Y. Kai, H. Masuda, *J. Am. Chem. Soc.* **1996**, *118*, 5562 – 5571.

[218] K. Endo, T. Koike, T. Sawaki, O. Hyashida, H. Masuda, Y. Aoyama, *J. Am. Chem. Soc.* **1997**, *119*, 4117 – 4122.

[219] K. Endo, T. Ezuhara, M. Koyanagi, H. Masuda, Y. Aoyama, *J. Am. Chem. Soc.* **1997**, *119*, 499 – 505.

[220] T. Dewa, K. Endo, Y. Aoyama, *J. Am. Chem. Soc.* **1998**, *120*, 8933 – 8940.

[221] P. Brunet, M. Simard, J. D. Wuest, *J. Am. Chem. Soc.* **1997**, *119*, 2737 – 2738.

[222] E. M. Flanigen, B. M. Lok, R. L. Patton, S. T. Wilson, *New Dev. Zeolite Sci. Technol. Proc. Int. Zeolite Conf. 7th* **1986** [*Stud. Surf. Sci. Catal.* **1986**, *28*].

[223] E. M. Flanigen, R. L. Patton, S. T. Wilson, *Innovation Zeolite Mater. Sci. Proc. Int. Symp.* **1987** [*Stud. Surf. Sci. Catal.* **1988**, *37*].

[224] M. Hartmann, L. Kevan, *Chem. Rev.* **1999**, *99*, 635 – 663.

[225] J. Rocha, M. W. Anderson, *Eur. J. Inorg. Chem.* **2000**, 801 – 818.

[226] S. R. Batten, B. F. Hoskins, R. Robson, *J. Am. Chem. Soc.* **1995**, *117*, 5385 – 5386.

[227] S. Decurtins, H. W. Schmalle, R. Pellaux, P. Schneuwly, A. Hauser, *Inorg. Chem.* **1996**, *35*, 1451 – 1460.

[228] R. Sieber, S. Decurtins, H. Stoeckli-Evans, C. Wilson, D. Yufit, J. A. K. Howard, S. C. Capelli, A. Hauser, *Chem. Eur. J.* **2000**, *6*, 361 – 368.

[229] K. Biradha, Y. Hongo, M. Fujita, *Angew. Chem.* **2000**, *112*, 4001 – 4003; *Angew. Chem. Int. Ed.* **2000**, *39*, 3843 – 3845.

[230] J. Sun, L. Weng, Y. Zhou, J. Chen, Z. Chen, Z. Liu, D. Zhao, *Angew. Chem.* **2002**, *114*, 4651 – 4653; *Angew. Chem. Int. Ed.* **2002**, *41*, 4471 – 4473.

[231] Y. Cui, S. J. Lee, W. Lin, *J. Am. Chem. Soc.* **2003**, *125*, 6014 – 6015.

[232] S. Kawata, S. Kitagawa, H. Kumagai, C. Kudo, H. Kamesaki, T. Ishiyama, R. Suzuki, M. Kondo, M. Katada, *Inorg. Chem.* **1996**, *35*, 4449 – 4461.

[233] S. Kawata, S. Kitagawa, H. Kumagai, T. Ishiyama, K. Honda, H. Tobita, K. Adachi, M. Katada, *Chem. Mater.* **1998**, *10*, 3902 – 3912.

[234] B. F. Abrahams, K. D. Lu, B. Moubaraki, K. S. Murray, R. Robson, *J. Chem. Soc. Dalton Trans.* **2000**, 1793 – 1797.
[235] M. Ohba, H. Tamaki, N. Matsumoto, H. Okawa, S. Kida, *Chem. Lett.* **1991**, 1157 – 1160.
[236] H. Tamaki, M. Mitsumi, K. Nakamura, N. Matsumoto, S. Kida, H. Okawa, S. Iijima, *Chem. Lett.* **1992**, 1975 – 1978.
[237] H. Okawa, N. Matsumoto, H. Tamaki, M. Ohba, *Mol. Cryst. Liq. Cryst.* **1993**, *233*, 257 – 262.
[238] C. Mathonière, S. G. Carling, D. Yusheng, P. Day, *J. Chem. Soc. Chem. Commun.* **1994**, 1551 – 1552.
[239] C. Mathonière, C. J. Nuttall, S. G. Carling, P. Day, *Inorg. Chem.* **1996**, *35*, 1201 – 1206.
[240] R. Pellaux, H. W. Schmalle, R. Huber, P. Fisher, T. Hauss, B. Ouladdiaf, S. Decurtins, *Inorg. Chem.* **1997**, *36*, 2301 – 2308.
[241] E. Coronado, J. R. Galán-Mascarós, C.-J. Gómez-García, *Synth. Met.* **1999**, *102*, 1459 – 1460.
[242] S. Bénard, P. Yu, T. Coradin, E. Riviére, K. Nakatani, R. Clément, *Adv. Mater.* **1997**, *9*, 981 – 984.
[243] Z. Gu, O. Sato, T. Iyoda, K. Hashimoto, A. Fujishima, *Mol. Cryst. Liq. Cryst.* **1996**, *286*, 469 – 474.
[244] M. Clemente-León, E. Coronado, J.-R. Galán-Mascarós, C.-J. Gómez-García, *Chem. Commun.* **1997**, 1727 – 1728.
[245] E. Coronado, J.-R. Galán-Mascarós, C.-J. Gómez-García, J. Ensling, P. Gütlich, *Chem. Eur. J.* **2000**, *6*, 552 – 563.
[246] E. Coronado, J.-R. Galán-Mascarós, C.-J. Gómez-García, V. Laukhin, *Nature* **2000**, *408*, 447 – 449.
[247] J. Cai, J.-S. Zhou, M.-L. Lin, *J. Mater. Chem.* **2003**, *13*, 1806 – 1811.
[248] A. P. Côté, M. J. Ferguson, K. A. Khan, G. D. Enright, A. D. Kulynych, S. A. Dalrymple, G. K. H. Shimizu, *Inorg. Chem.* **2002**, *41*, 287 – 292.
[249] T. J. Prior, D. Bradshaw, S. J. Teat, M. J. Rosseinsky, *Chem. Commun.* **2003**, 500 – 501.
[250] IUPAC Manual of Symbols and Terminology, Appendix 2, Pt. 1, Colloid and Surface Chemistry [*Pure Appl. Chem.* **1972**, *31*, 578].
[251] S. Brunauer, P. H. Emmett, E. Teller, *J. Am. Chem. Soc.* **1938**, *60*, 309 – 319.
[252] S. Brunauer, L. S. Deming, W. E. Deming, E. Teller, *J. Am. Chem. Soc.* **1940**, *62*, 1723.
[253] S. J. Gregg, K. S. W. Sing, *Adsorption*, *Surface Area*, *and Porosity*, Academic Press, London, **1984**.
[254] C. Martin, N. Tosi-Pellenq, J. Patarin, J. P. Coulomb, *Langmuir* **1998**, *14*, 1774 – 1778.
[255] L. Mentasty, A. M. Woestyn, G. Zgrablich, *Adsorpt. Sci. Technol.* **1994**, *11*, 123 – 133.
[256] G. A. Ozin, A. Kuperman, A. Stein, *Angew. Chem.* **1989**, *101*, 373 – 390; *Angew. Chem. Int. Ed. Engl.* **1989**, *28*, 359 – 376.
[257] B. Smit, T. L. M. Maesen, *Nature* **1995**, *374*, 42 – 44.
[258] K. Kaneko, K. Shimizu, T. Suzuki, *J. Chem. Phys.* **1992**, *97*, 8705 – 8711.
[259] K. Kaneko, K. Murata, *Adsorption* **1997**, *3*, 197 – 208.
[260] K. R. Matranga, A. L. Myers, E. D. Glandt, *Chem. Eng. Sci.* **1992**, *47*, 1569 – 1579.
[261] P. N. Aukett, N. Quirke, S. Riddiford, S. R. Tennison, *Carbon* **1992**, *30*, 913 – 924.
[262] R. K. Agarwal, J. A. Schwarz, *J. Colloid Interface Sci.* **1989**, *130*, 137 – 145.
[263] M. J. Bojan, W. A. Steele, *Carbon* **1998**, *36*, 1417 – 1423.
[264] K. Seki, W. Mori, *J. Phys. Chem. B* **2002**, *106*, 1380 – 1385.
[265] K. Seki, *Chem. Commun.* **2001**, 1496 – 1497.
[266] K. Seki, S. Takamizawa, W. Mori, *Chem. Lett.* **2001**, 332 – 333.
[267] G. Horvath, K. Kawazoe, *J. Chem. Eng. Jpn.* **1983**, *16*, 470 – 475.
[268] N. Khosrovani, A. W. Sleight, *J. Solid State Chem.* **1996**, *121*, 2 – 11.
[269] T. Takaishi, K. Tsutsumi, K. Chubachi, A. Matsumoto, *J. Chem. Soc. Faraday Trans.* **1998**, *94*, 601 – 608.
[270] T. G. Amos, A. W. Sleight, *J. Solid State Chem.* **2001**, *160*, 230 – 238.
[271] R. L. Withers, Y. Tabira, J. S. O. Evans, I. J. King, A. W. Sleight, *J. Solid State Chem.* **2001**, *157*, 186 – 192.
[272] D. C. S. Souza, V. Pralong, A. J. Jacobson, L. F. Nazar, *Science* **2002**, *296*, 2012 – 2015.
[273] S. M. Kuznicki, V. A. Bell, S. Mair, H. W. Hillhouse, R. M. Jacubinas, C. M. Braunbarth, B. H. Toby, M. Tsapatsis, *Nature* **2001**, *412*, 720 – 724.
[274] B. Rather, M. J. Zaworotko, *Chem. Commun.* **2003**, 830 – 831.
[275] K. Seki, *Langmuir* **2002**, *18*, 2441 – 2443.
[276] M. Eddaoudi, J. Kim, N. Rosi, D. Vodak, J. Wachter, M. O'Keeffe, O. M. Yaghi, *Science* **2002**, *295*, 469 – 472.
[277] D. Li, K. Kaneko, *J. Phys. Chem. B* **2000**, *104*, 8940 – 8945.
[278] S. S.-Y. Chui, S. M.-F. Lo, J. P. H. Charmant, A. G. Orpen, I. D. Williams, *Science* **1999**, *283*, 1148 – 1150.
[279] T. Ohkubo, J. Miyawaki, K. Kaneko, R. Ryoo, N. A. Seaton, *J. Phys. Chem. B* **2002**, *106*, 6523 – 6528.
[280] N. Setoyama, T. Suzuki, K. Kaneko, *Carbon* **1998**, *36*, 1459 – 1467.
[281] K. Kaneko, R. F. Cracknell, D. Nicholson, *Langmuir* **1994**, *10*, 4606 – 4609.
[282] *Organometallic Conjugation*: *Structures*, *Reactions and Functions of d-d and d-π Conjugated Systems* (Eds.: A. Nakamura, N. Ueyama, K. Yamaguchi), Kodansha-Springer, Tokio, **2002**.
[283] T. Sawaki, T. Dewa, Y. Aoyama, *J. Am. Chem. Soc.* **1998**, *120*, 8539 – 8640.
[284] T. Sawaki, Y. Aoyama, *J. Am. Chem. Soc.* **1999**, *121*, 4793 – 4798.
[285] K. Barthelet, J. Marrot, D. Riou, G. Férey, *Angew. Chem.* **2002**, *114*, 291 – 294; *Angew. Chem. Int. Ed.* **2002**, *41*, 281 – 284.
[286] F. Millange, C. Serre, G. Férey, *Chem. Commun.* **2002**, 822 – 823.
[287] C. Serre, F. Millange, C. Thouvenot, M. Nogués, G. Marsolier, D. Louer, G. Férey, *J. Am. Chem. Soc.* **2002**, *124*, 13519 – 13526.
[288] G. J. Halder, C. J. Kepert, B. Moubaraki, K. S. Murray, J. D. Cashion, *Science* **2002**, *298*, 1762 – 1765.
[289] A. Kamiyama, T. Noguchi, T. Kajiwara, T. Ito, *Angew. Chem.* **2000**, *112*, 3260 – 3262; *Angew. Chem. Int. Ed.* **2000**, *39*, 3130 – 3132.
[290] J.-H. Liao, S.-H. Cheng, C.-T. Su, *Inorg. Chem. Commun.* **2002**, *5*, 761 – 764.
[291] L. G. Beauvais, M. P. Shores, J. R. Long, *J. Am. Chem. Soc.* **2000**, *122*, 2763 – 2772.
[292] L. Pan, H. Liu, X. Lei, X. Huang, D. H. Olson, N. J. Turro, J. Li, *Angew. Chem.* **2003**, *115*, 560 – 564; *Angew. Chem. Int. Ed.* **2003**, *42*, 542 – 546.
[293] Y.-Q. Tian, C.-X. Cai, Y. Ji, X.-Z. You, S.-M. Peng, G.-H. Lee, *Angew. Chem.* **2002**, *114*, 1442 – 1444; *Angew. Chem. Int. Ed.* **2002**, *41*, 1384 – 1386.
[294] C. J. Kepert, M. J. Rosseinsky, *Chem. Commun.* **1999**, 375 – 376.
[295] E. J. Cussen, J. B. Claridge, M. J. Rosseinsky, C. J. Kepert, *J. Am. Chem. Soc.* **2002**, *124*, 9574 – 9581.
[296] A. J. Fletcher, E. J. Cussen, T. J. Prior, M. J. Rosseinsky, C. J. Kepert, K. M. Thomas, *J. Am. Chem. Soc.* **2001**, *123*, 10001 – 10011.
[297] K. Biradha, Y. Hongo, M. Fujita, *Angew. Chem.* **2002**, *114*, 3545 – 3548; *Angew. Chem. Int. Ed.* **2002**, *41*, 3395 – 3398.
[298] K. S. Min, M. P. Suh, *Chem. Eur. J.* **2001**, *7*, 303 – 313.
[299] C. J. Kepert, T. J. Prior, M. J. Rosseinsky, *J. Am. Chem. Soc.* **2000**, *122*, 5158 – 5168.
[300] N. Guillou, C. Livage, W. van Beek, M. Nogués, G. Férey, *Angew. Chem.* **2003**, *115*, 668 – 671; *Angew. Chem. Int. Ed.* **2003**, *42*, 644 – 647.
[301] O. M. Yaghi, H. Li, T. L. Groy, *Inorg. Chem.* **1997**, *36*, 4292 – 4293.

[302] T. Ohmura, W. Mori, M. Hasegawa, T. Takei, A. Yoshizawa, *Chem. Lett.* **2003**, *32*, 34–35.

[303] R. Kitaura, S. Kitagawa, Y. Kubota, T. C. Kobayashi, K. Kindo, Y. Mita, A. Matsuo, M. Kobayashi, H.-C. Chang, T. C. Ozawa, M. Suzuki, M. Sakata, M. Takata, *Science* **2002**, *298*, 2358–2361.

[304] R. Nukada, W. Mori, S. Takamizawa, M. Mikuriya, M. Handa, H. Naono, *Chem. Lett.* **1999**, 367–368.

[305] W. Mori, F. Inoue, K. Yoshida, H. Nakayama, S. Takamizawa, M. Kishita, *Chem. Lett.* **1997**, 1219–1220.

[306] K. Seki, S. Takamizawa, W. Mori, *Chem. Lett.* **2001**, 122–123.

[307] M. Eddaoudi, J. Kim, J. B. Wachter, H. K. Chae, M. O'Keeffe, O. M. Yaghi, *J. Am. Chem. Soc.* **2001**, *123*, 4368–4369.

[308] L. C. Tabares, J. A. R. Navarro, J. M. Salas, *J. Am. Chem. Soc.* **2001**, *123*, 383–387.

[309] J. W. Ko, K. S. Min, M. P. Suh, *Inorg. Chem.* **2002**, *41*, 2151–2157.

[310] D. V. Soldatov, J. A. Ripmeester, S. I. Shergina, I. E. Sokolov, A. S. Zanina, S. A. Gromilov, Y. A. Dyadin, *J. Am. Chem. Soc.* **1999**, *121*, 4179–4188.

[311] D. V. Soldatov, J. A. Ripmeester, *Chem. Mater.* **2000**, *12*, 1827–1839.

[312] A. Y. Manakov, D. V. Soldatov, J. A. Ripmeester, J. Lipkowski, *J. Phys. Chem. B* **2000**, *104*, 12 111–12 118.

[313] D. V. Soldatov, E. V. Grachev, J. A. Ripmeester, *Cryst. Growth Des.* **2002**, *2*, 401–408.

[314] D. Li, K. Kaneko, *Chem. Phys. Lett.* **2001**, *335*, 50–56.

[315] L. Carlucci, G. Ciani, M. Moret, D. M. Proserpio, S. Rizzato, *Angew. Chem.* **2000**, *112*, 1566–1570; *Angew. Chem. Int. Ed.* **2000**, *39*, 1506–1510.

[316] L. Carlucci, G. Ciani, D. W. v. Gudenberg, D. M. Proserpio, *New J. Chem.* **1999**, *23*, 397–401.

[317] D. Maspoch, D. Ruiz-Molina, K. Wurst, N. Domingo, M. Cavallini, F. Biscarini, J. Tejada, C. Rovira, J. Veciana, *Nat. Mater.* **2003**, *2*, 190–195.

[318] J. Y. Lu, A. M. Babb, *Chem. Commun.* **2002**, 1340–1341.

[319] O. M. Yaghi, H. Li, *J. Am. Chem. Soc.* **1995**, *117*, 10 401–10 402.

[320] N. L. Rosi, J. Eckert, M. Eddaoudi, D. T. Vodak, J. Kim, M. O'Keeffe, O. M. Yaghi, *Science* **2003**, *300*, 1127–1129.

[321] H. K. Chae, M. Eddaoudi, J. Kim, S. I. Hauck, J. F. Hartwig, M. O'Keeffe, O. M. Yaghi, *J. Am. Chem. Soc.* **2001**, *123*, 11 482–11 483.

[322] H. Li, M. Eddaoudi, T. L. Groy, O. M. Yaghi, *J. Am. Chem. Soc.* **1998**, *120*, 8571–8572.

[323] M. Eddaoudi, H. Li, O. M. Yaghi, *J. Am. Chem. Soc.* **2000**, *122*, 1391–1397.

[324] H. Li, C. E. Davis, T. L. Groy, D. G. Kelley, O. M. Yaghi, *J. Am. Chem. Soc.* **1998**, *120*, 2186–2187.

[325] O. M. Yaghi, C. E. Davis, G. Li, H. Li, *J. Am. Chem. Soc.* **1997**, *119*, 2861–2868.

[326] M. Edgar, R. Mitchell, A. M. Z. Slawin, P. Lightfoot, P. A. Wright, *Chem. Eur. J.* **2001**, *7*, 5168–5175.

[327] D. M. L. Goodgame, D. A. Grachvogel, D. J. Williams, *Angew. Chem.* **1999**, *111*, 217–219; *Angew. Chem. Int. Ed.* **1999**, *38*, 153–156.

[328] S. Takamizawa, W. Mori, M. Furihata, S. Takeda, K. Yamaguchi, *Inorg. Chim. Acta* **1998**, *283*, 268–274.

[329] W. Mori, H. Hoshino, Y. Nishimoto, S. Takamizawa, *Chem. Lett.* **1999**, 331–332.

[330] S. Takamizawa, T. Hiroki, E.-i. Nakata, K. Mochizuki, W. Mori, *Chem. Lett.* **2002**, 1208–1209.

[331] S. Takamizawa, E.-i. Nakata, H. Yokoyama, K. Mochizuki, W. Mori, *Angew. Chem.* **2003**, *115*, 4467–4470; *Angew. Chem. Int. Ed.* **2003**, *42*, 4331–4334.

[332] B. H. Hamilton, K. A. Kelly, T. A. Wagler, M. P. Espe, C. J. Ziegler, *Inorg. Chem.* **2002**, *41*, 4984–4986.

[333] S. K. Mäkinen, N. J. Melcer, M. Parvez, G. K. H. Shimizu, *Chem. Eur. J.* **2001**, *7*, 5176–5182.

[334] G. B. Gardner, Y.-H. Kiang, S. Lee, A. Asgaonkar, D. Venkataraman, *J. Am. Chem. Soc.* **1996**, *118*, 6946–6953.

[335] B. F. Abrahams, P. A. Jackson, R. Robson, *Angew. Chem.* **1998**, *110*, 2801–2804; *Angew. Chem. Int. Ed.* **1998**, *37*, 2656–2659.

[336] O.-S. Jung, Y. J. Kim, K. M. Kim, Y.-A. Lee, *J. Am. Chem. Soc.* **2002**, *124*, 7906–7907.

[337] K. S. Min, M. P. Suh, *J. Am. Chem. Soc.* **2000**, *122*, 6834–6840.

[338] O.-S. Jung, Y. J. Kim, Y.-A. Lee, H. K. Chae, H. G. Jang, J. Hong, *Inorg. Chem.* **2001**, *40*, 2105–2110.

[339] O. M. Yaghi, H. Li, *J. Am. Chem. Soc.* **1996**, *118*, 295–296.

[340] O.-S. Jung, Y. J. Kim, Y.-A. Lee, K. H. Yoo, *Chem. Lett.* **2002**, 500–501.

[341] L. Pan, E. B. Woodlock, X. Wang, K.-C. Lam, A. L. Rheingold, *Chem. Commun.* **2001**, 1762–1763.

[342] A. N. Khlobystov, N. R. Champness, C. J. Roberts, S. J. B. Tendler, C. Thompson, M. Schröder, *CrystEngComm* **2002**, *4*, 426–431.

[343] O.-S. Jung, Y. J. Kim, Y.-A. Lee, J. K. Park, H. K. Chae, *J. Am. Chem. Soc.* **2000**, *122*, 9921–9925.

[344] S. Muthu, J. H. K. Yip, J. J. Vittal, *J. Chem. Soc. Dalton Trans.* **2002**, 4561–4568.

[345] O.-S. Jung, Y. J. Kim, Y.-A. Lee, K.-M. Park, S. S. Lee, *Inorg. Chem.* **2003**, *42*, 844–850.

[346] X. Xu, M. Nieuwenhuyzen, S. L. James, *Angew. Chem.* **2002**, *114*, 790–793; *Angew. Chem. Int. Ed.* **2002**, *41*, 764–767.

[347] T. M. Reineke, M. Eddaoudi, M. O'Keeffe, O. M. Yaghi, *Angew. Chem.* **1999**, *111*, 2712–2716; *Angew. Chem. Int. Ed.* **1999**, *38*, 2590–2594.

[348] Y. Yokomichi, K. Seki, S. Kitagawa, unpublished results.

[349] L. Schlapbach, A. Züttel, *Nature* **2001**, *414*, 353–358.

[350] J. Weitkamp, M. Fritz, S. Ernst, *Int. J. Hydrogen Energy* **1995**, *20*, 967–970.

[351] A. C. Dillon, K. M. Jones, T. A. Bekkedahl, C. H. Kiang, D. S. Bethune, M. J. Heben, *Nature* **1997**, *386*, 377–379.

[352] A. Chambers, C. Park, R. T. K. Baker, N. M. Rodriguez, *J. Phys. Chem. B* **1998**, *102*, 4253–4256.

[353] Y. Ye, C. C. Ahn, C. Witham, B. Fultz, *Appl. Phys. Lett.* **1999**, *74*, 2307–2309.

[354] C. Liu, Y. Y. Fan, M. Liu, H. T. Cong, H. M. Cheng, M. S. Dresselhaus, *Science* **1999**, *285*, 1127–1129.

[355] P. Chen, X. Wu, J. Lin, K. L. Tan, *Science* **1999**, *285*, 91–93.

[356] C. M. Brown, T. Yildirim, D. A. Neumann, M. J. Heben, T. Gennett, A. C. Dillon, J. L. Alleman, J. E. Fischer, *Chem. Phys. Lett.* **2000**, *329*, 311–316.

[357] A. Kuznetsova, D. B. Mawhinney, V. Naumenko, J. T. J. Yates, J. Liu, R. E. Smalley, *Chem. Phys. Lett.* **2000**, *321*, 292–296.

[358] R. T. Yang, *Carbon* **2000**, *38*, 623–641.

[359] H. W. Zhu, *J. Mater. Sci. Lett.* **2000**, *19*, 1237–1239.

[360] V. Meregalli, M. Parrinello, *Appl. Phys. A* **2001**, *72*, 143–146.

[361] A. C. Dillon, M. J. Heben, *Appl. Phys. A* **2001**, *72*, 133–142.

[362] A. Cao, H. Zhu, X. Zhang, X. Li, D. Ruan, C. Xu, B. Wei, J. Liang, D. Wu, *Chem. Phys. Lett.* **2001**, *342*, 510–514.

[363] G. E. Froudakis, *J. Phys. Condens. Matter* **2002**, *14*, R453–R465.

[364] P. M. Forster, J. Eckert, J.-S. Chang, S.-E. Park, G. Férey, A. K. Cheetham, *J. Am. Chem. Soc.* **2003**, *125*, 1309–1312.

[365] J. Fan, L. Gan, H. Kawaguchi, W.-Y. Sun, K.-B. Yu, W.-X. Tang, *Chem. Eur. J.* **2003**, *9*, 3965–3973.

[366] W. Hölderich, M. Hesse, F. Naumann, *Angew. Chem.* **1988**, *100*, 232–251; *Angew. Chem. Int. Ed. Engl.* **1988**, *27*, 226–246.

[367] J. M. Tanski, P. T. Wolczanski, *Inorg. Chem.* **2001**, *40*, 2026–2033.

[368] B. Gomez-Lor, E. Gutiérrez-Puebla, M. Iglesias, M. A. Monge, C. Ruiz-Valero, N. Snejko, *Inorg. Chem.* **2002**, *41*, 2429–2432.

[369] R. Tannenbaum, *Chem. Mater.* **1994**, *6*, 550–555.

[370] R. Tannenbaum, *J. Mol. Catal. A* **1996**, *107*, 207–215.
[371] I. Feinstein-Jaffe, A. Efraty, *J. Mol. Catal.* **1987**, *40*, 1–7.
[372] S. Naito, T. Tanibe, E. Saito, T. Miyao, W. Mori, *Chem. Lett.* **2001**, 1178–1179.
[373] B. Xing, M.-F. Choi, B. Xu, *Chem. Eur. J.* **2002**, *8*, 5028–5032.
[374] M. P. Suh, J. W. Ko, H. J. Choi, *J. Am. Chem. Soc.* **2002**, *124*, 10976–10977.
[375] G. R. Desiraju, *Angew. Chem.* **1995**, *107*, 2541–2558; *Angew. Chem. Int. Ed. Engl.* **1995**, *34*, 2311–2327.
[376] C. J. Kepert, D. Hesek, P. D. Beer, M. J. Rosseinsky, *Angew. Chem.* **1998**, *110*, 3335–3337; *Angew. Chem. Int. Ed.* **1998**, *37*, 3158–3160.
[377] K. Nagayoshi, M. K. Kabir, H. Tobita, K. Honda, M. Kawahara, M. Katada, K. Adachi, H. Nishikawa, I. Ikemoto, H. Kumagai, Y. Hosokoshi, K. Inoue, S. Kitagawa, S. Kawata, *J. Am. Chem. Soc.* **2003**, *125*, 221–232.
[378] H. J. Choi, T. S. Lee, M. P. Suh, *Angew. Chem.* **1999**, *111*, 1490–1493; *Angew. Chem. Int. Ed.* **1999**, *38*, 1405–1408.
[379] D. V. Soldatov, A. T. Henegouwen, G. D. Enright, C. I. Ratcliffe, J. A. Ripmeester, *Inorg. Chem.* **2001**, *40*, 1626–1636.
[380] S.-i. Noro, S. Kitagawa, *Stud. Surf. Sci. Catal.* **2002**, *141*, 363–370.
[381] H. J. Choi, M. P. Suh, *J. Am. Chem. Soc.* **1998**, *120*, 10622–10628.
[382] K. S. Min, M. P. Suh, *Eur. J. Inorg. Chem.* **2001**, 449–455.
[383] B. F. Abrahams, M. J. Hardie, B. F. Hoskins, R. Robson, G. A. Williams, *J. Am. Chem. Soc.* **1992**, *114*, 10641–10643.
[384] A. Mercedes, F. Belen, G. Hermenegildo, R. Fernando, *Chem. Commun.* **2002**, 2012–2013.
[385] N. K. Mal, M. Fujiwara, Y. Tanaka, *Nature* **2003**, *421*, 350–353.
[386] P. J. Langley, J. Hulliger, *Chem. Soc. Rev.* **1999**, *28*, 279–291.
[387] A. I. Yanson, G. R. Bollinger, H. E. van den Brom, N. Agrait, J. M. Ruitenbeek, *Nature* **1998**, *395*, 783–785.
[388] J. D. Holmes, K. P. Jonston, R. C. Doty, B. A. Korgel, *Science* **2000**, *287*, 1471–1473.
[389] Y. Kondo, K. Takayanagi, *Science* **2000**, *289*, 606–608.
[390] T. Hertzsch, F. Budde, E. Weber, J. Hulliger, *Angew. Chem.* **2002**, *114*, 2385–2388; *Angew. Chem. Int. Ed.* **2002**, *41*, 2281–2284.
[391] B. H. Hong, S. C. Bae, C.-W. Lee, S. Jeong, K. S. Kim, *Science* **2001**, *294*, 348–351.
[392] O. König, H.-B. Burgi, T. Armbruster, J. Hulliger, T. Weber, *J. Am. Chem. Soc.* **1997**, *119*, 10632–10640.
[393] K. T. Holman, A. M. Pivovar, M. D. Ward, *Science* **2001**, *294*, 1907–1911.
[394] V. A. Russell, C. C. Evans, W. Li, M. D. Ward, *Science* **1997**, *276*, 575–579.
[395] K. T. Holman, M. D. Ward, *Angew. Chem.* **2000**, *112*, 1719–1722; *Angew. Chem. Int. Ed.* **2000**, *39*, 1653–1656.
[396] Z. Liu, Y. Sakamoto, T. Ohsuna, K. Hiraga, O. Terasaki, C. H. Ko, H. J. Shin, R. Ryoo, *Angew. Chem.* **2000**, *112*, 3237–3240; *Angew. Chem. Int. Ed.* **2000**, *39*, 3107–3110.
[397] A. Fukuoka, Y. Sakamoto, S. Guan, S. Inagaki, N. Sugimoto, Y. Fukushima, K. Hirahara, S. Iijima, M. Ichikawa, *J. Am. Chem. Soc.* **2001**, *123*, 3373–3374.
[398] Y.-P. Ren, L.-S. Long, B.-W. Mao, Y.-Z. Yuan, R.-B. Huang, L.-S. Zheng, *Angew. Chem.* **2003**, *115*, 550–553; *Angew. Chem. Int. Ed.* **2003**, *42*, 532–535.
[399] W. Mori, T. C. Kobayashi, J. Kurobe, K. Amaya, Y. Narumi, T. Kumada, K. Kindo, H. A. Katori, T. Goto, N. Miura, S. Takamizawa, H. Nakayama, K. Yamaguchi, *Mol. Cryst. Liq. Cryst.* **1997**, *306*, 1–7.
[400] H. Kanoh, A. Zamma, N. Setoyama, Y. Hanzawa, K. Kaneko, *Langmuir* **1997**, *13*, 1047–1053.
[401] H. Kanoh, K. Kaneko, *J. Phys. Chem.* **1996**, *100*, 755–759.
[402] C. D. Gray, *Phys. Rev. B* **1981**, *23*, 4714–4740.
[403] H. J. Jodl, F. Bolduan, H. D. Hochheimer, *Phys. Rev. B* **1985**, *31*, 7376–7384.
[404] Y. Nozue, T. Kodaira, T. Goto, *Phys. Rev. Lett.* **1992**, *68*, 3789–3792.
[405] H. Yano, S. Yoshizaki, S. Inagaki, Y. Fukushima, N. Wada, *Low Temp. Phys.* **1998**, *110*, 573.
[406] W. E. Buhro, V. Colvin, *Nat. Mater.* **2003**, *2*, 138.
[407] B. Moulton, M. Zawortotko, *Curr. Opin. Solid State Mater. Sci.* **2002**, *6*, 117–123.